

Electronic Supplementary Information

Supramolecular ensemble of PBI derivative and copper nanoparticles: A light harvesting antenna for photocatalytic C(sp²)-H functionalization

Sandeep Kaur, Manoj Kumar and Vandana Bhalla*

Department of Chemistry, UGC Sponsored Centre for Advanced Studies-II, Guru Nanak Dev University, Amritsar 143005, Punjab, India

vanmanan@yahoo.co.in

- S4 Comparison of present method over other reported procedure in literature for the preparation of CuNPs.
- S5 Comparison of catalytic activity of CuNPs in C(sp²)-H alkylation of arenes over other reported methods.
- S6 Comparison of photocatalytic activity of CuNPs for C(sp²)-H amination reaction over other reported methods.
- S7 Comparison of photocatalytic activity in C(sp²)-H activation over other photocatalytic systems.
- S8 Absorption and fluorescence spectra of derivative **3** (5 μM) in different fraction of H₂O/THF mixture.
- S9 Concentration dependent ¹H NMR spectrum of derivative **3** in CDCl₃ and SEM image of derivative **3** in H₂O/THF mixture (6:4, v/v).
- S10 UV-vis spectra of compound **3** upon additions of various metal ions as their chloride and perchlorate salt in H₂O/THF (6:4, v/v).
- S11 UV-Vis spectra of compound **3** (5 μM) in presence of Cu²⁺ ion in THF and UV-vis spectroelectrochemical studies of PBI derivative **3** in presence of Cu²⁺ ions.
- S12 Detection limit of Cu²⁺ by using derivative **3** in H₂O/THF (6:4, v/v).
- S13 Competitive and selectivity graph of derivative **3** towards various metal ions as their chloride and perchlorate salt in H₂O/THF (6:4, v/v).
- S14 XRD diffraction patterns of CuNPs prepared by derivative **3** and DLS studies showing the variation in particle size of CuNPs by varying concentration of aggregates of derivative **3** and Cu²⁺ ions in H₂O/THF (6:4, v/v).
- S15 Normalized LSPR band of CuNPs. Fluorescence spectra of derivative **3** and Cu²⁺ ions in H₂O/THF (6:4, v/v) by mixing in different ratio.
- S16 Overlay of ¹H NMR spectra of **3** and CuCl₂ after filtration with THF.
- S17 Overlay of NMR spectra of oxidized species **4** and derivative **3**.
- S18 FT-IR spectra and ESI-MS mass spectra of oxidized species **4**.

- S19** Fluorescence spectrum of oxidised derivative **4** and spectral overlap of absorption spectrum of CuNPs and emission spectrum of oxidized species of **4**.
- S20** Fluorescence spectrum of oxidised derivative **4** in presence of bare CuNPs and Cu²⁺ ions.
- S21** Time resolved fluorescence studies of derivative **4** in presence of CuNPs in H₂O/THF (6:4, v/v).
- S22** UV-Vis spectra of compound **3** (5 μM) showing the response to the Cu²⁺ ion (0-15 equiv.) in H₂O/THF (6:4, v/v) mixture. Catalytic efficiency of supramolecular ensemble **4**:CuNPs for photocatalytic C-H activation of oxazoline substituted benzamide (**5**) and phenyl acetylene (**6a**).
- S23** Atomic absorption Studies (AAS) showed the leaching of CuNPs (8-20 nm) after 4th catalytic cycle.
- S24** Catalytic efficiency of supramolecular ensemble **4**:CuNPs using 10 μM of derivative **3** and 30 equiv. Cu²⁺ ions for photocatalytic C-H activation reaction of **5** with **6a**. AAS studies showed the leaching of CuNPs (5-8 nm) after 4th catalytic cycle.
- S25** Recyclability and catalytic efficiency of supramolecular ensemble **4**:CuNPs for photocatalytic C-H activation of oxazoline substituted benzamides (**5**) and *p*-nitro aniline (**9a**).
- S26** ¹H NMR of spectrum of derivative **3**.
- S27** ¹³C NMR of spectrum of derivative **3**.
- S28** MALDI-TOF spectrum of derivative **3**.
- S29** FT-IR spectra of derivative **3**.
- S30** ¹H NMR of spectrum of derivative **7a** and **7b**.
- S31** ¹³C NMR and ESI-MS spectrum of derivative **7b**.
- S32** ¹H and ¹³C NMR of spectrum of derivative **7c**.
- S33** ESI-MS spectrum of derivative **7c**.
- S34** ¹H and ¹³C NMR of spectrum of derivative **7d**.
- S35** ESI-MS spectrum of derivative **7d**.
- S36** ¹H and ¹³C NMR spectrum of derivative **7e**.
- S37** ESI-MS spectrum of derivative **7e**.
- S38** ¹H and ¹³C NMR spectrum of derivative **7f**.
- S39** ESI-MS spectrum of derivative **7f**.
- S40** ¹H NMR spectrum of derivative **7g** and **7h**.

- S41** ^1H NMR spectrum of derivative **7i**.
- S42** ^1H and ^{13}C NMR spectrum of derivative **7j**.
- S43** ESI-MS spectrum of derivative **7j** and ^1H NMR spectrum of derivative **7k**.
- S44** ^1H and ^{13}C NMR NMR spectrum of derivative **7l**.
- S45** ESI-MS spectrum of derivative **7l**.
- S46** ^1H and ^{13}C NMR spectrum of derivative **7m**.
- S47** ESI-MS spectrum of derivative **7m**.
- S48** ^1H and ^{13}C NMR spectrum of derivative **6n**.
- S49** ESI-MS spectrum of derivative **6n**.
- S50** ^1H and ^{13}C NMR spectrum of derivative **7n**.
- S51** ESI-MS spectrum of derivative **7n**.
- S52** ^1H NMR spectrum of derivative **10a** and **10b**
- S53** ^1H NMR spectrum of derivative **10c** and **10d**.
- S54** ^1H and ^{13}C NMR spectrum of derivative **10e**.
- S55** ESI-MS spectrum of derivative **10e**.
- S56** ^1H and ^{13}C NMR spectrum of derivative **10f**.
- S57** ESI-MS spectrum of derivative **10f**.
- S58** ^1H and ^{13}C NMR spectrum of derivative **10g**
- S59** ESI-MS spectrum of derivative **10g**.
- S60** ^1H and ^{13}C NMR spectrum of derivative **10h**.
- S61** ESI-MS spectrum of derivative **10h**.
- S62** ^1H and ^{13}C NMR spectrum of derivative **10i**.
- S63** ESI-MS spectrum of derivative **10i**.
- S64** ^1H and ^{13}C NMR spectrum of derivative **10j**
- S65** ESI-MS spectrum of derivative **10j**.
- S66** ^1H and ^{13}C NMR spectrum of derivative **10k**.
- S67** ESI-MS spectrum of derivative **10k**.
- S68** ^1H and ^{13}C NMR spectrum of derivative **10l**.
- S69** ESI-MS spectrum of derivative **10l**.
- S70** ^1H and ^{13}C NMR spectrum of derivative **11**
- S71** ^1H and ^{13}C NMR spectrum of derivative **12**

Table S1: Comparison of present method over other reported procedure in literature for the preparation of CuNPs.

Sr. No.	Publication	Method of formation of CuNPs	Reagent Used	Reducing agent Used	Reaction time to prepare CuNPs	Temp. (°C)	Shape of Cu(0)NPs	Size	Reusability of CuNPs after reaction
1	Present manuscript	Wet Chemical Method	Compound 3 in Water/THF (6:4) and CuCl₂	No	30 min	Room Temperature	Spherical	8-20 nm	Yes
2	<i>ACS Nano</i> , 2015, 9 , 12104-12114	Hydrothermal	Cu(NO ₃) ₂ , propylene glycol and ethylene glycol, PVP	propylene glycol and ethylene glycol	60 min	150	spherical	360 (12 nm)	No
3	<i>ACS Appl. Mater. Interfaces</i> , 2015, 7 , 19382-19389	Solution synthesis, low-temperature sintering,	Ethylene Glycol, Cu(OAc) ₂ , 3-amino-1-propanol, hydrazine monohydrate	hydrazine monohydrate	24 h	stirring at 1100 rpm and at room temperature	Spherical	3-10 nm	No
4	<i>Sci. Rep.</i> , 2015, 5 , 8294	Hydrothermal condition	Cu(acac) ₃ , phenol formaldehyde resin and triblock copolymer Pluronic-F127, N ₂ H ₄ .H ₂ O	N ₂ H ₄ .H ₂ O	24 h	100	Spherical	9.8-14.3 nm	Yes
5	<i>Catal. Sci. Technol.</i> , 2015, 5 , 1251-1260	Simple one-pot method	Graphite powder, sulfuric acid, H ₂ O ₂ , potassium permanganate, ascorbic Acid, Cu(CH ₃ COO) ₂ .H ₂ O,	ascorbic acid	1 h	80	Spherical	10-20 nm	Yes
6	<i>Faraday Discuss.</i> , 2015, 181 , 383-401	Feld-stimulated assembly of copper nanoparticles	L-ascorbic acid, CTAB, CuCl ₂ .2H ₂ O	L-ascorbic acid	42 h	45°C, centrifugation at 10000 rpm	Film	3.2 ± 0.74 nm	No
7	<i>Angew. Chem.</i> , 2014, 126 , 2004 – 2008	Reduction	Graphene oxide and copper Acetate, absolute ethanol, diethylene glycol, H ₂ (5 vol%) and Ar at 500°C	H ₂ (5 vol%)	2 h	180/500	Spherical	15 nm	No
8	<i>ACS Appl. Mater. Interfaces</i> , 2014, 6 , 560-567	Solvothermal	Cu(OH) ₂ , PEG-2000, L-ascorbic acid, ethylene glycol butyl ether, methylcellulose,	L-ascorbic acid	30 min	80	Spherical	90-180 nm	No
9	<i>ACS Sustainable Chem. Eng.</i> , 2014, 2 , 2658-2665	Agarose-Supported Copper Catalyst	Agarose, CuBr, NaBH ₄ ,	NaBH ₄	24 h	80	Spherical	4-8 nm	No
10	<i>ACS Sustainable Chem. Eng.</i> , 2014, 2 , 1933-1939	Plant Tea Reducing Agent	CuSO ₄ ·5H ₂ O, lemongrass tea, deionized water	lemongrass tea	2 weeks	Room Temperature	Spherical	2.90 ± 0.64 nm,	No
11	<i>RSC Adv.</i> , 2014, 4 , 25155-25159	Through T-shaped microfluidic chip	CuSO ₄ ·5H ₂ O, NaBH ₄ , polyvinylpyrrolidone, NH ₄ OH, NaOH, polydimethylsiloxane	NaBH ₄	2 days	Room temp	Spherical	8.95 nm	No
12	<i>RSC Adv.</i> , 2014, 4 , 27381-27388	Photoreduction	CuCl ₂ , photoinitiator 184, diethanol amine, and ethanol, PEI, PVP, dark and Oxygen free environment	photoinitiator 184	30 min	Room Temp	Spherical	10-200 nm	No
13	<i>ACS Appl. Mater. Interfaces</i> , 2013, 5 , 3839-3846	Chemical reduction of copper ions in aqueous solution	Copper(II) acetate monohydrate, hydrazine hydrate solution (50%), lactic acid, glycolic acid, acetic acid, citric acid, glycine, alanine, and ammonia-water	hydrazine hydrate	3 h	40°C for 3 h in an inert atmosphere and 11000 rpm for 15 min	Spherical /Film	9.2 ± 1.5 Mm	No
14	<i>J. Mater. Chem.</i> , 2012, 22 , 987-993	Reduction	Copper(II) chloride dehydrate, sodium borohydride, trisodium citrate dehydrate, diethylene glycol, ethanol, isopropanol	NaBH ₄	12 h	100	Irregular	15-45 nm	No
15	<i>Green Chem.</i> , 2012, 14 , 1589-1592	Cooperative assembly	CuSO ₄ ·5H ₂ O, SDS and ascorbic acid, NaBH ₄ (or N ₂ H ₄)	NaBH ₄ (or N ₂ H ₄)	4 h	60	Spherical	20 nm	No

Table S2: Comparison of catalytic activity of CuNPs for C(sp²)-H alkylation reaction over other reported methods:

Serial No.	Publication	Catalyst used	Reagent used	Base used	Solvent used	Reusable	Reaction time	Photocatalytic/Thermal condition required	Isolated Yield (Product, %)
1	Present manuscript C(sp ²)-H activation	CuNPs (1 mol %)	Benzamides with Terminal alkynes	K ₂ CO ₃	DMSO	Yes	6h	Photochemical (60 W tungsten bulb, r.t.)	78
2	<i>Org. Lett.</i> , 2016, 18 , 1064–1067	[RhCl(COD)] ₂ (1.5 mol %), Cu(OAc) ₂ ·H ₂ O	2H-[1,2'-bipyridin]-2-ones with propargyl alcohols	-	Toluene	No	4 h	125°C	62
3	<i>Catal. Sci. Technol.</i> , 2016, 6 , 1946-1951	Ni(OTf) ₂ (5 mol %) 10 mol % of benzoic acid	N-(quinolin-8-yl)benzamide with (triisopropylsilyl)ethynyl bromide	Na ₂ CO ₃	Toluene	No	24 h	110°C	75
4	<i>Angew. Chem. Int. Ed.</i> , 2015, 54 , 10012-10015	CoC ₂ O ₄ ·4H ₂ O AgOAc	2-benzamidopyridine 1-oxide (1a) with phenylacetylene	NaOAc	DMSO	No	12 h	100°C	85
5	<i>Org. Lett.</i> , 2015, 17 , 5316-5319	[Cp*CoI ₂] ₂ AgSbF ₆	Indole and silylated bromoalkynes	K ₂ CO ₃	TFE	No	16 h	80°C	96
6	<i>Chem. Commun.</i> , 2015, 51 , 6388-6391	Ni(OTf) ₂	benzamides and bromoalkynes	NaHCO ₃	Pivalonitrile	No	12 h	150°C	81
7	<i>Chem. Commun.</i> , 2015, 51 , 14497-14500	-	C(sp ²)-H oxidative alkylation of aldehydes with ethynyl benziodoxolones (EBX)	TBHP	PhCl	No	3 h	120°C	68
8	<i>J. Am. Chem. Soc.</i> , 2014, 136 , 11590-11593	Cu(OAc) ₂ (0.1 Mmol)	(Hetero)Arenes with Terminal Alkynes	NaOAc	DMSO	No	12 h	60°C	85
9	<i>Org. Lett.</i> , 2014, 16 , 2884-2887	Cu(OAc) ₂	N-(quinolin-8-yl)benzamide with Terminal Alkynes		t-AmylOH		24 h	140 °C under an N ₂ atmosphere	91
10	<i>Org. Lett.</i> , 2012, 14 , 2948-2951	Pd(OAc) ₂ , oPBA	R-substituted benzylamine With TIPS protected acetylenic bromide	KHCO ₃	DCE	No	24 h	100°C	90
11	<i>Org. Lett.</i> , 2011, 13 , 1474-1477	Pd(PPh ₃) ₄	5-Methylbenzoxazole and phenylacetylene	LiOtBu	Toluene	No	12 h	100°C	67
12	<i>J. Org. Chem.</i> , 2010, 75 , 1764-1766	[CuI]:[phen]	1,3,4-oxadiazoles with alkynyl bromides	LiO-t-Bu	Toluene	No	1 h	r.t.	70

Table S3: Comparison of catalytic activity of CuNPs for C(sp²)-H amination reaction over other reported methods:

Serial No.	Publication	Catalyst used	Reagent used	Additives/Base	Solvent used	Reusable	Reaction time	Photocatalytic/Thermal condition required	Isolated Yield (Product, %)
1	Present manuscript C(sp ²)-H activation	CuNPs (5 mol %)	Benzamides with amines	K ₂ CO ₃	DMSO	Yes	4h	Photochemical (60 W tungsten bulb, r.t.)	86
2	<i>J. Am. Chem. Soc.</i> , 2016, 138 , 4601	Cu(OAc) ₂ (30 mol %)	8-aminoquinoline benzamide with morpholine	Pyridine	Pyridine	No	6 h	80-110°C	92
3	<i>Angew. Chem. Int. Ed.</i> , 2016, 55 , 1519–1522	Bu ₄ N[Fe(CO) ₃ (NO)] (TBA[Fe]) (5 mol%)	α-azidobiaryls and (azidoaryl)alkenes	microwave irradiation (200 W, 1008C)	1,2-dichloroethane	No	68 h	100°C	79
4	<i>ACS Catal.</i> , 2016, 6 , 2341–2351	Cu(OAc) ₂ (20 mol%), 1,10-phenanthroline	ortho-alkynylanilines to react with oxadiazoles	K ₂ CO ₃	Toluene	No	10 h	120°C	85
5	<i>Org. Lett.</i> , 2016, 18 , 1318–1321	Co(OAc) ₂ ·4H ₂ O, AgTFA,	2-benzamidopyridine 1-oxide (1a) and morpholine	NaOAc	p-xylene	No	12 h	120°C	82
6	<i>Adv. Synth. Catal.</i> , 2015, 357 , 3868–3874	I ₂ (2.5), FeCl ₃ ·6H ₂ O (10),	Chalcone and N-phenylbenzimidamide	1,10-phen (ligand)	1,2-DCB	No	24 h	120°C	92
7	<i>ACS Catal.</i> , 2015, 5 , 7008–7014	Cu(MeCN) ₄ BF ₄ , (10 mol%)	carbocyclic arenes followed by diaryl-λ ₃ -iodanes	-	MeCN/DMSO, 1:4	No	40 h	40 °C	68
8	<i>Angew. Chem. Int. Ed.</i> , 2015, 54 , 11809 – 11812	TiCl ₃ , HCL	o-nitrostyrenes	-	Acetone	No	8 h	R. T.	90
9	<i>Org. Lett.</i> , 2015, 17 , 2748–2751	(PhSe) ₂	ortho-vinyl anilines and vinylated aminopyridines	4 Å molecular Sieves	Toluene	No	16 h	100°C	71
10	<i>Org. Lett.</i> , 2015, 17 , 2482–2485	Ni(OAc) ₂	8-aminoquinoline benzamide and morpholine	Ag ₂ CO ₃ , N ₂ , Na ₂ CO ₃	Toluene	No	10 h	140°C	66
11	<i>J. Am. Chem. Soc.</i> , 2015, 137 , 4924–4927	NiI ₂ (10 mol %), Cu(acac) ₂ (20 mol %),	N-(quinolin-8-yl)benzamide	THAB (1.0 equiv), O ₂ (1 atm), Li ₂ CO ₃ (0.4 equiv),	DMF	No	24 h	160°C	85
12	<i>Angew. Chem. Int. Ed.</i> , 2014, 53 , 9884–9888	Pd(OAc) ₂ (0.05 equiv),	phenylpropylamine	PhI(OAc) ₂ (2 equiv), Ar	toluene or (HFIP)	No	24 h	100°C	83
13	<i>Chem. Sci.</i> , 2014, 5 , 2422-2427	3 mol % [Co(Por)]	aldehyde (0.2 M) and 1.2 equiv. of azide	4 Å MS	PhCl	No	24 h	80°C	77
14	<i>Chem. Eur. J.</i> , 2014, 20 , 4474–4480	[RhCl ₂ (Cp*)] ₂ (3 mol %),	benzoic acids with N-chlorocarbamates/N-chloromorpholines	AgOAc (1.5), N ₂ Atmosphere	DCE	No	12 h	60°C	86
15	<i>Journal of Catalysis</i> , 2014, 320 , 9–15	Cu(BTC)	N-benzoyl-8-aminoquinoline, morpholine	AgOAc (25 mol%), NMO (2 equiv., 117 mg)	NMP	No	6 h	90°C	65
16	<i>J. Am. Chem. Soc.</i> , 2014, 136 , 3354–3357	Cu(OAc) ₂	Benzamides with amines	Na ₂ CO ₃	DMSO	No	6h	80 °C	94

Table S4: Comparison of photocatalytic activity C(sp²)-H activation reaction over other reported photocatalytic systems:

Serial No.	Publication	Photocatalytic condition (Light Source)	Photocatalyst	Reagent used	Reaction Temperature and atm.	Base used	Solvent used	Reusability	Reaction time	Isolated Yield (Product %)
1	Present manuscript C(sp ²)-H activation)	60 W tungsten bulb	4:CuNPs(1/5 mol %)	Benzamides with Terminal alkynes/aryl amines	R.T./Aerial	K ₂ CO ₃	DMSO	Yes	4/6	78/86
2	<i>Angew. Chem. Int. Ed.</i> , 2016, 55 , 1–5	blue LEDs (450-500 nm)	CuI, Me ₂ NCH ₂ COOH	Azole and aryl halide	R.T./N ₂ atm.	LiOtBu	Et ₂ O	No	16 h	80
3	<i>Chem. Eur. J.</i> , 2016, 22 , 2236–2242	1.5 W blue LED	Pd(TFA) ₂ (0.01 mmol), and 9-mesityl-10-methylacridinium perchlorate (PC-A, Photoredox catalyst)	Azobenzene (36.4 mg, 0.20 mmol), 2-oxo-2-phenylacetic Acid	R.T./Aerial	-	Toluene	No	16 h	84-52

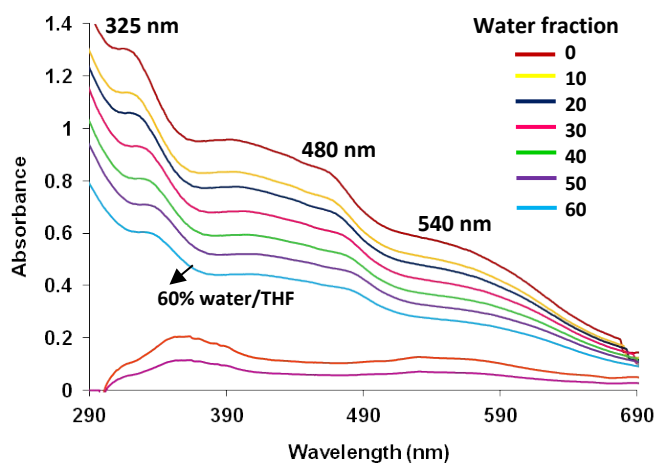


Fig. S1 Absorption spectra of derivative **3** (5 μM) showing the variation of absorption intensity in different H₂O/THF fractions.

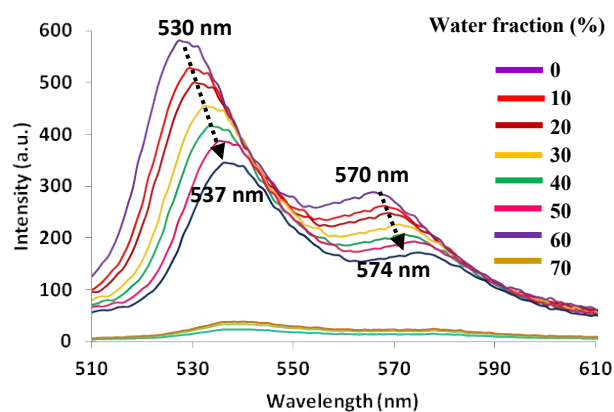


Fig. S2 Fluorescence spectrum of derivative **3** (5 μM) showing the variation of fluorescence intensity in H₂O/THF mixtures; $\lambda_{\text{ex}} = 485$ nm.

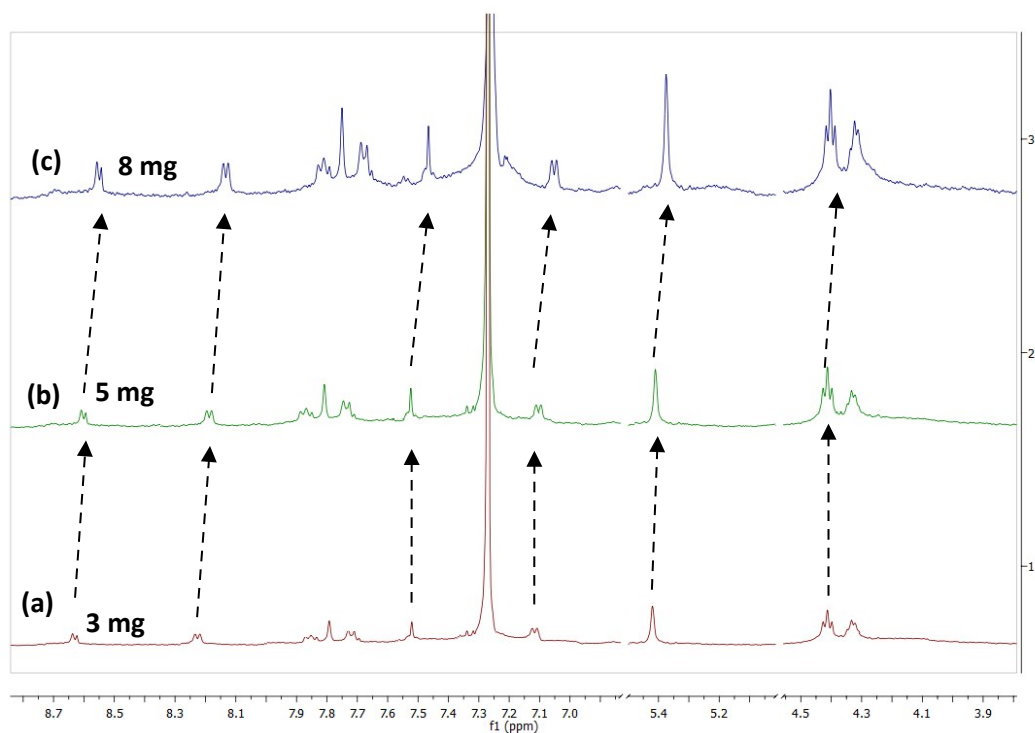


Fig. S3 Concentration dependent ¹H NMR spectrum of compound **3**, (a) 3 mg (b) 5 mg and (c) 8 mg each in 0.6 ml CDCl₃. NMR frequency 300 MHz.

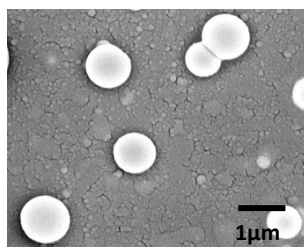


Fig. S4 SEM image of derivative **3** showing the formation of spherical aggregates (H₂O/THF, 6:4, v/v). Scale bar 1 μm.

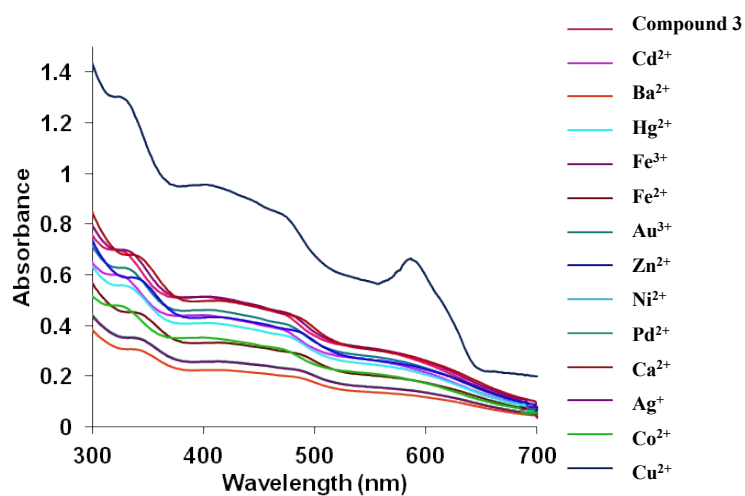


Fig. S5A UV-vis spectra of derivative **3** (5 μM) upon additions of 30 equiv. of various metal ions as their chloride salt in H₂O/THF (6:4, v/v) mixture.

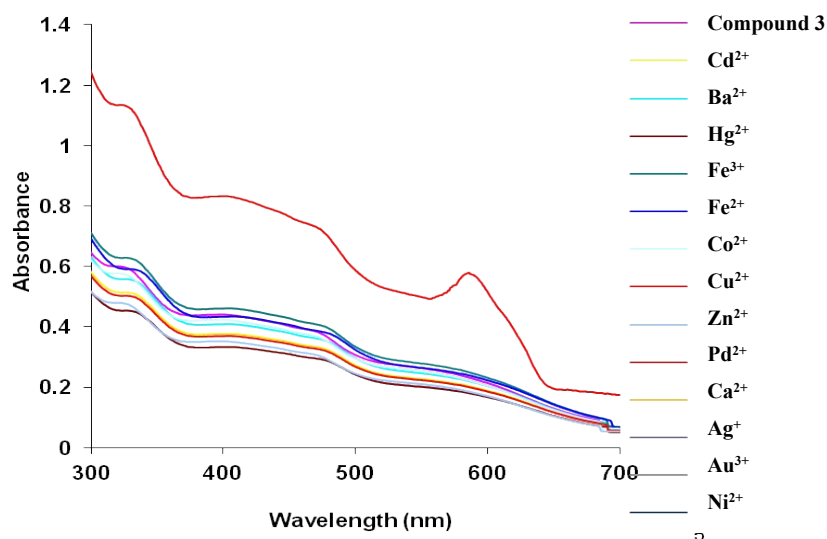


Fig. S5B UV-vis spectra of derivative **3** (5 μM) upon additions of 30 equiv. of various metal ions as their perchlorate salt in H₂O/THF (6:4, v/v) mixture.

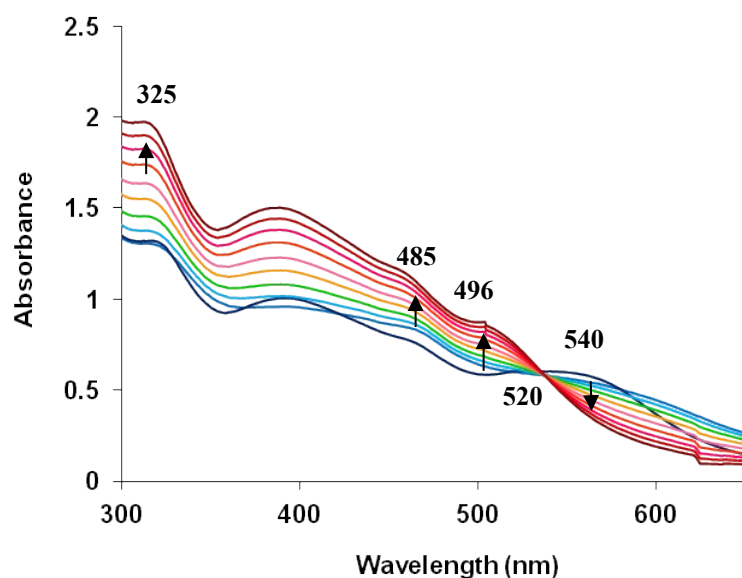


Fig. S6 UV-Vis spectra of compound **3** (5 μM) in pure THF showing the response in presence of Cu^{2+} ion (0-55 equiv.).

Compound	1 st red potential	2 nd red potential	1 st ox potential	2 nd ox potential
3	-0.14	-0.45	0.21	0.47

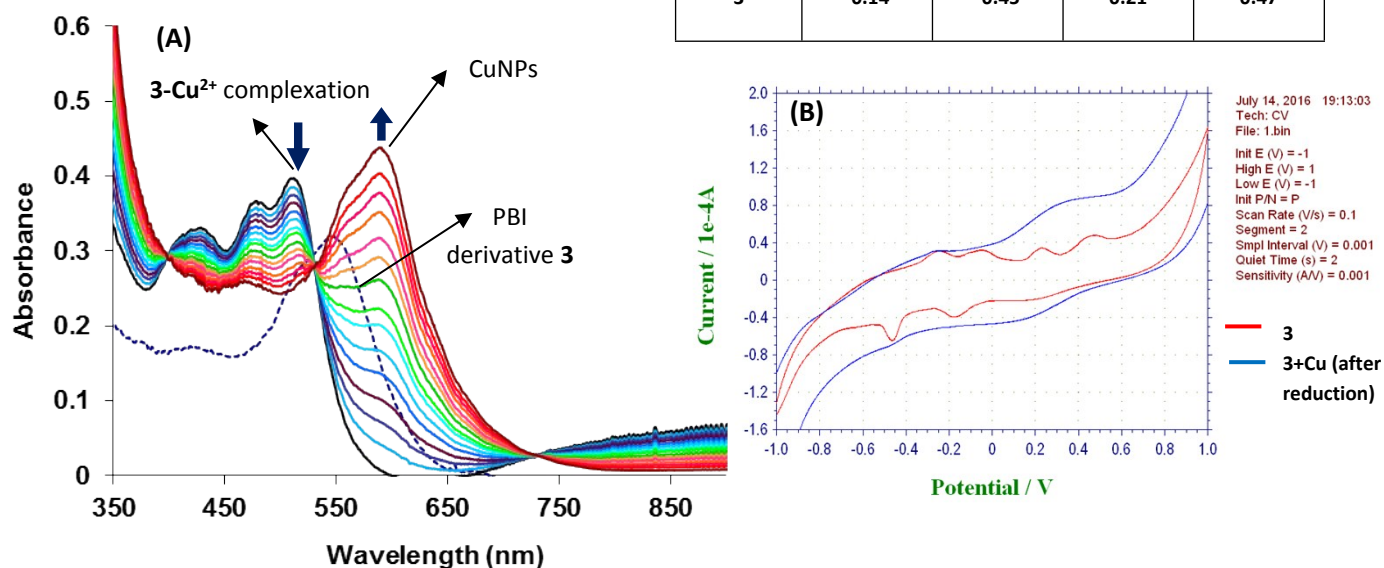


Fig. S7 (A) UV-vis spectroelectrochemical studies of PBI derivative **3** in $\text{H}_2\text{O}:\text{CH}_3\text{CN}$ (1:9) containing 0.1 M TBAPF_6 (supporting electrolyte) and Ag/AgCl (reference electrode) showing the change in the electronic absorption spectra observed during application of controlled potential -0.45 eV; (B) Cyclic voltammogram of the electrochemical analysis of compound **3** with Cu^{2+} ions.

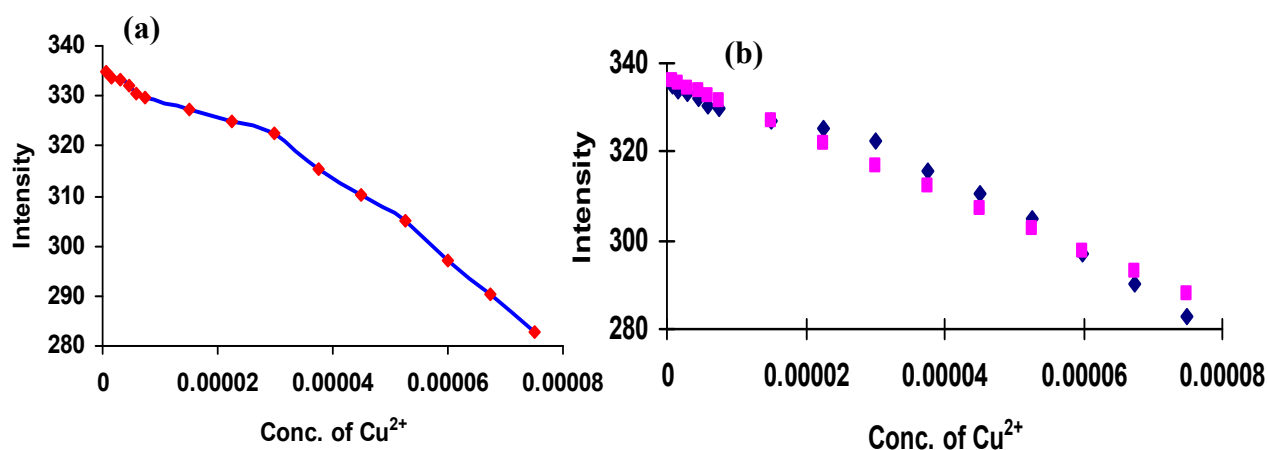


Fig. S8 (a) Showing the fluorescence intensity of compound **3** and (b) Calibrated curve showing the fluorescence intensity of compound **3** at 537 nm as a function of Cu²⁺ ions concentration (equiv.) in H₂O/THF (4:6, v/v) buffered with HEPES, pH = 7.05, λ_{ex} = 485nm.

Multiple R = 0.986075,

R² = 0.972344,

Standard deviation = 0.008,

Observation = 10,

Intercept = 336.4618,

Slope = 647167

The detection limit was calculated based on the fluorescence titration. To determine the S/N ratio, the emission intensity of receptor **3** without Cu²⁺ was measured by 10 times and the standard deviation of blank measurements was determined. The detection limit is then calculated with the following equation:

$$DL = 3 \times SD/S$$

Where SD is the standard deviation of the blank solution measured by 10 times; S is the slope of the calibration curve.

From the graph we get slope

S = **647167**, and SD value is 0.008

Thus using the formula we get the Detection Limit (**DL**) = **3 × 0.008/647167 = 3.7 × 10⁻⁸ M = 37 nM**

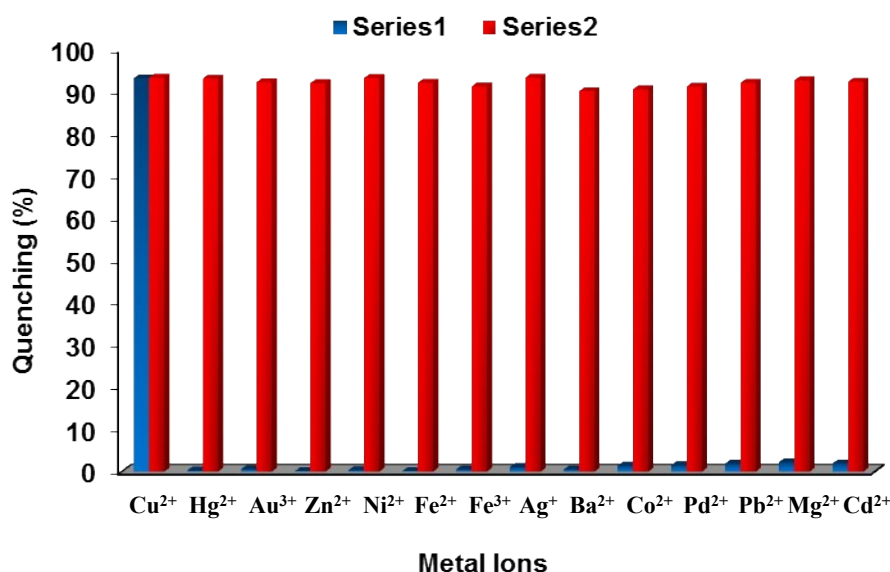


Fig. S9A Fluorescence response of **3** (5.0 μM) to various metal ions of **chloride salts** (30 equiv.) in H₂O/THF (6:4, v/v) mixture buffered with HEPES; pH = 7.05; λ_{ex} = 485 nm. Bars represent the emission intensity ratio (I₀-I)/I₀×100 (I₀ and I are the initial and final fluorescence intensity at 537 nm before and after the addition of metal ions). (Series 1) Sky blue bars represent selectivity of **3** upon addition of different metal ions. (Series 2) Red bars represent competitive selectivity of derivative **3** toward Cu²⁺ ions (30 equiv.) in the presence of other metal ions (60 equiv.).

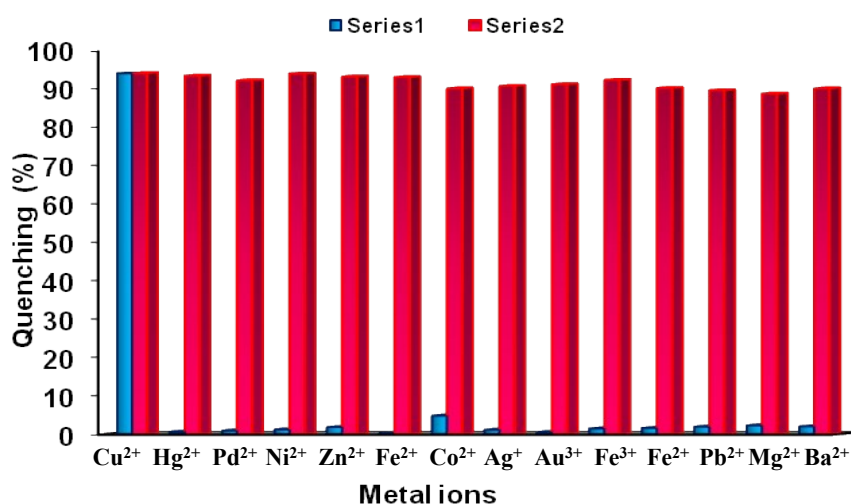


Fig. S9B Fluorescence response of **3** (5.0 μM) to various metal ions of **perchlorate salts** (30 equiv.) in H₂O/THF (6:4, v/v) mixture buffered with HEPES; pH = 7.05; λ_{ex} = 485 nm. Bars represent the emission intensity ratio (I₀-I)/I₀×100 (I₀ and I are the initial and final fluorescence intensity at 537 nm before and after the addition of metal ions). (Series 1) Sky blue bars represent selectivity of **3** upon addition of different metal ions. (Series 2) pink bars represent competitive selectivity of derivative **3** toward Cu²⁺ ions (30 equiv.) in the presence of other metal ions (60 equiv.).

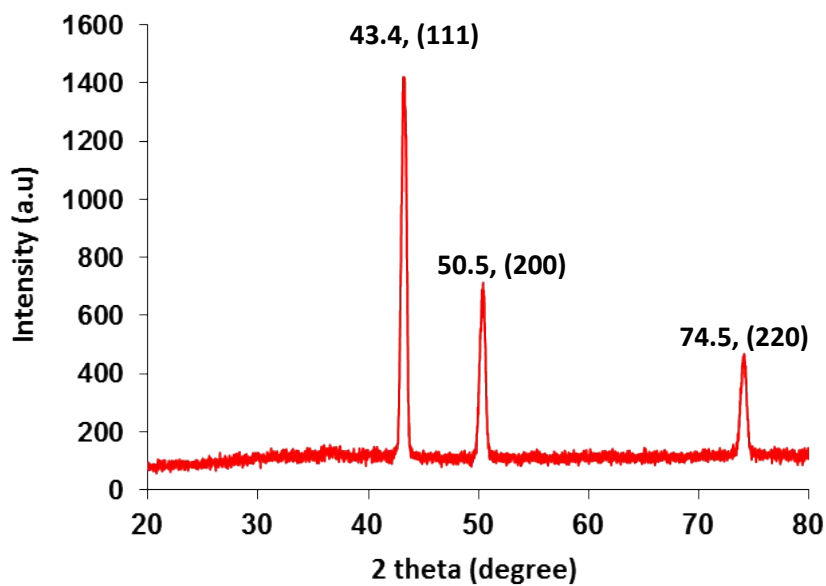


Fig. S10 Representative XRD diffraction patterns of CuNPs prepared by derivative **3**.

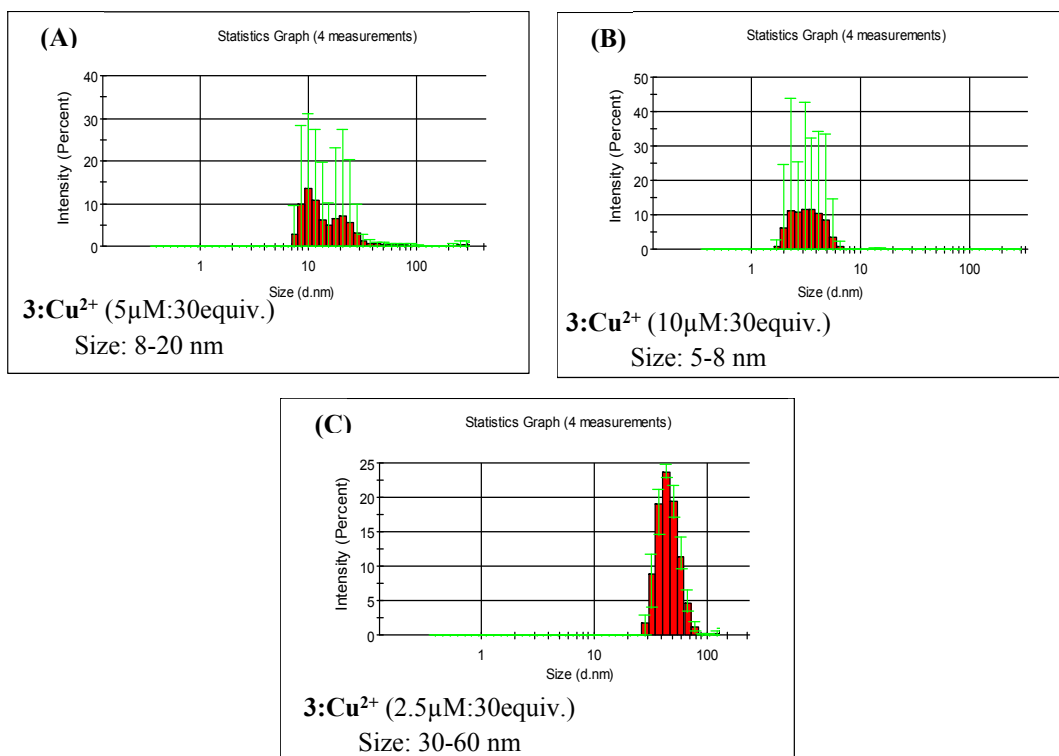


Fig. S11 DLS studies showed the variation in particle size of CuNPs by mixing aggregates of derivative **3** in H₂O/THF (6:4, v/v) and Cu²⁺ ions in different ratio.

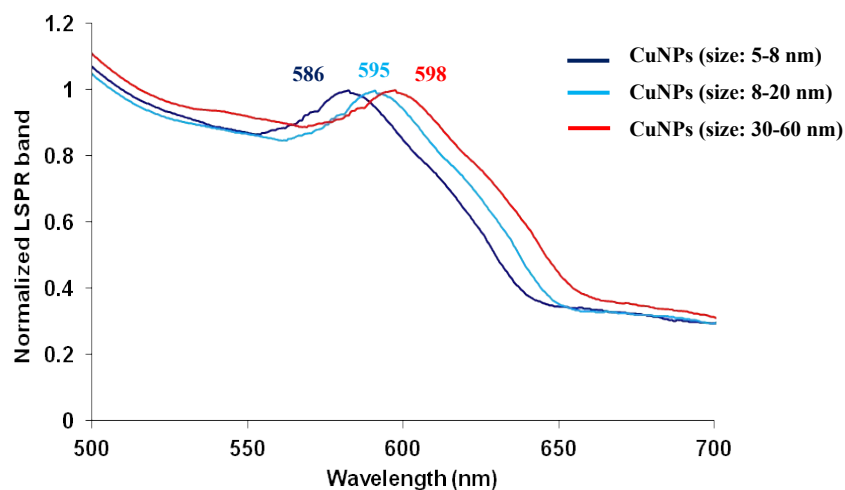


Fig. S12 Normalized UV-vis spectra showing the shifting of LSPR band of CuNPs by mixing aggregates of derivative **3** in H₂O/THF (6:4, v/v) and Cu²⁺ ions in different ratio.

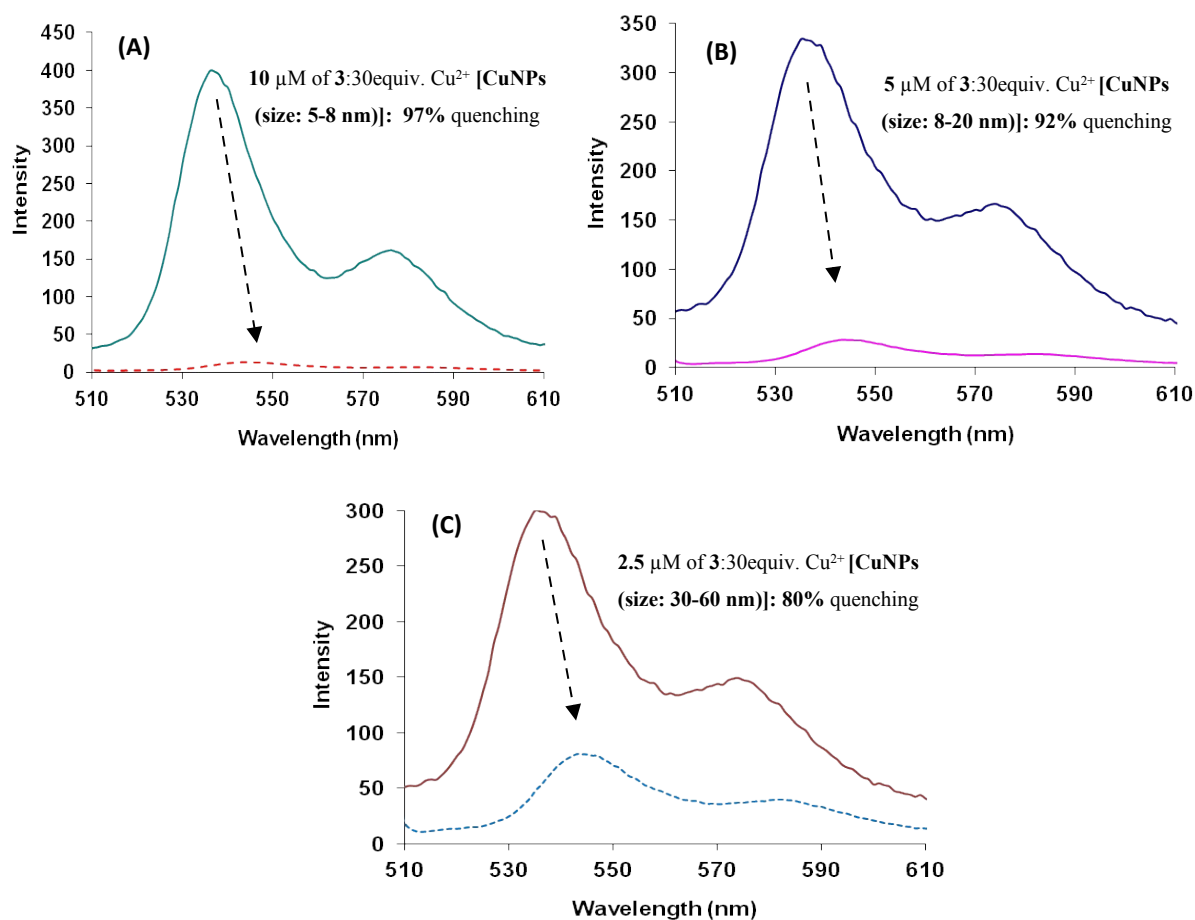


Fig. S13 Fluorescence studies showed the quenching in emission intensity with the variation in particle size of CuNPs by mixing aggregates of derivative **3** in H₂O/THF (6:4, v/v) and Cu²⁺ ions in different ratio: (A) 97% quenching: 10 μM of **3**:30 equiv. Cu²⁺, (B) 92% quenching: 5 μM of **3**:30 equiv. Cu²⁺; (C) 80% quenching: 2.5 μM of **3**:30 equiv. Cu²⁺

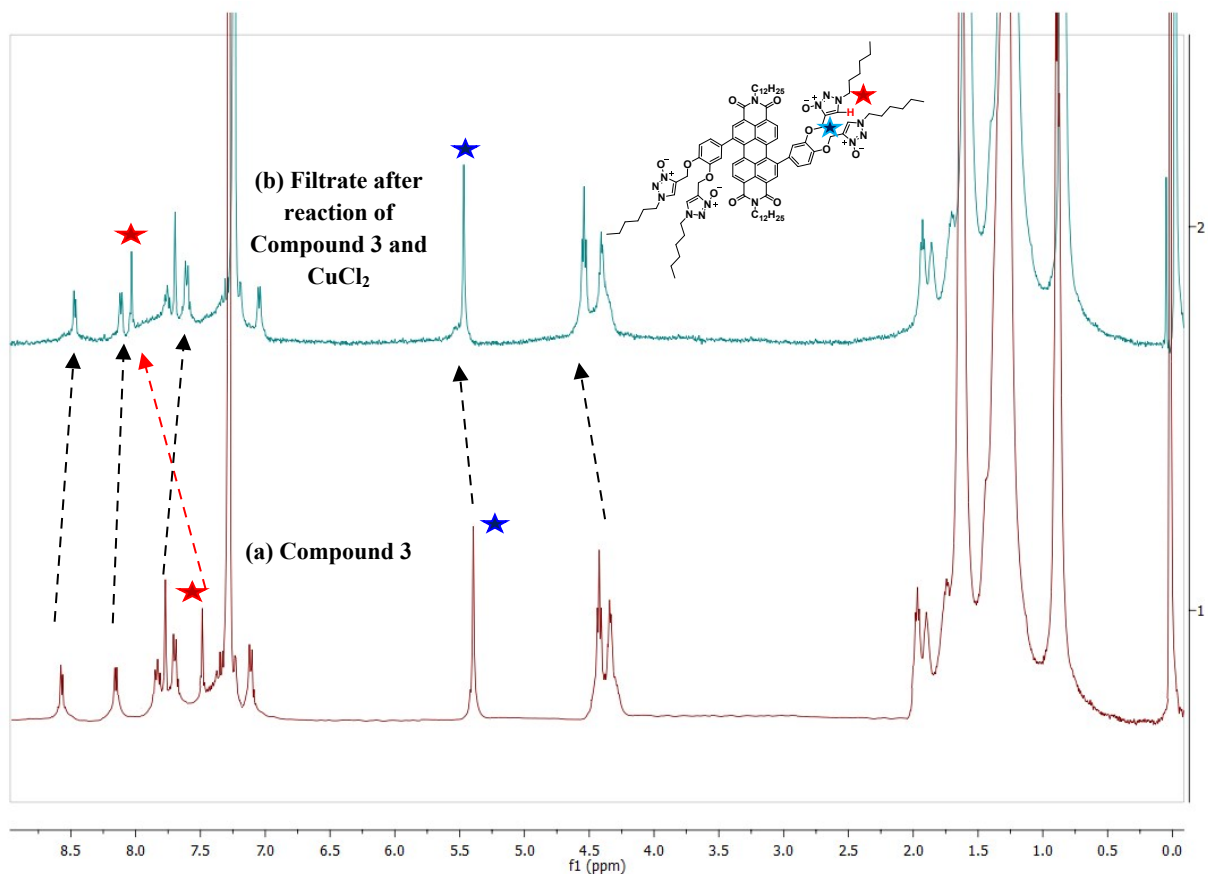


Fig. S14 Overlay ^1H NMR spectra of (a) compound **3** and (b) compound **3** + CuCl_2 after filtration with THF in CDCl_3 .

(a) Compound 3 (δ_1 , ppm)	(b) Compound 3 + Cu^{2+} , after filtration by THF (δ_2 , ppm)	$\Delta\delta = \delta_1 - \delta_2$
8.55 (d, aromatic)	8.48	0.07
8.13 (d, aromatic)	8.08	0.05
7.81 (t, aromatic)	7.76	0.05
7.75 (s, aromatic)	7.70	0.05
7.68 (t, aromatic)	7.62	0.06
★ 7.47 (s, Triazole C-H)	★ 8.06	-0.59 (downfield)
7.06 (d, aromatic)	7.02	0.04
★ 5.38 (s, O- CH_2 -)	★ 5.44	-0.06 (downfield)
4.40 (t, triazole-N- CH_2 -)	4.44	-0.04 (downfield)

Table S5: Change in chemical shift (δ) value of ^1H NMR spectra of derivative **3** in CDCl_3 and oxidized species of derivative **3** after reaction of derivative **3** and CuCl_2 .

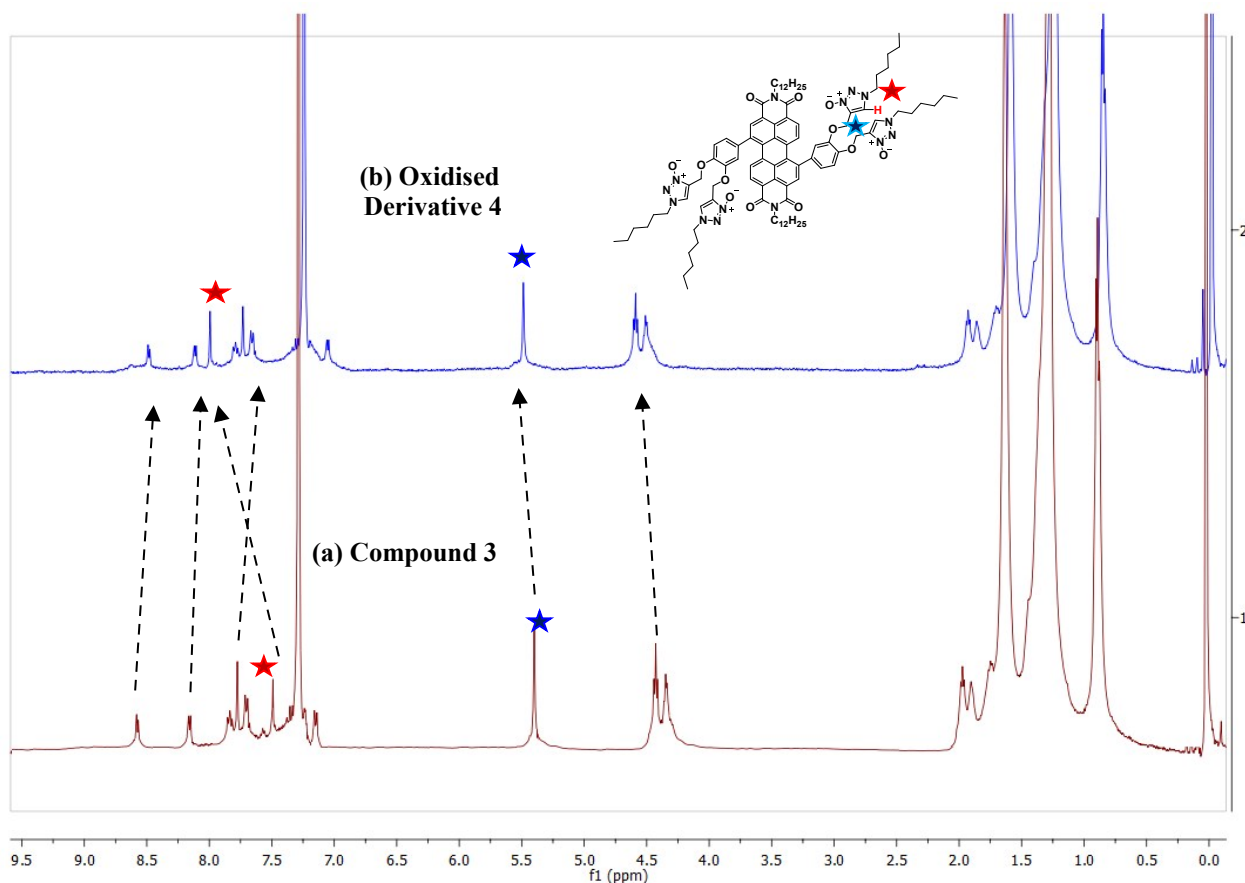


Fig. S15 Overlay ¹H NMR spectra of (a) compound **3** and (b) Oxidised derivative **4** in CDCl₃.

(a) Compound 3 (δ_1 , ppm)	(b) Oxidised derivative 4 (δ_2 , ppm)	$\Delta\delta = \delta_1 - \delta_2$
8.55 (d, aromatic)	8.46	0.09
8.13 (d, aromatic)	8.07	0.06
7.81 (t, aromatic)	7.75	0.06
7.75 (s, aromatic)	7.68	0.07
7.68 (t, aromatic)	7.60	0.08
★ 7.47 (s, Triazole C-H)	★ 8.08	-0.61 (downfield)
7.06 (d, aromatic)	7.00	0.06
★ 5.38 (s, O-CH ₂ -)	★ 5.45	-0.07 (downfield)
4.40 (t, triazole-N-CH ₂ -)	4.46	-0.06 (downfield)

Table S6: Change in chemical shift (δ) value of ¹H NMR spectra of derivative **3** in CDCl₃ and Oxidised species **4**.

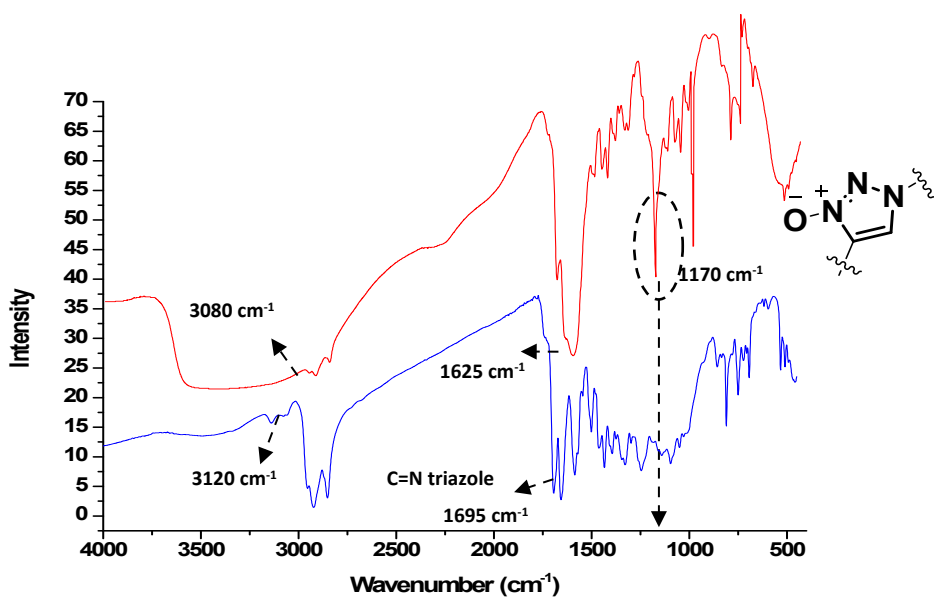


Fig. S16 FT-IR spectrum of oxidized species **4** showed stretching band at around 1170 cm^{-1} corresponding to $\text{N}^+\text{-O}^-$ stretching frequency.

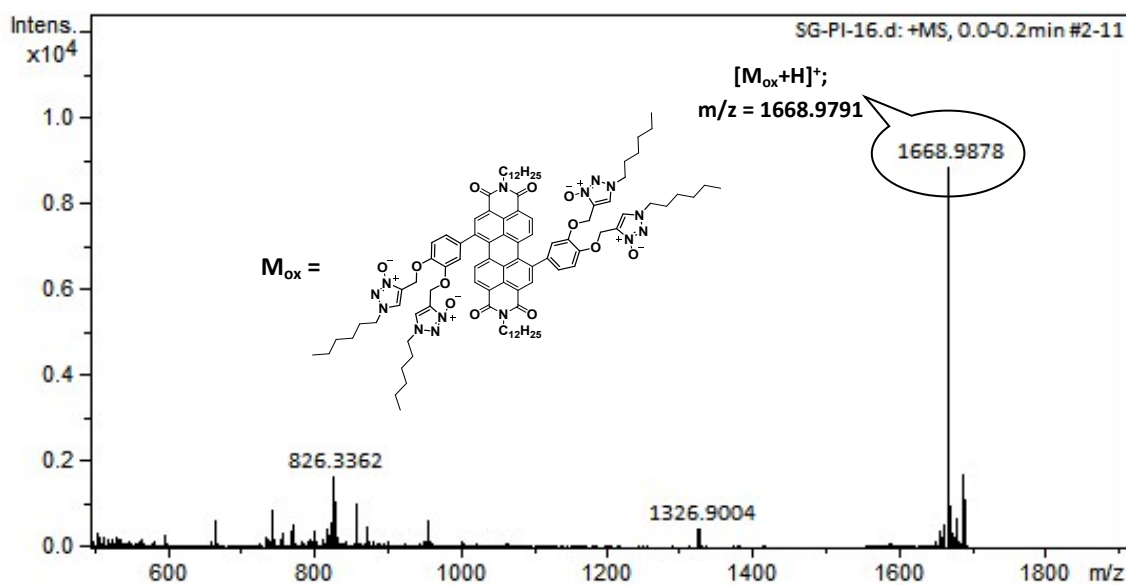


Fig. S17 ESI-MS mass spectrum of residue obtained showed a parent ion peak, $m/z = 1668.98$ of oxidized species **4**.

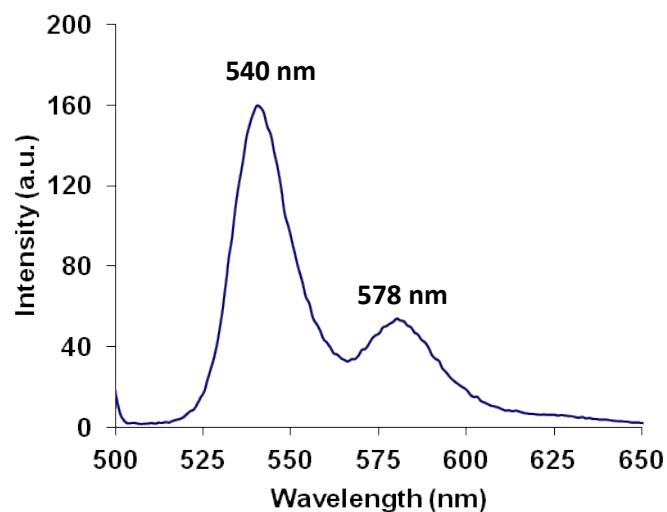


Fig. S18 Fluorescence spectrum of oxidized species **4** ($5\mu\text{M}$) in $\text{H}_2\text{O}/\text{THF}$ (6:4, v/v) mixture.

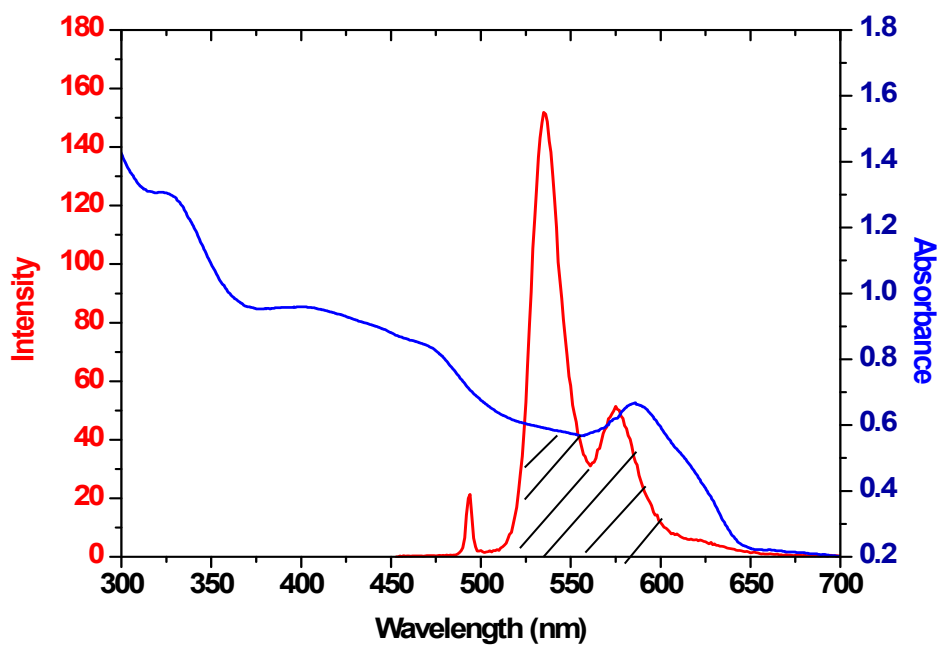


Fig. S19 Spectral overlap of emission spectrum of oxidized species **4** and absorption spectrum of CuNPs.

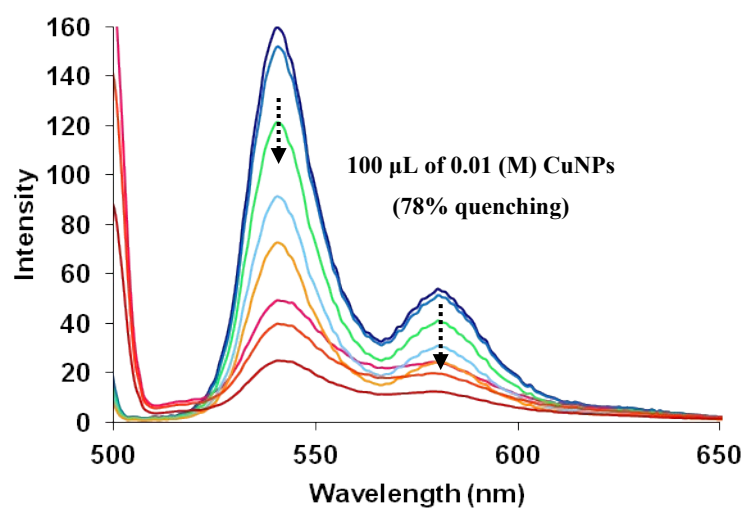


Fig. S20 Fluorescence spectrum of oxidized species **4** (5 μM) in H₂O/THF (6:4, v/v) mixture upon gradual addition of CuNPs up to 100 μL of 0.01 (M).

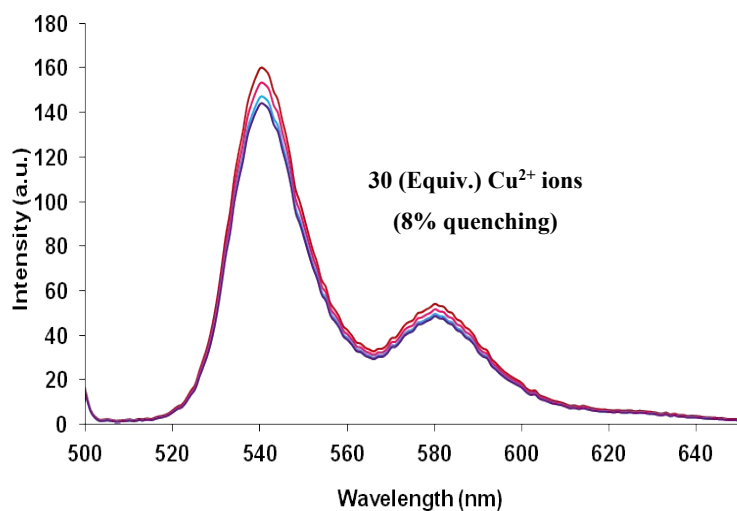


Fig. S21 Fluorescence spectrum of oxidized species **4** (5 μM) in H₂O/THF (6:4, v/v) in presence of 30 (Equiv.) Cu²⁺ ions.

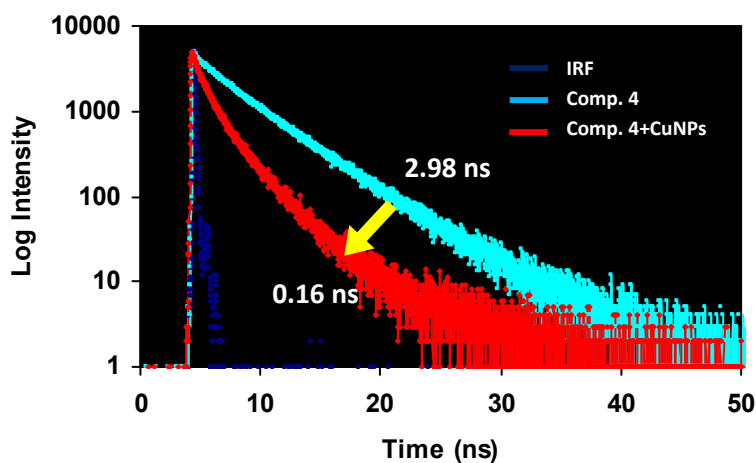


Fig. S22 Exponential fluorescence decays of oxidised species **4** on addition of CuNPs measured at 540 nm. Spectra were acquired in H₂O/THF (6:4, v/v) mixture buffered with HEPES; pH = 7.05; $\lambda_{\text{ex}} = 486$ nm.

Entry	Quantum Yield	A ₁ /A ₂	Life time (ns)			k_f (10 ⁹ S ⁻¹)	k_{nr} (10 ⁹ S ⁻¹)
			τ_1	τ_2	τ_{avg}		
Oxidized species 4 (4:6, THF/Water)	0.21	40/60	0.95	3.96	2.98	0.070	0.265
Oxidized species 4 + CuNPs	0.06	10/90	0.71	1.26	0.16	0.37	5.87

Table S7 Fluorescence lifetime of oxidised species **4** in H₂O/THF (6:4, v/v) and in the presence of CuNPs for the emission at 540 nm. A₁, A₂: fractional amount of molecules in each environment. τ_1 , τ_2 and τ_{avg} : mono, bi-exponential and average life time of aggregates in 60 vol% of water in THF; k_f : radiative rate constant ($k_f = \Phi_f/\tau_{avg}$); k_{nr} : non-radiative rate constant ($k_{nr} = (1 - \Phi_f)/\tau_{avg}$); $\lambda_{\text{ex}} = 486$ nm.

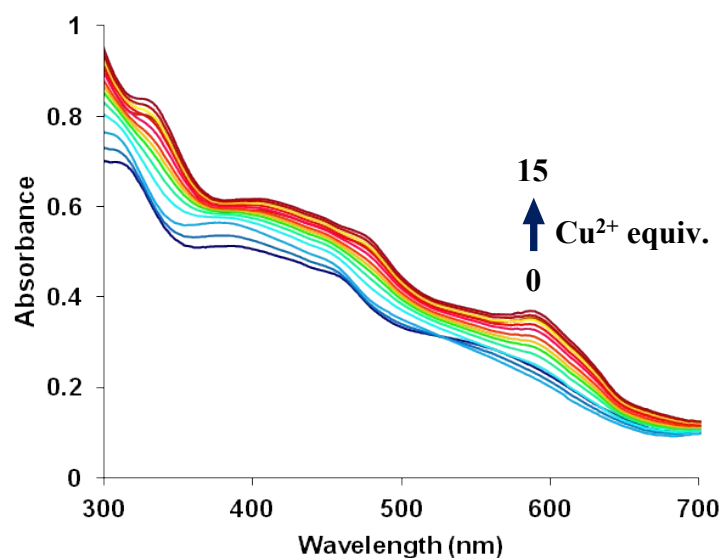


Fig. S23: UV-Vis spectra of compound **3** (5 μM) showing the response to the Cu^{2+} ion (0-15 equiv.) in $\text{H}_2\text{O}/\text{THF}$ (6:4, v/v) mixture.

Table S8: Catalytic efficiency of supramolecular ensemble **4**:CuNPs for photocatalytic C(sp²)-H alkylation reaction of oxazoline substituted benzamide (**5**) with phenylacetylene (**6a**).

Entry	CuNPs (ppm)	Time (hours)	Yield (%)	TON	TOF (h ⁻¹)
1	10000 (1 mol%)	8	72	7.2	0.9
2	5000 (0.5 mol%)	10	68	13.6	1.36
3	1000 (0.1 mol%)	10	65	65	6.5
4	100 (0.01 mol%)	15	60	600	40
5	10 (0.001 mol%)	20	50	5000	250
6	0 mol%	24	0	0	0

Analyst
Date Started 15:45 31-03-2016 GMT: 10:15 31-03-2016
Worksheet Sandeep31032016
Comment
Methods Cu
Computer name HP-PC
Serial Number:

Method: Cu (Flame)

Sample ID	Conc mg/L	%RSD	SD	Mean Abs		
CAL ZERO	0.000	7.8	0.0001	0.0012		
	Readings					
	0.0011	0.0011	0.0013		31-03-2016	15:48:50
	ISF					
	1.0000					
STANDARD 1	1.000	1.2	0.0008	0.0711		
	Readings					
	0.0703	0.0712	0.0719		31-03-2016	15:49:22
	ISF					
	1.0000					
STANDARD 2	3.000	0.6	0.0013	0.2223		
	Readings					
	0.2239	0.2219	0.2213		31-03-2016	15:49:54
	ISF					
	1.0000					
STANDARD 3	5.000	0.5	0.0019	0.3516		
	Readings					
	0.3494	0.3525	0.3529		31-03-2016	15:50:26
	ISF					
	1.0000					
Sample 001	0.558	1.6	0.0007	0.0400		
	Readings					
	0.0392	0.0404	0.0404		31-03-2016	15:57:20
	ISF					
	1.0000					

Fig. S24 Atomic absorption studies (AAS) of the residual liquid left after the recycling (4th cycle) of the catalyst [prepared by mixing aggregates of derivative **3** (5 μ M) and Cu²⁺ ions (30 equiv.)] and found that only 0.558 mg/lit = 0.558 ppm of copper leached into the solution after 4th catalytic cycle.

Table S9: Catalytic efficiency of supramolecular ensemble **4**:CuNPs prepared by mixing aggregates of derivative **3** (10 μ M) and Cu²⁺ ions (30 equiv.) for photocatalytic C-H alkynylation reaction of oxazoline substituted benzamide (**5**) with phenylacetylene (**6a**).

Entry	Supramolecular ensemble 4 :CuNPs (1 mol%)	Catalytic cycle	Time (hours)	Yield of 7a (%)
1	Prepared by mixing derivative 3 (10 μ M) and Cu ²⁺ ions (30 equiv.)	1 st	11	69
2	Prepared by mixing derivative 3 (10 μ M) and Cu ²⁺ ions (30 equiv.)	4 th	12	62

SpectrAA Report.

17:04 01-06-2016

Page 1 of 11

Analyst
 Date Started 16:11 31-05-2016 GMT: 10:41 31-05-2016
 Worksheet cu
 Comment
 Methods Cu
 Computer name HP-PC
 Serial Number:

Method: Cu (Flame)

Sample ID	Conc mg/L	%RSD	SD	Mean Abs	
CAL ZERO	0.000	23.8	0.0003	0.0011	
	Readings				
	0.0014	0.0010	0.0009	31-05-2016	16:32:26
	ISF				
	1.0000				
STANDARD 1	1.000	2.5	0.0008	0.0327	
	Readings				
	0.0329	0.0318	0.0334	31-05-2016	16:33:06
	ISF				
	1.0000				
STANDARD 2	3.000	1.5	0.0020	0.1398	
	Readings				
	0.1390	0.1382	0.1421	31-05-2016	16:33:44
	ISF				
	1.0000				
STANDARD 3	5.000	1.1	0.0024	0.2230	
	Readings				
	0.2240	0.2247	0.2202	31-05-2016	16:34:30
	ISF				
	1.0000				
Sample 001	0.114	9.6	0.0005	0.0050	
	Readings				
	0.0052	0.0053	0.0044	31-05-2016	16:55:42
	ISF				
	1.0000				

Fig. S25 Atomic absorption studies (AAS) of the residual liquid left after the recycling (4th cycle) of the catalyst [prepared by mixing aggregates of derivative **3** (10 μ M) and Cu²⁺ ions (30 equiv.)] and found that only 0.114 mg/lit = 0.114 ppm of copper leached into the solution after 4th catalytic cycle.

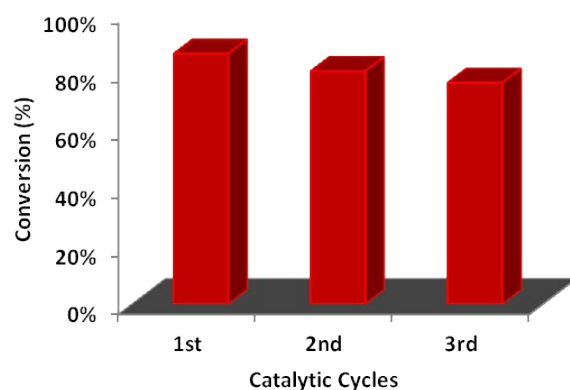


Fig.S26 Recyclability of supramolecular ensemble 4:CuNPs catalyst for C(sp²)-H amination reaction of oxazoline substituted benzamide (**5**) with *p*-nitro aniline (**9a**).

Table S10: Catalytic efficiency of supramolecular ensemble 4:CuNPs for photocatalytic C-H amination reaction of oxazoline substituted benzamide (**5**) with *p*-nitro aniline (**9a**).

Entry	CuNPs (ppm)	Time (hours)	Yield (%)	TON	TOF (h ⁻¹)
1	50000 (5 mol%)	4	86	1.72	0.43
2	10000 (1 mol%)	5	84	8.4	1.68
1	5000 (0.5 mol%)	7	75	15	2.14
2	1000 (0.1 mol%)	9	70	70	7.77
3	100 (0.01 mol%)	12	66	660	55
4	10 (0.001 mol%)	16	60	6000	375
5	0 mol%	24	0	0	0

^1H NMR spectrum of derivative **3** in CDCl_3

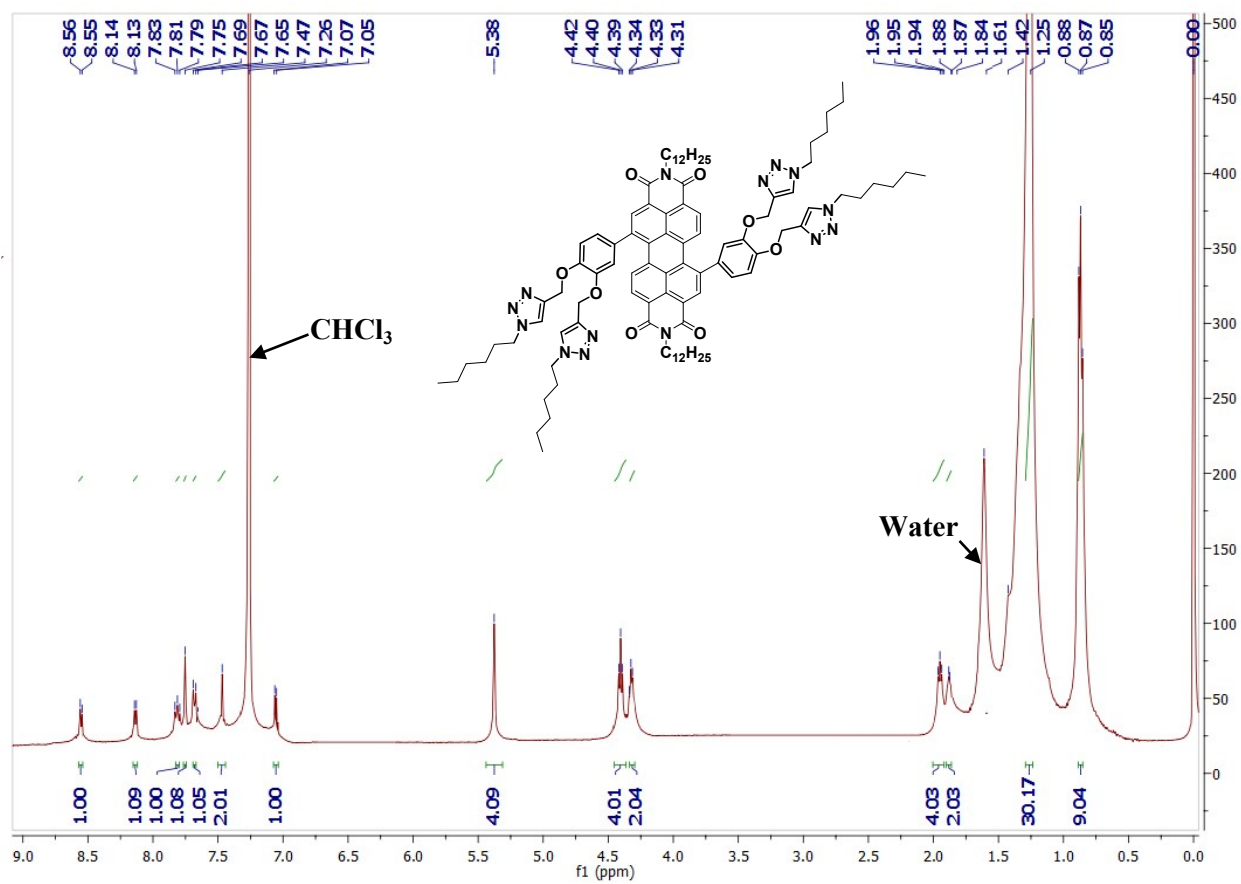


Fig. S27 ^1H NMR spectrum of derivative **3** in CDCl_3 .

^{13}C NMR spectrum of derivative **3** in CDCl_3

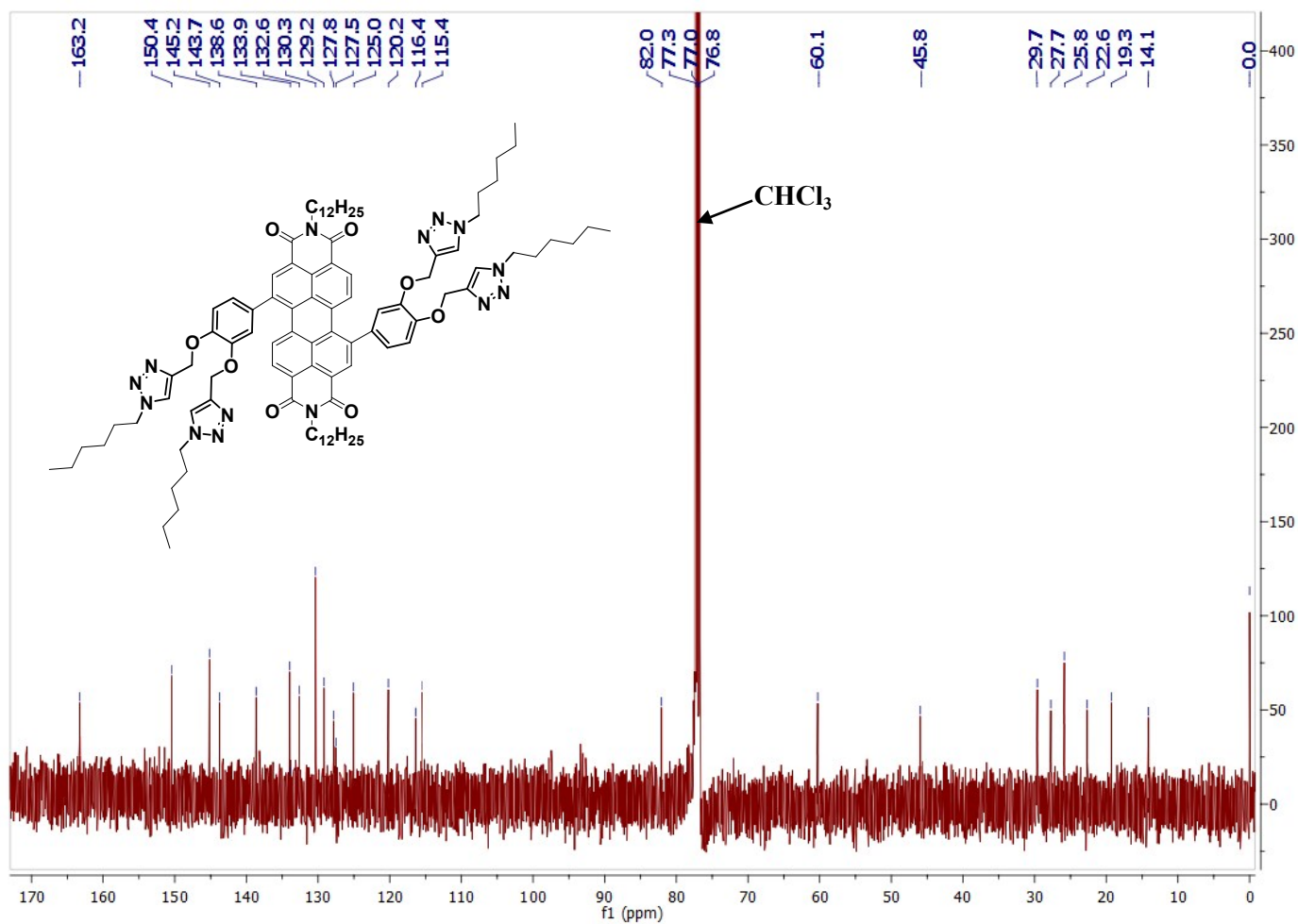


Fig. S28 ^{13}C NMR spectrum of derivative **3** in CDCl_3 .

MALDI-TOF analysis of derivative 3:

Applied Biosystems MDS Analytical Technologies TOF/TOF™ Series Explorer™ 72027

TOF/TOF™ Reflector Spec #1 MC[BP = 1604.0, 8875]

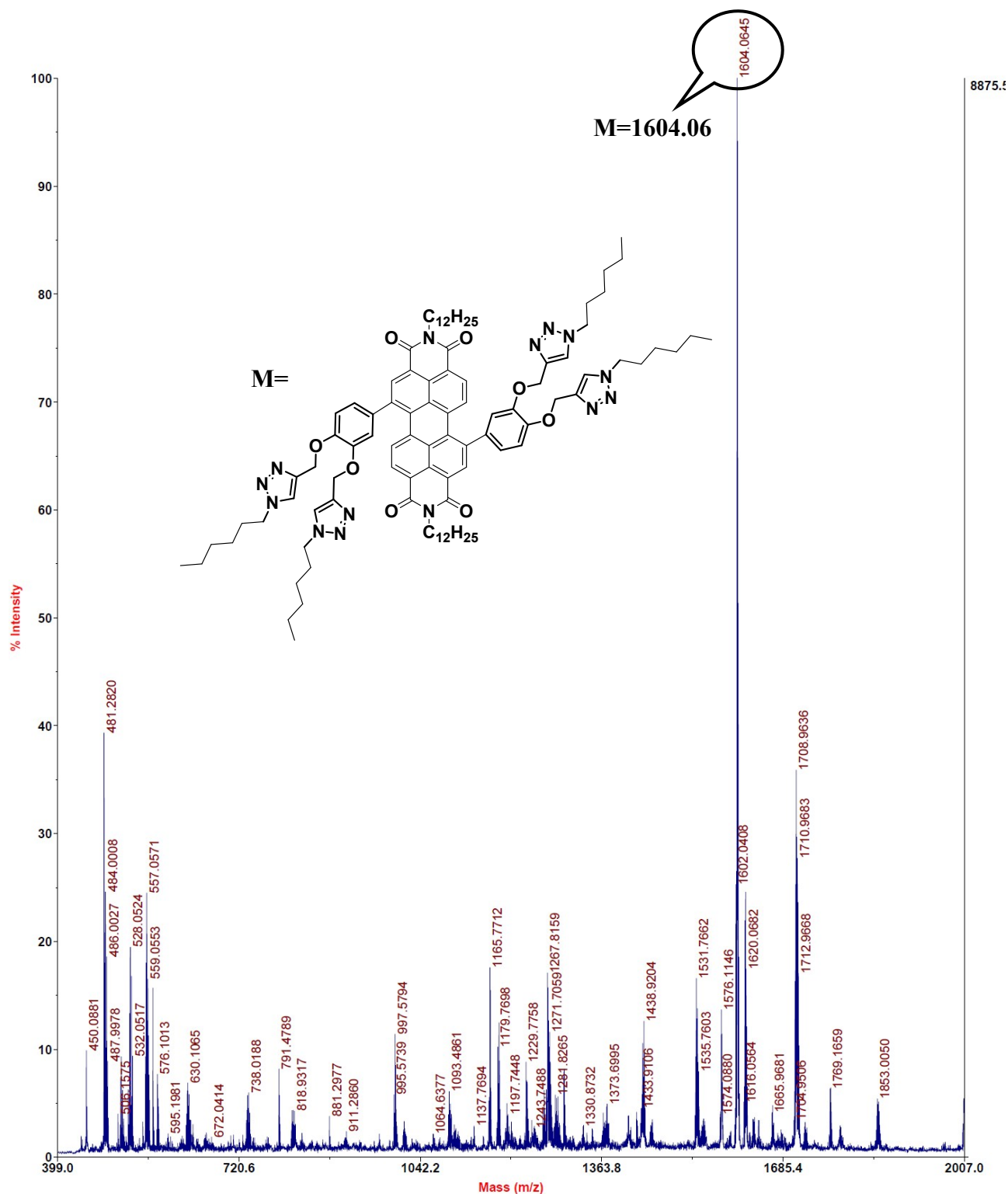


Fig. S29 MALDI-TOF analysis of derivative 3.

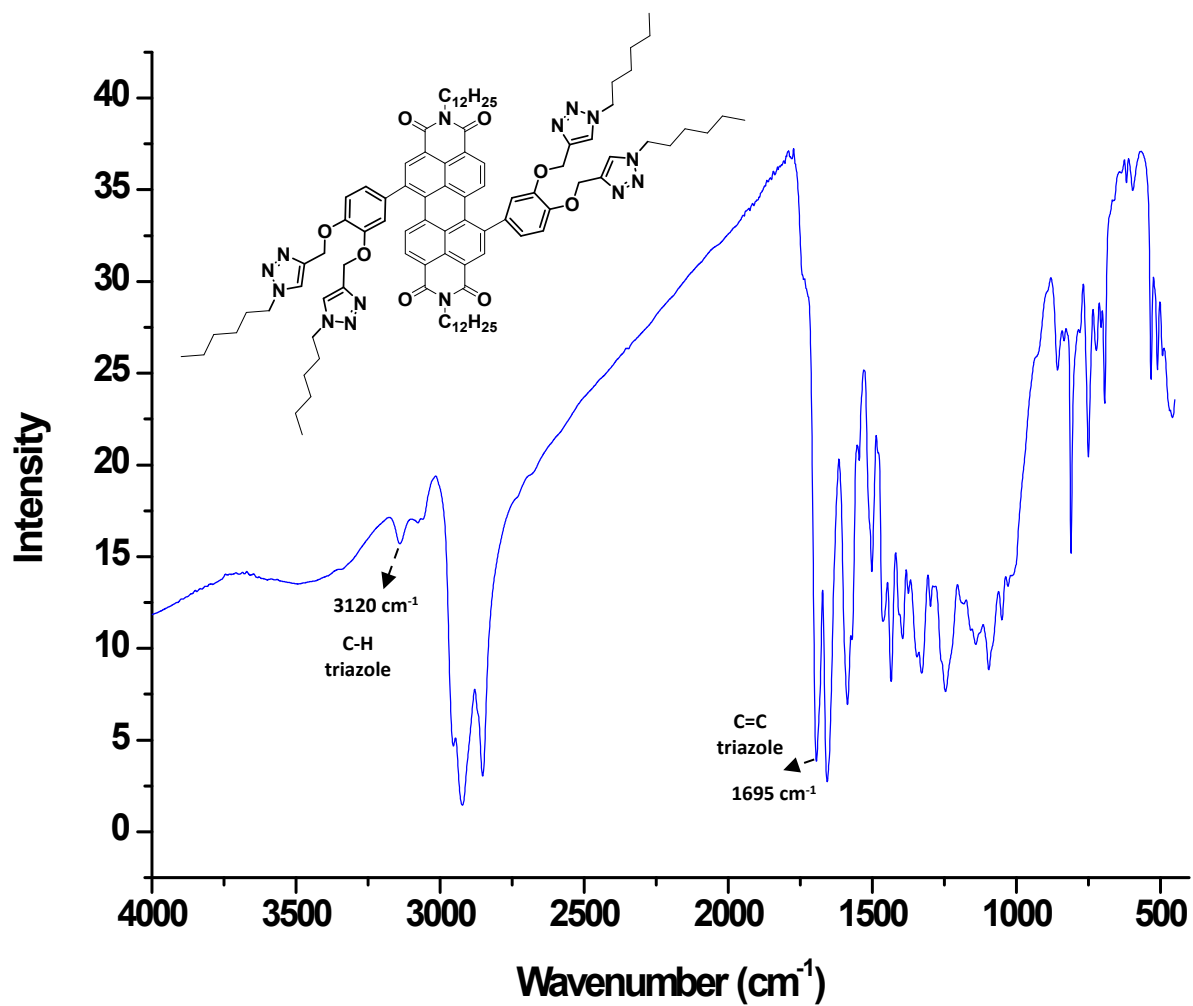


Fig. S30 FT-IR spectrum of derivative 3.

Fig. S31 ^1H NMR spectrum of derivative **7a** in CDCl_3

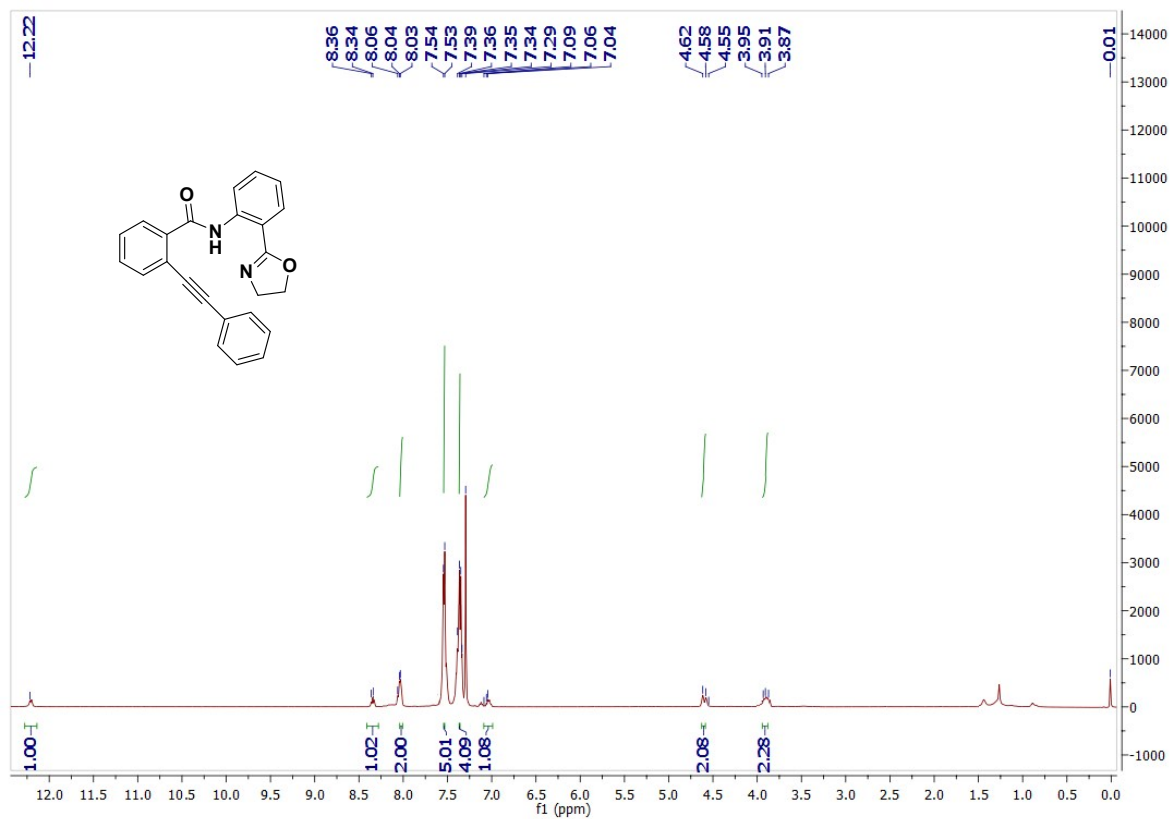


Fig. S32A ^1H NMR spectrum of derivative **7b** in CDCl_3

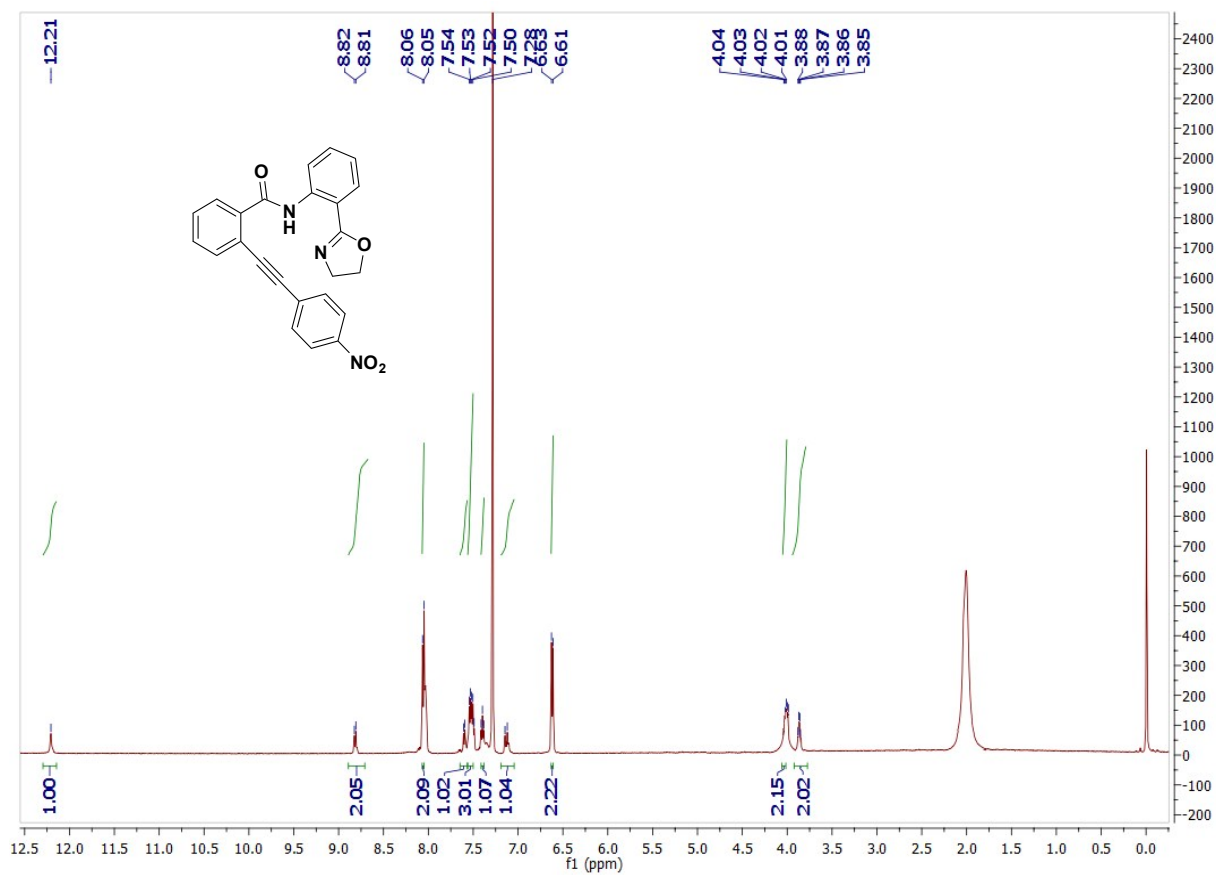


Fig. S32B ^{13}C NMR spectrum of derivative **7b** in CDCl_3

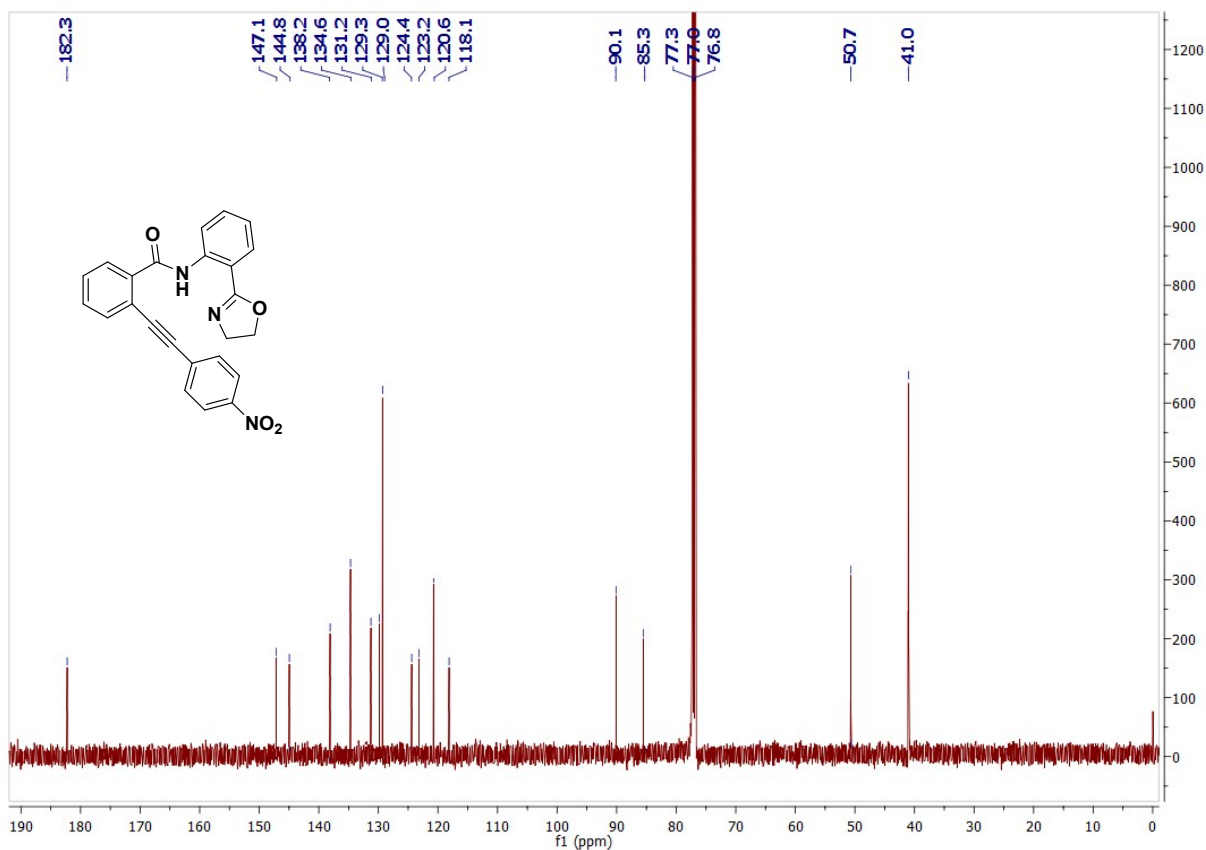


Fig. S32C ESI-MS spectrum of derivative **7b**

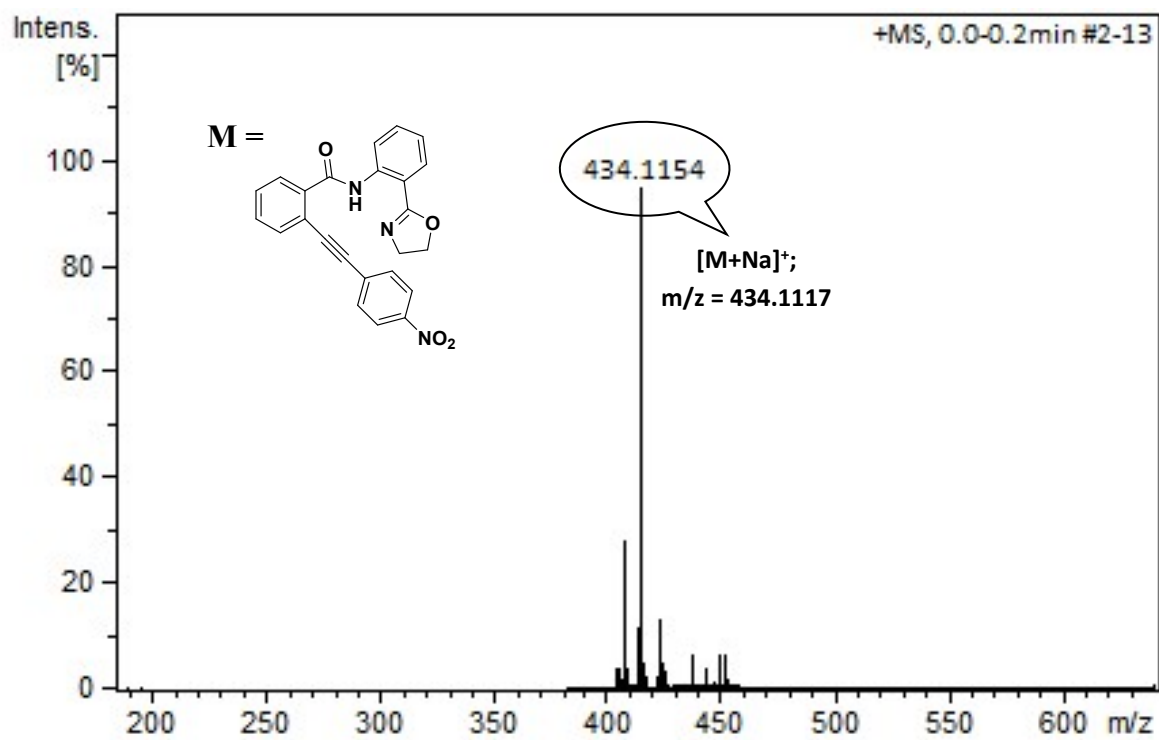


Fig. S33A ^1H NMR spectrum of derivative **7c** in CDCl_3

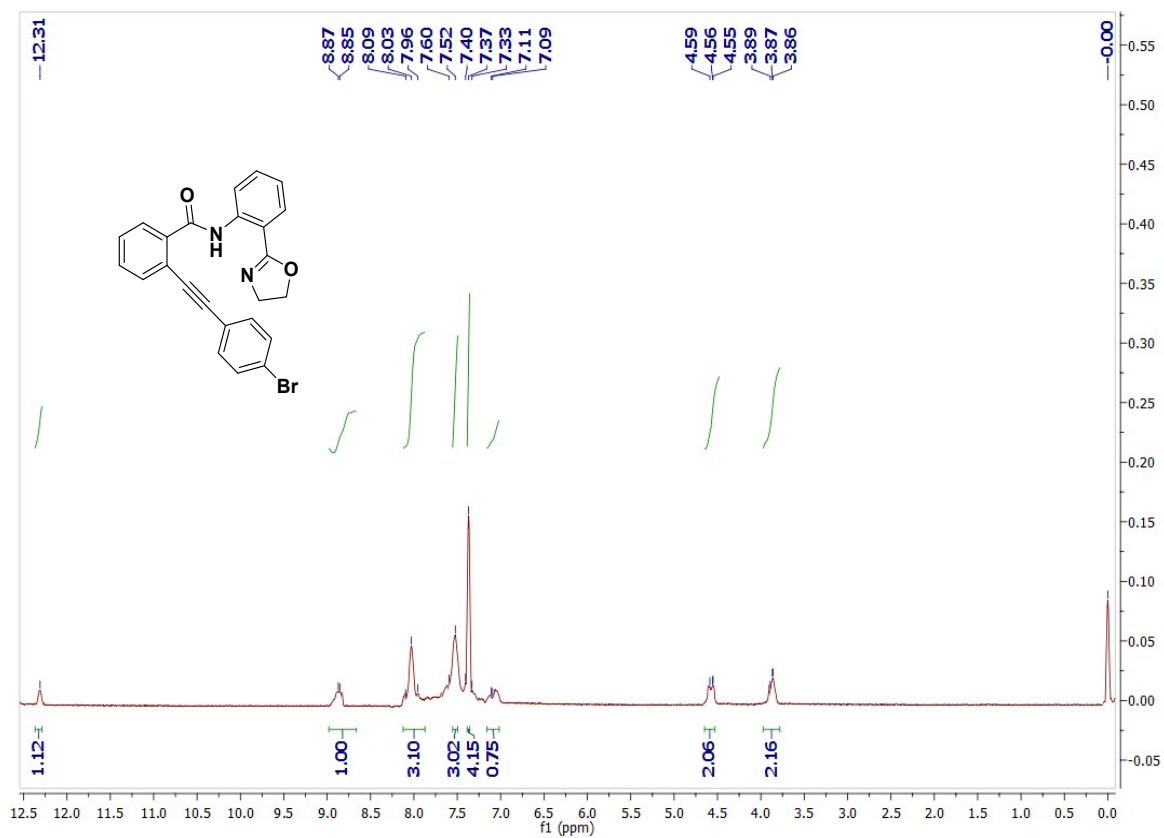


Fig. S33B ^{13}C NMR spectrum of derivative **7c** in CDCl_3

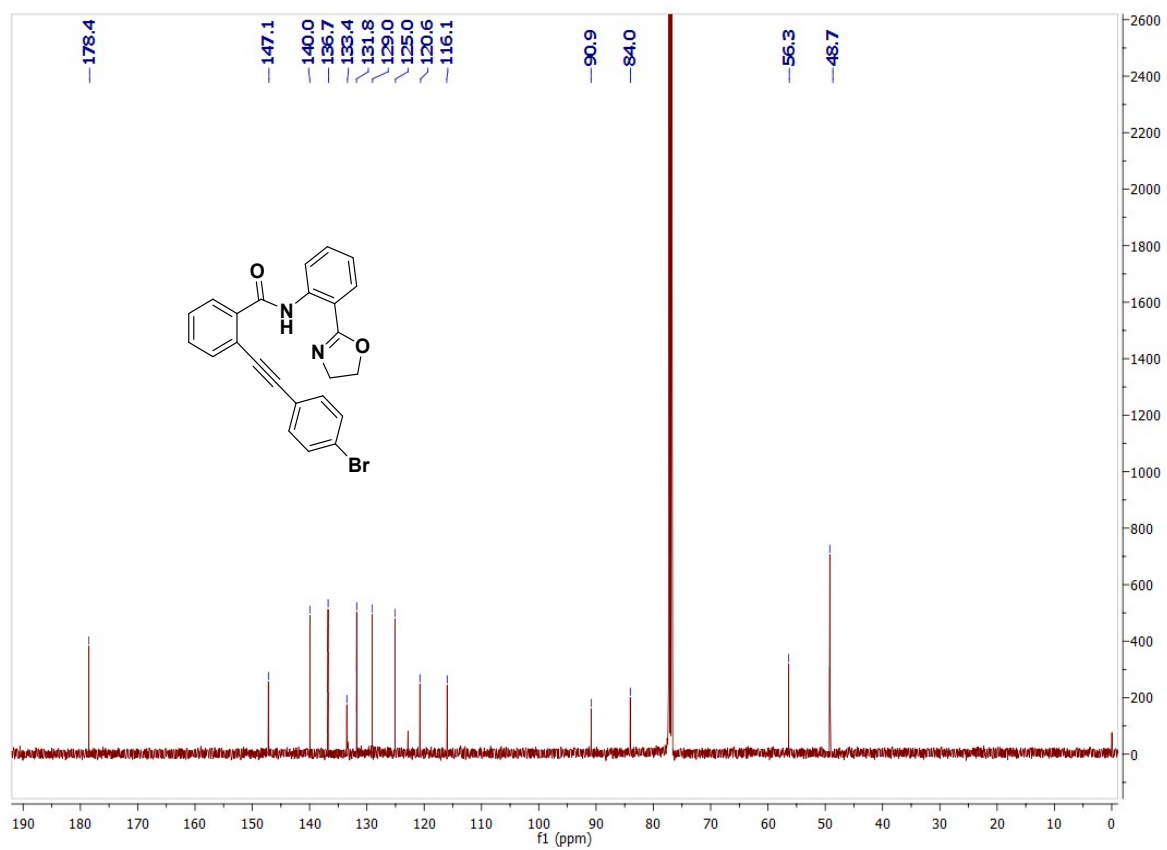


Fig. S33C ESI-MS spectrum of derivative 7c

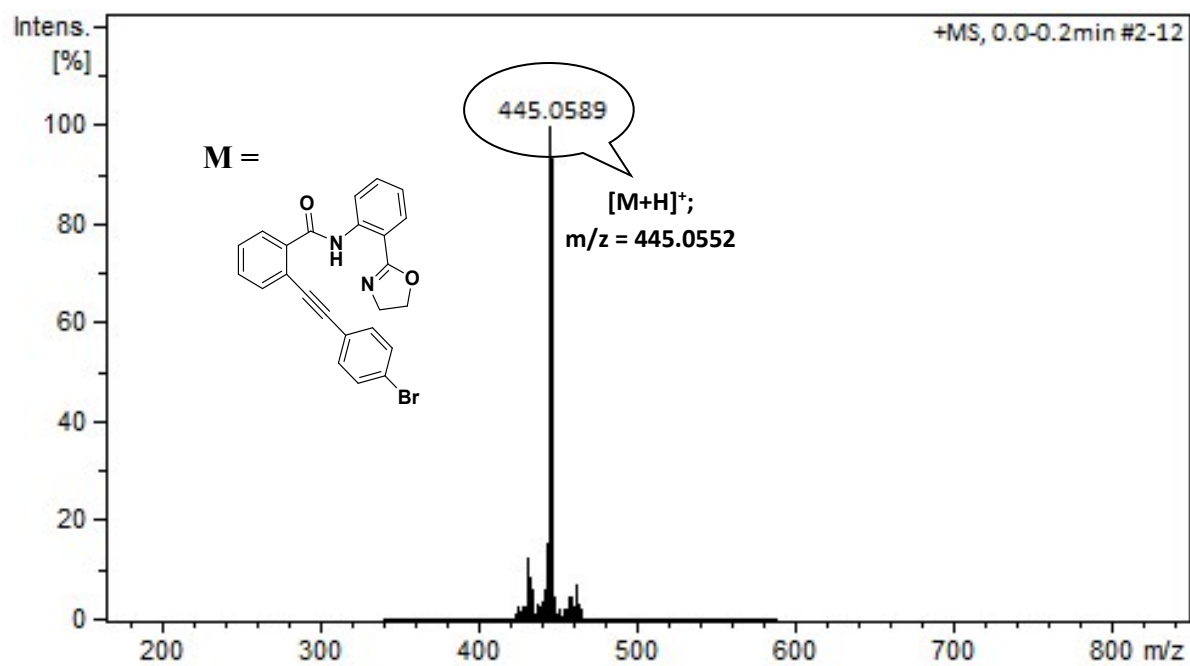


Fig. S34A ¹H NMR spectrum of derivative 7d in CDCl₃

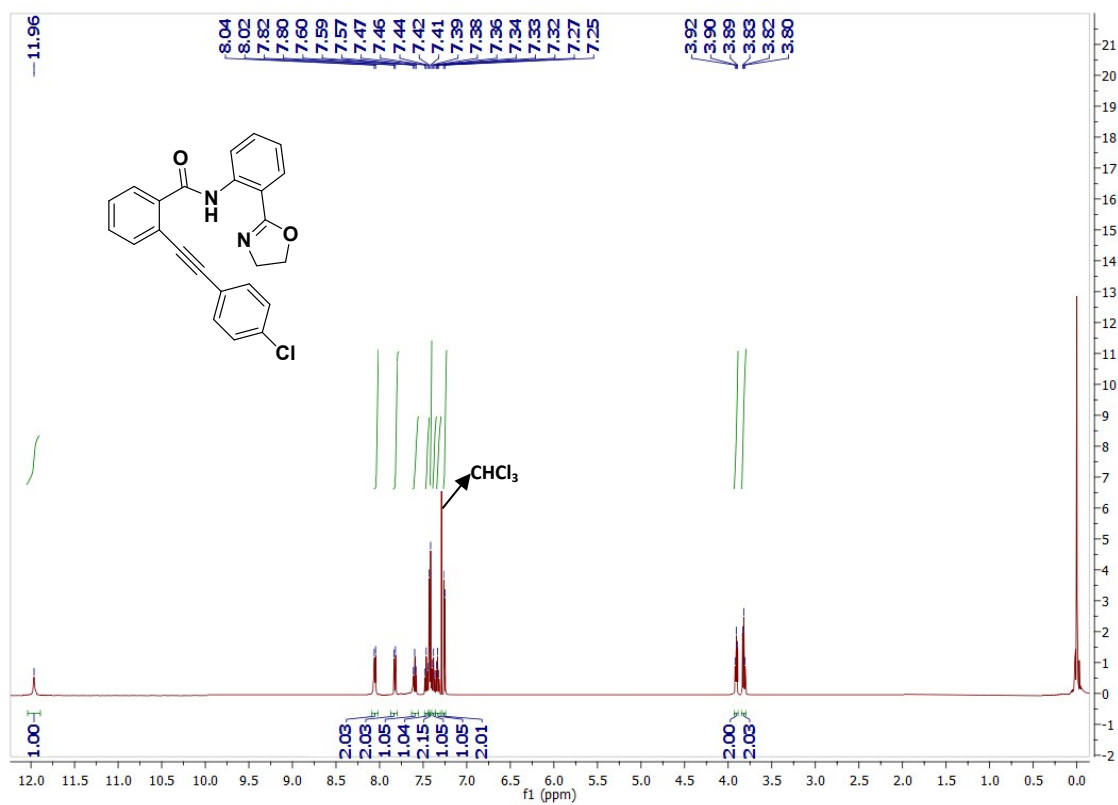


Fig. S34B ¹³C NMR spectrum of derivative 7d in CDCl₃

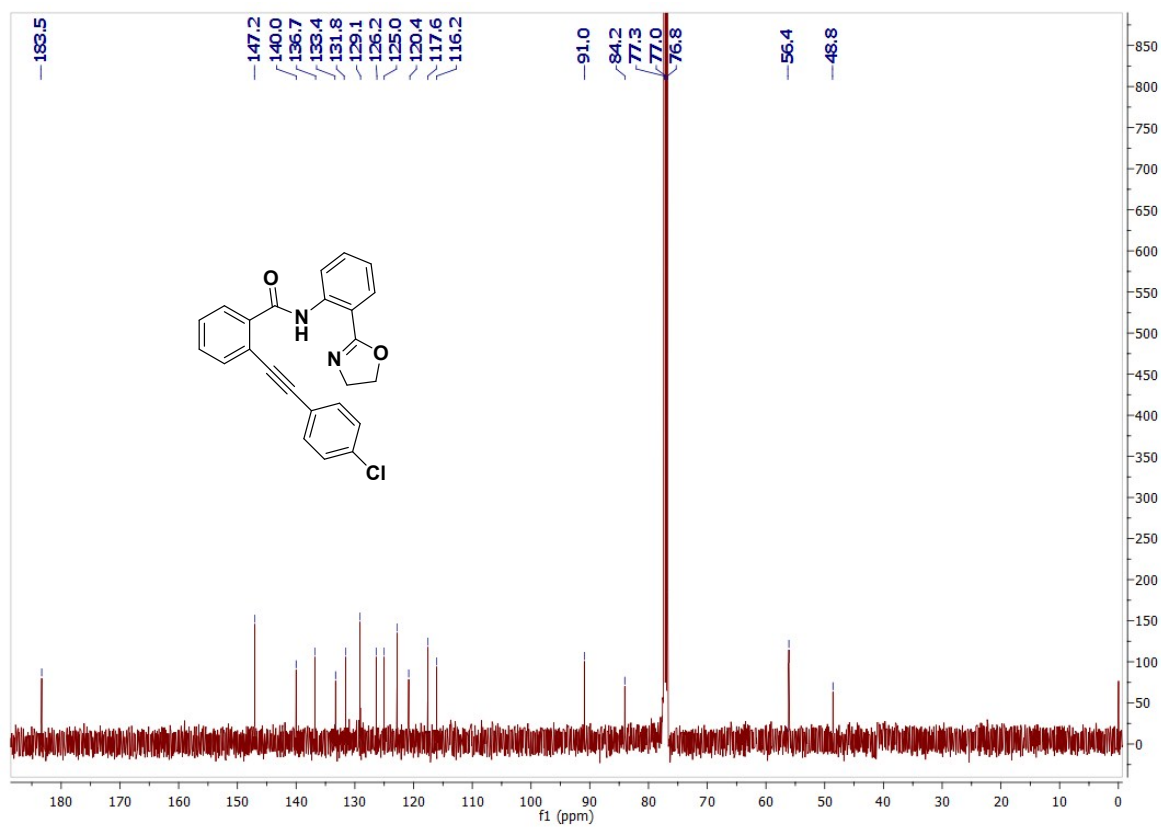


Fig. S34C ESI-MS spectrum of derivative 7d

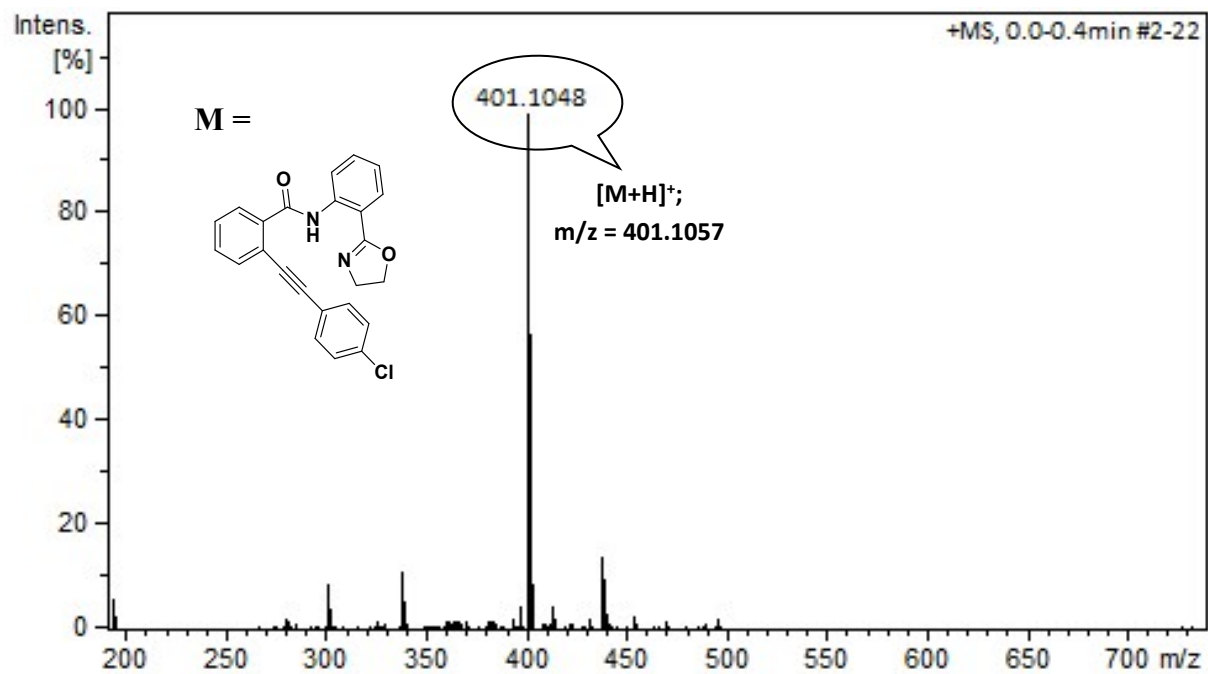


Fig. S35A ^1H NMR spectrum of derivative **7e** in CDCl_3

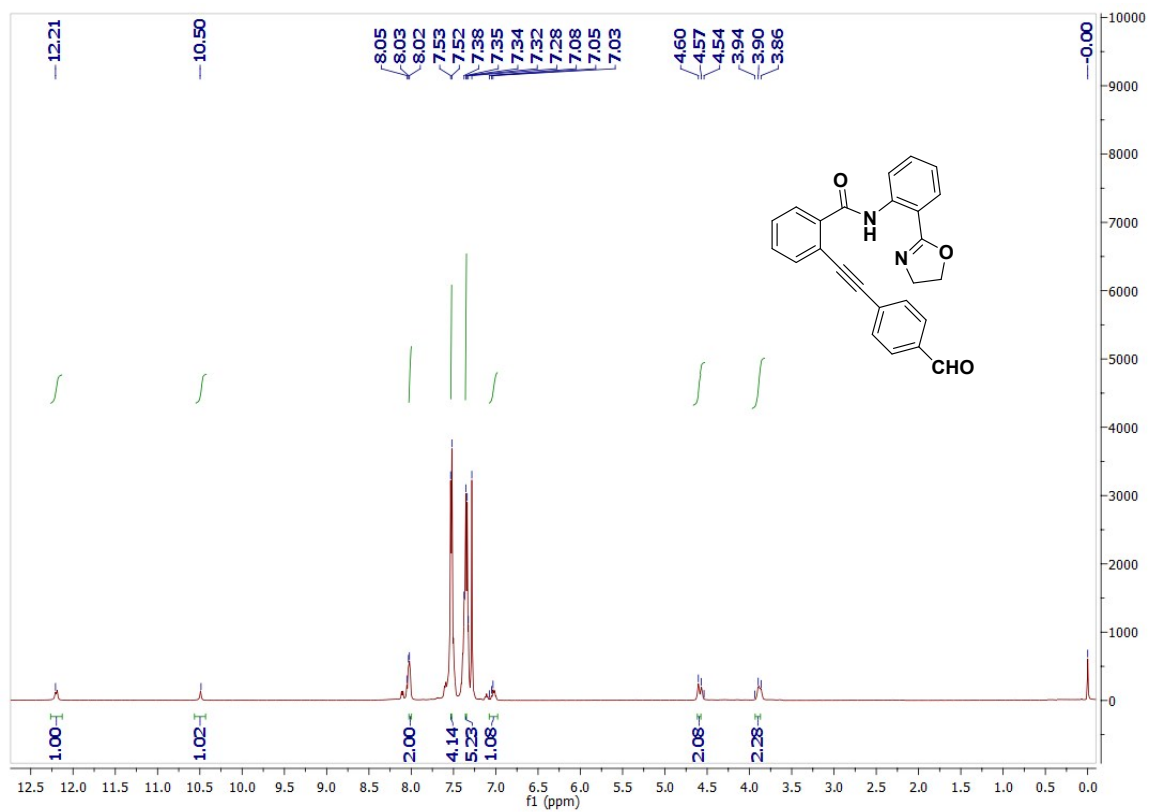


Fig. S35B ^{13}C NMR spectrum of derivative **7e** in CDCl_3

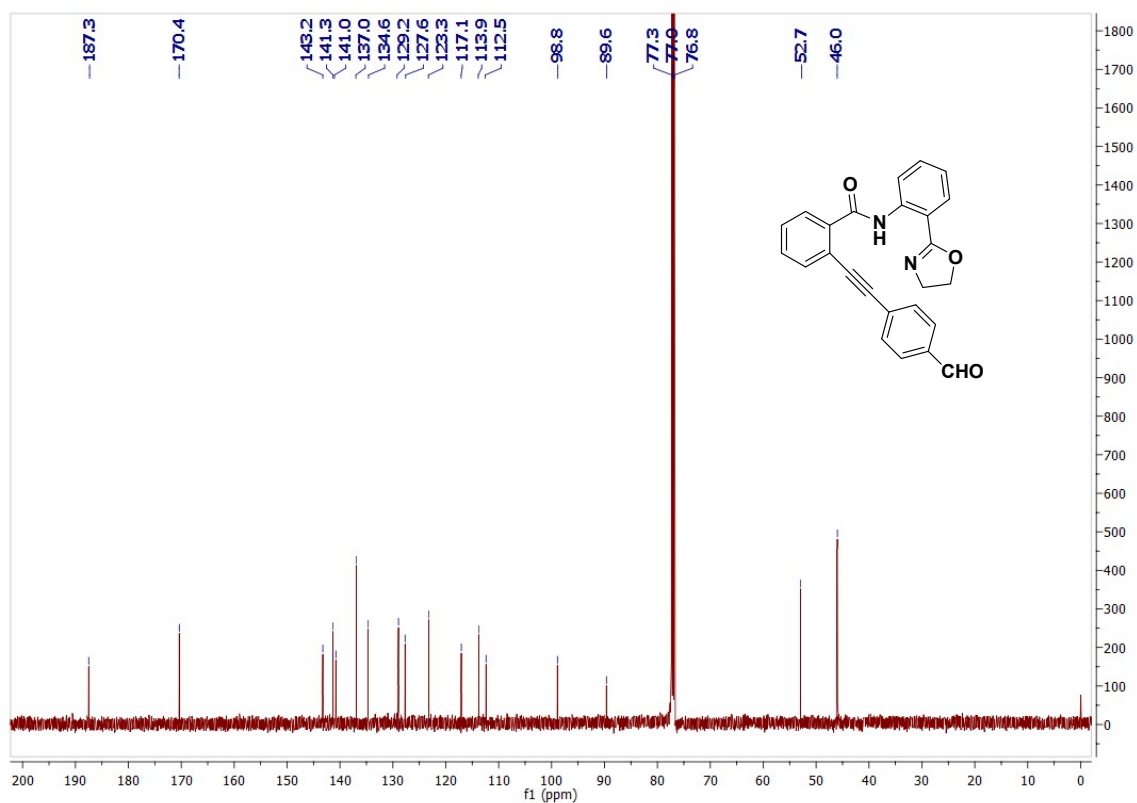


Fig. S35C ESI-MS spectrum of derivative 7e

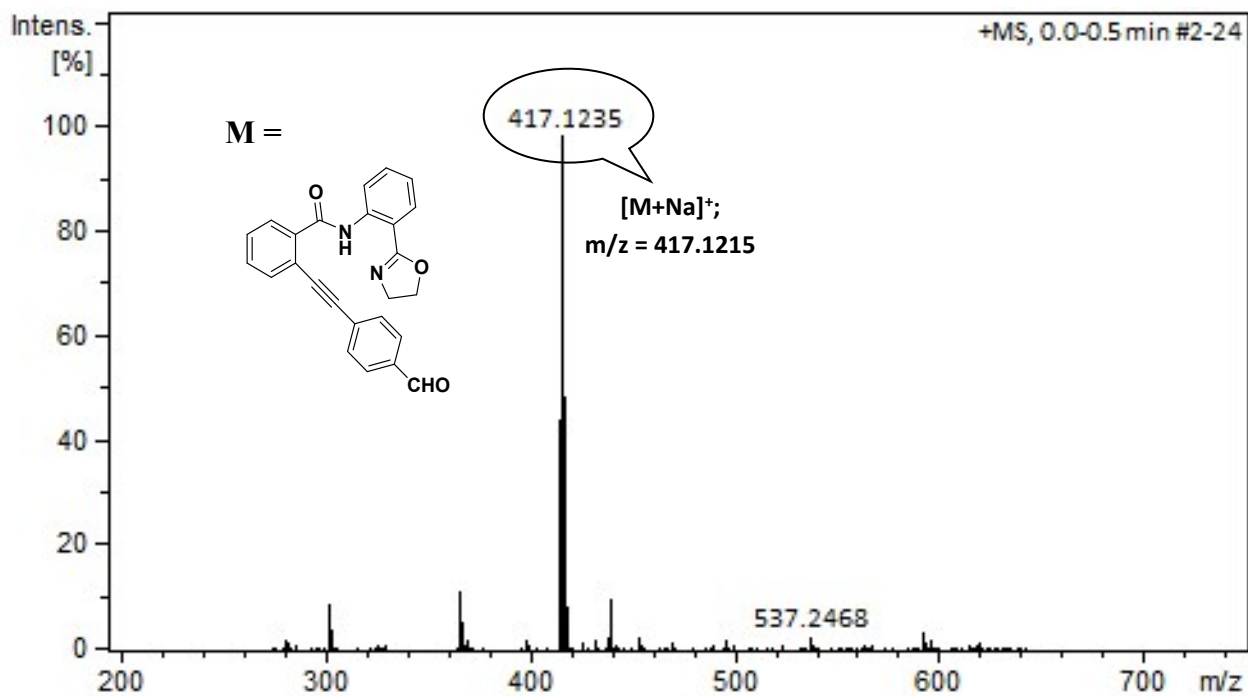


Fig. S36A ^1H NMR spectrum of derivative **7f** in CDCl_3

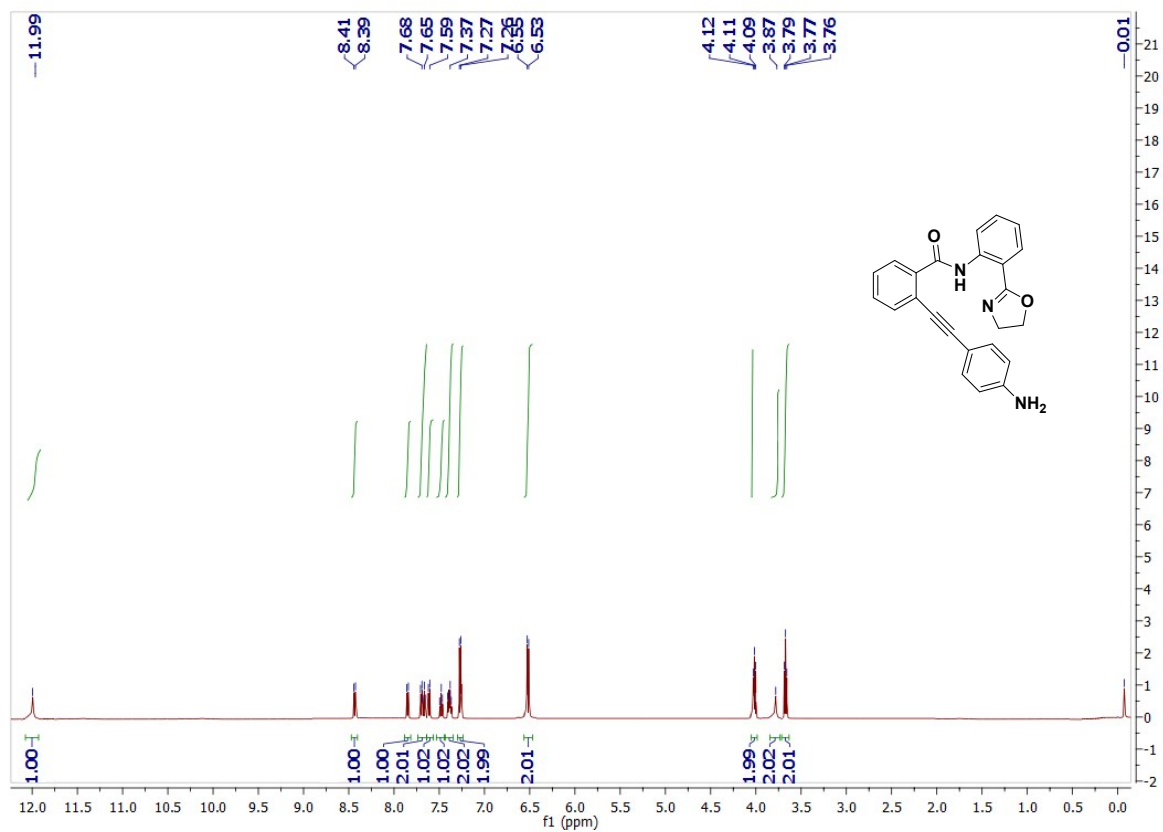


Fig. S36B ^{13}C NMR spectrum of derivative **7f** in CDCl_3

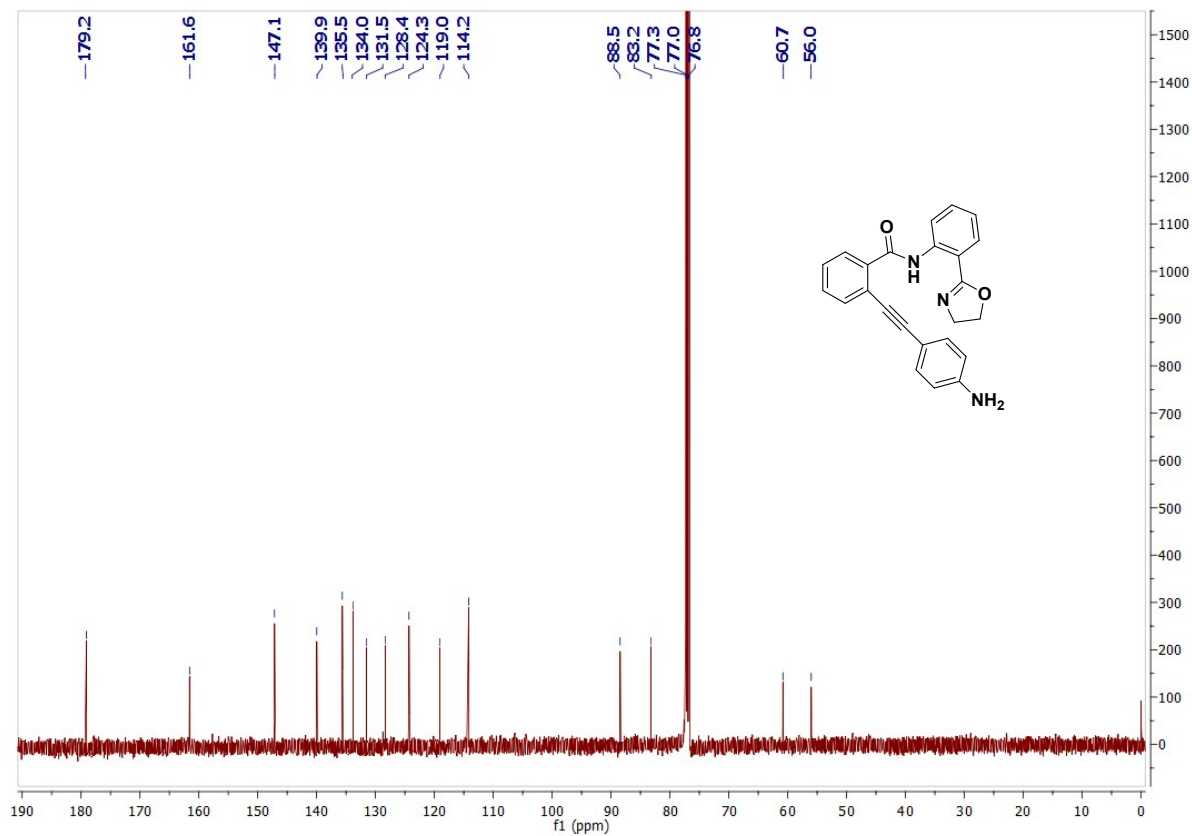


Fig. S36C ESI-MS spectrum of derivative 7f

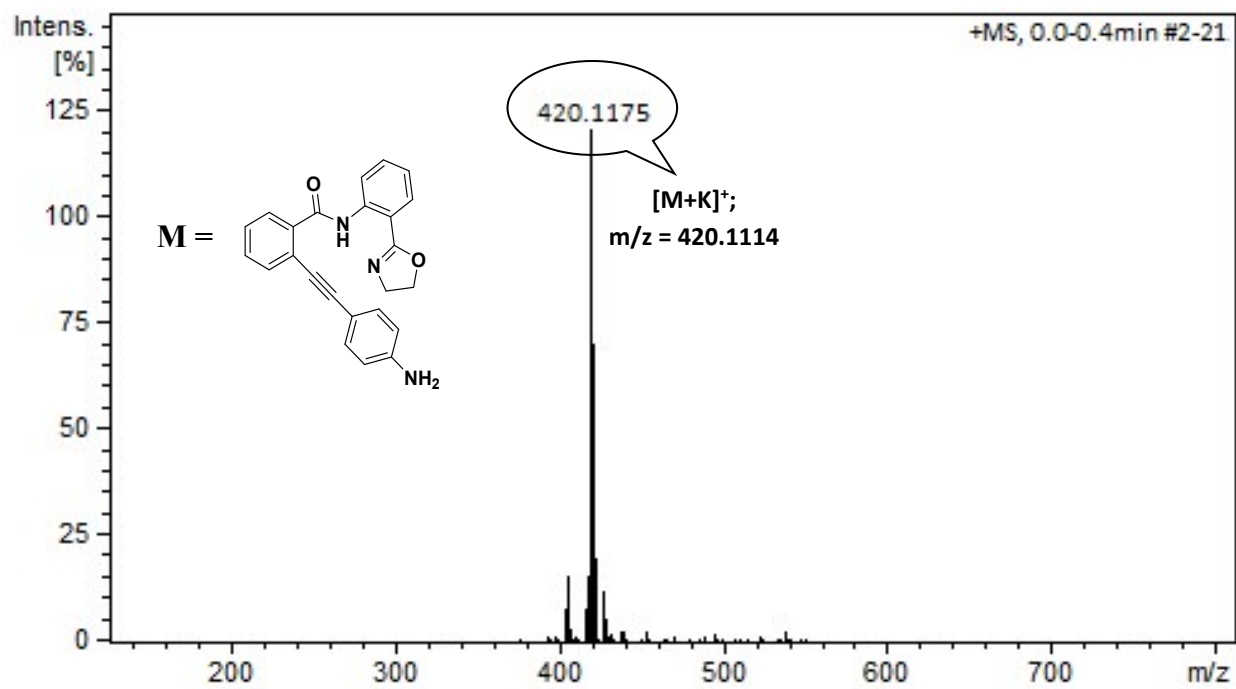


Fig. S37 ^1H NMR spectrum of derivative **7g** in CDCl_3

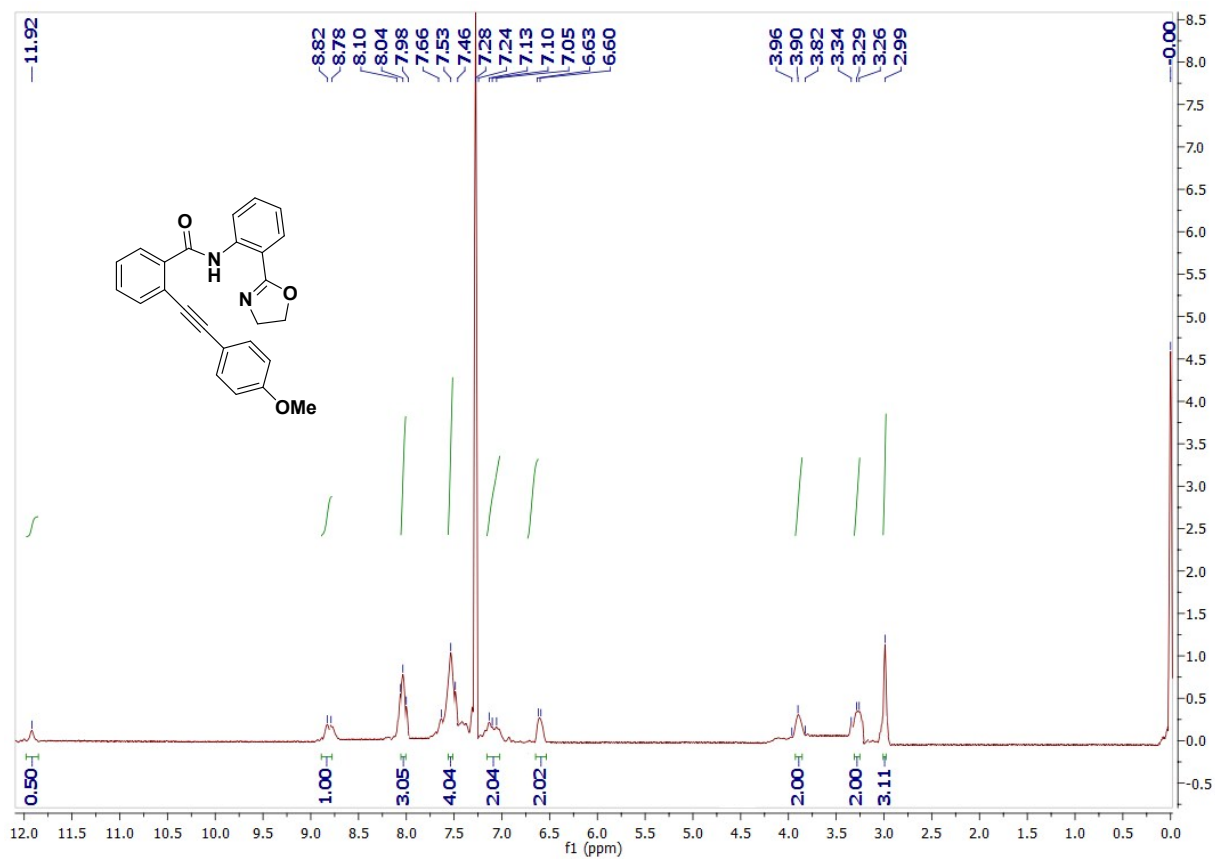


Fig. S38 ^1H NMR spectrum of derivative **7h** in CDCl_3

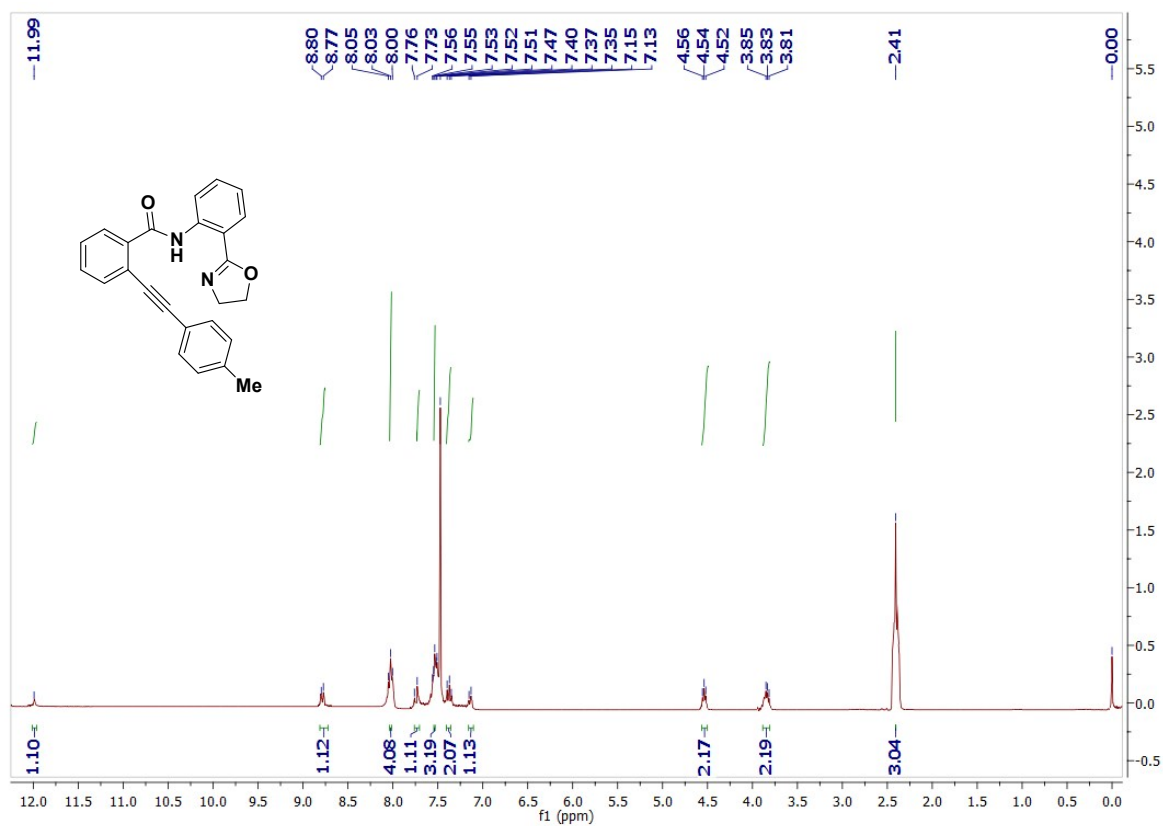


Fig. S39 ¹H NMR spectrum of derivative 7i in CDCl₃

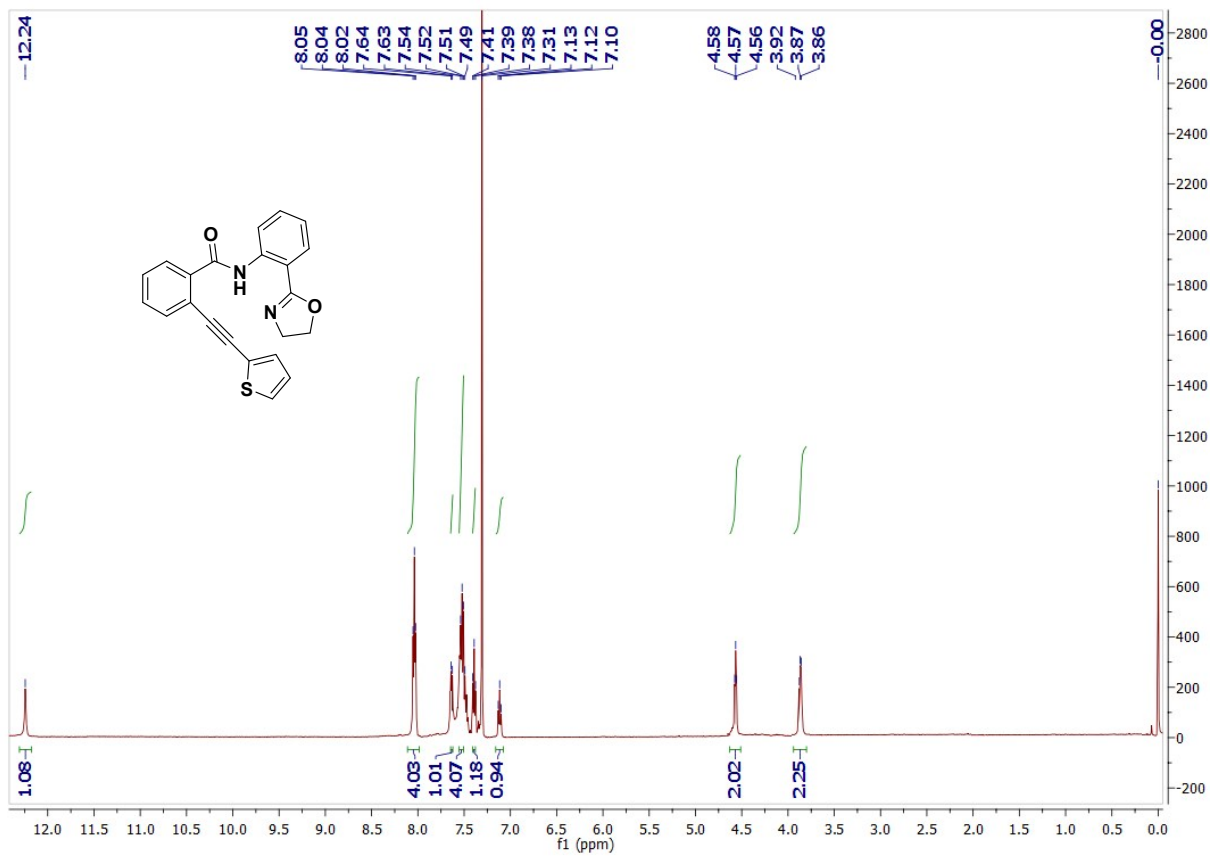


Fig. S40A ¹H NMR spectrum of derivative 7j in CDCl₃

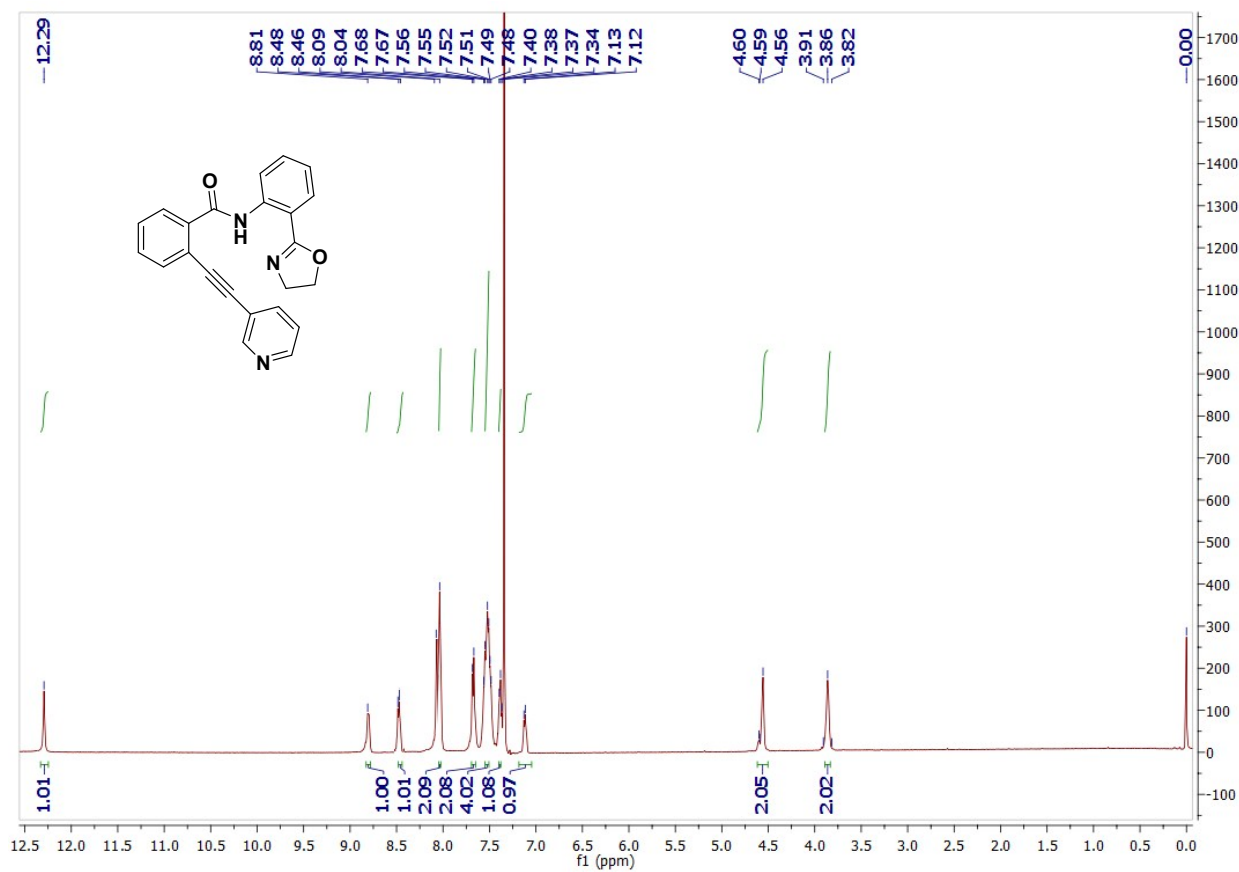


Fig. S40B ¹³C NMR spectrum of derivative 7j in CDCl₃

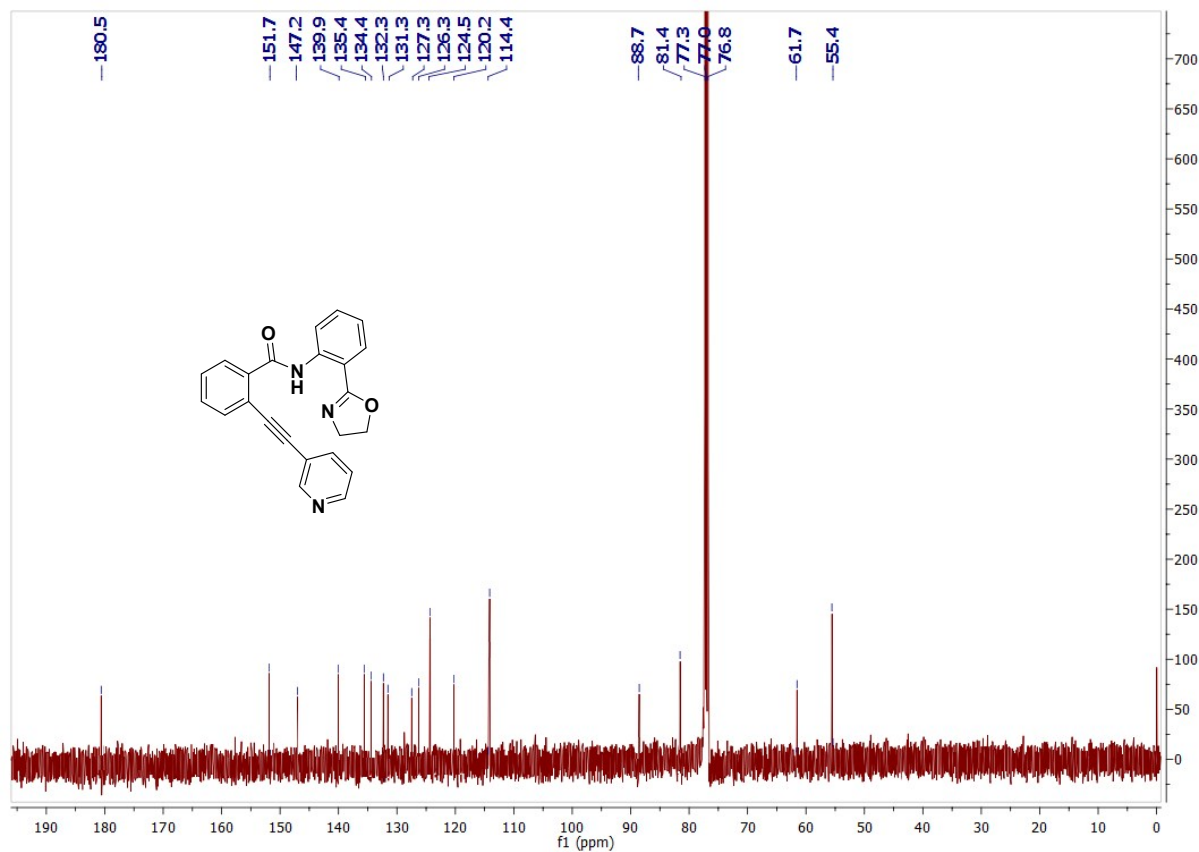


Fig. S40C ESI-MS spectrum of derivative 7j

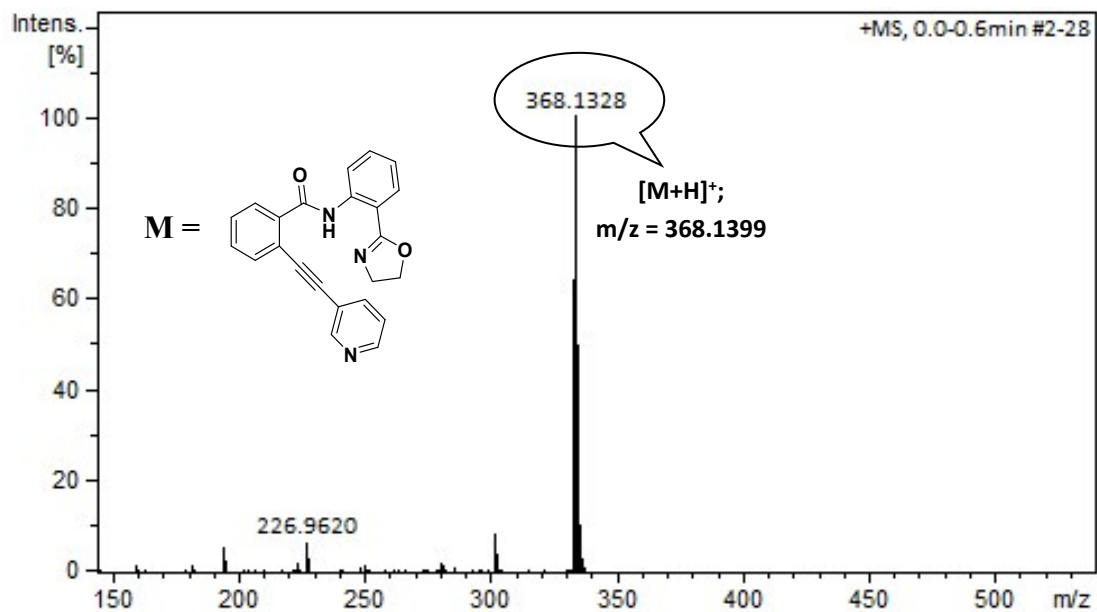


Fig. S41 ¹H NMR spectrum of derivative 7k in CDCl₃

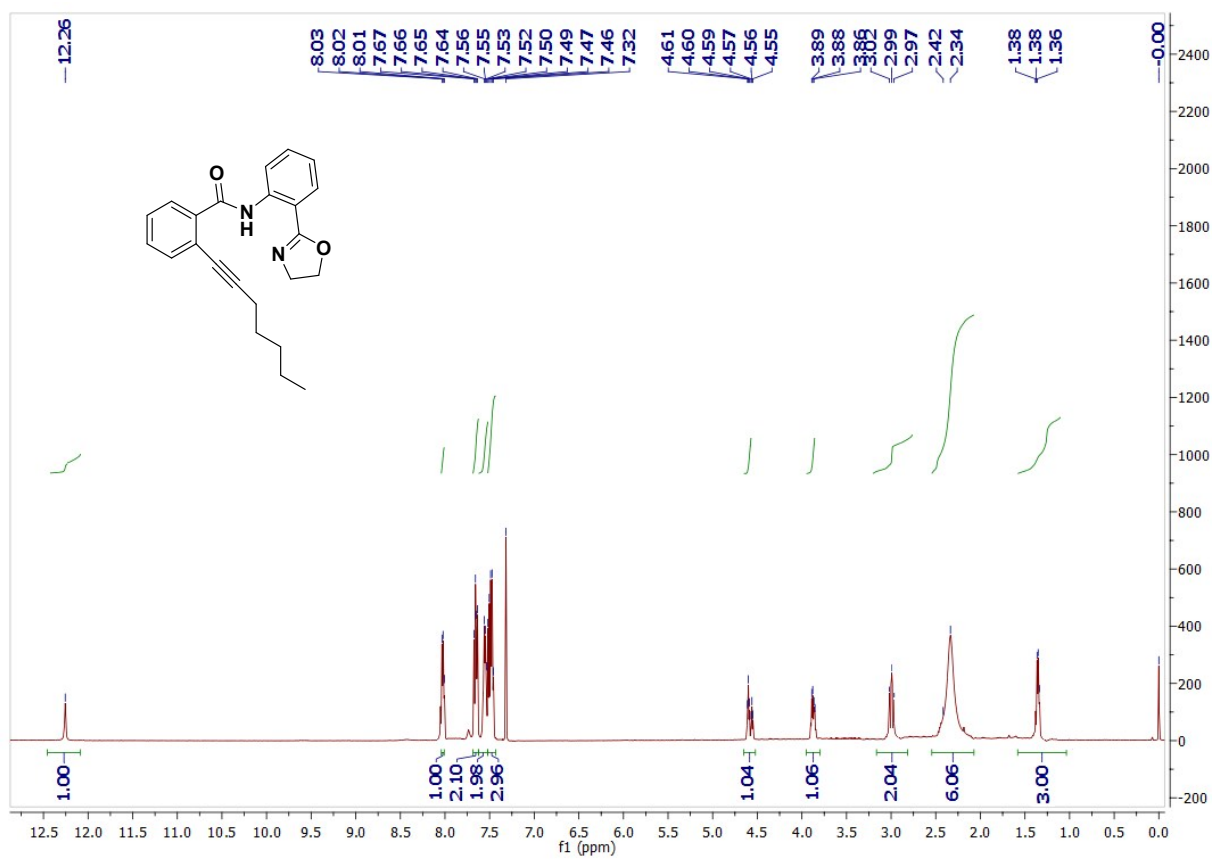


Fig. S42A ^1H NMR spectrum of derivative **7I** in CDCl_3

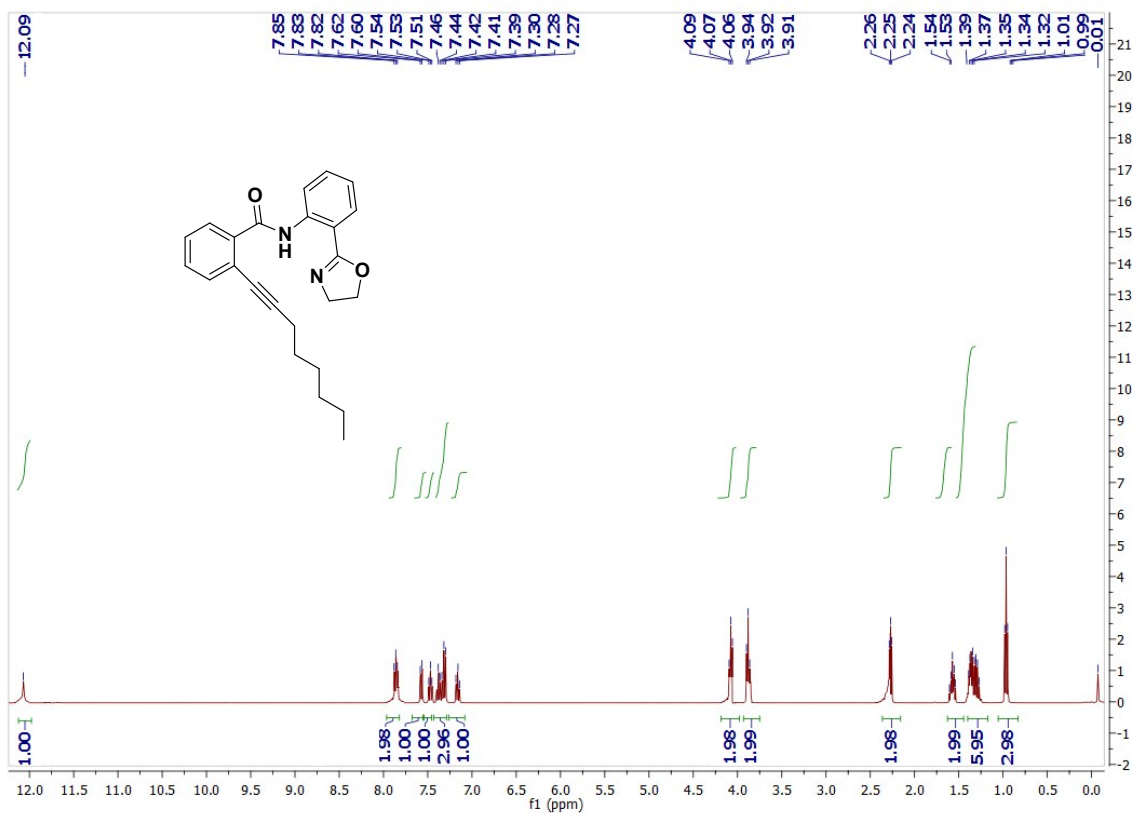


Fig. S42B ^{13}C NMR spectrum of derivative **7I** in CDCl_3

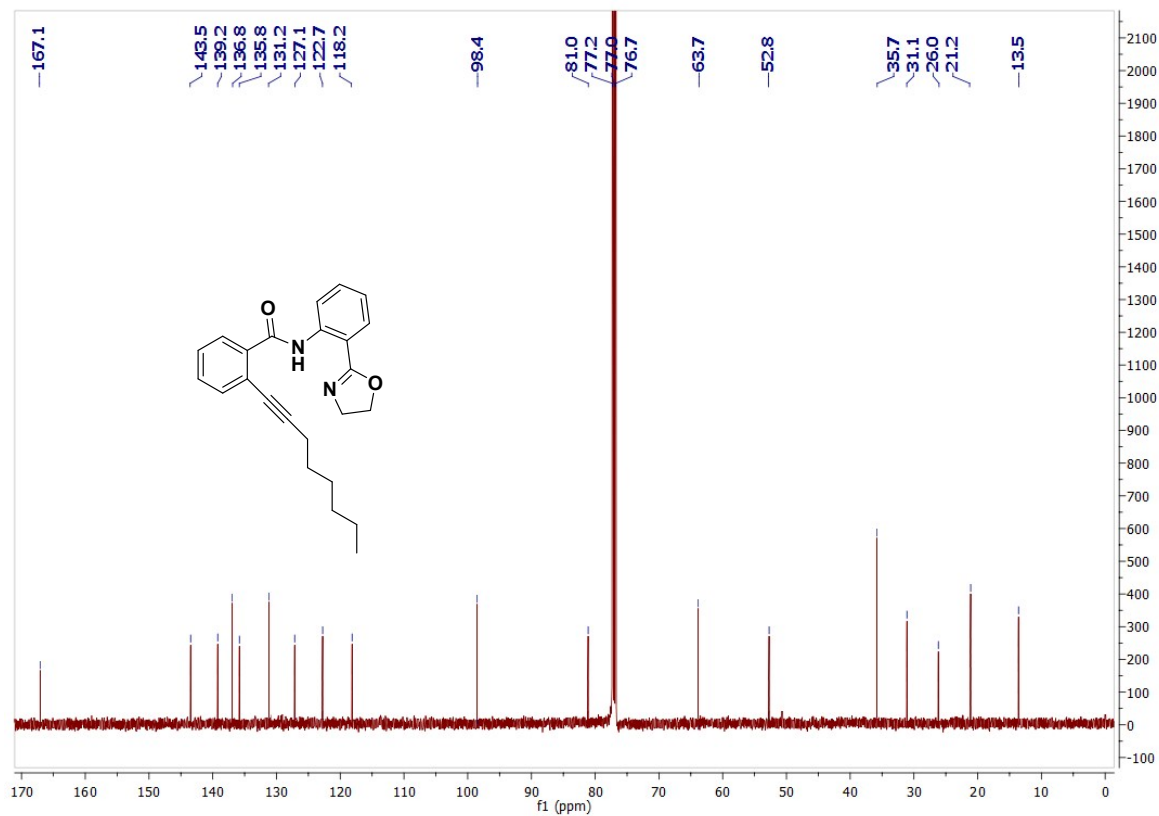


Fig. S42C ESI-MS spectrum of derivative 71

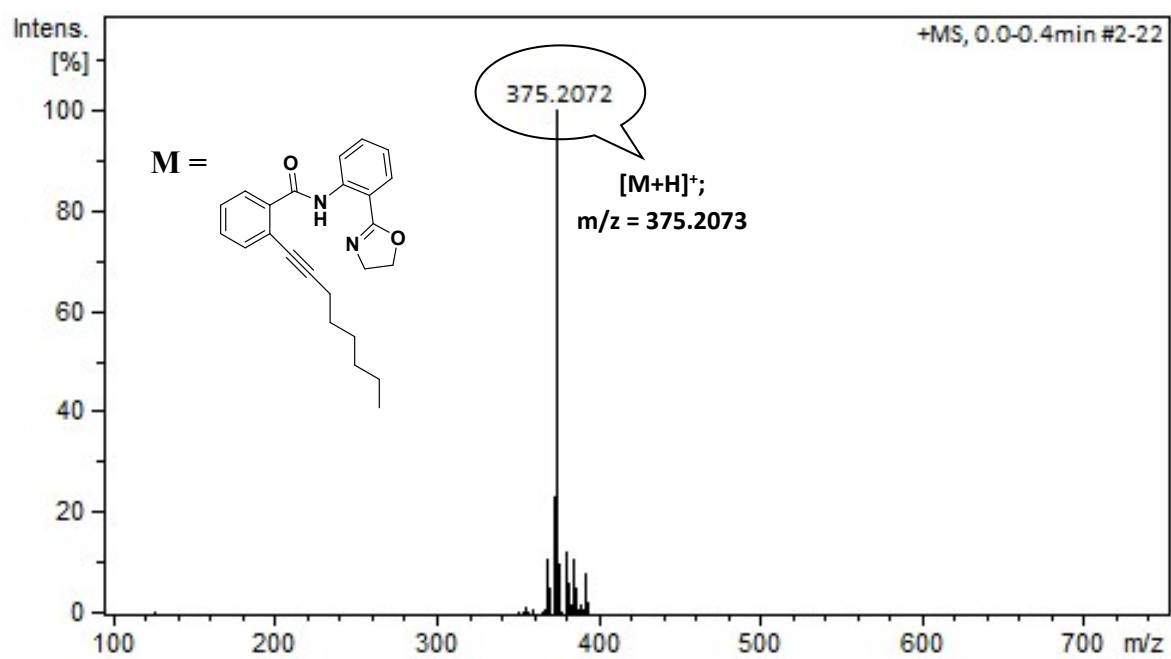


Fig. S43A ¹H NMR spectrum of derivative **7m** in CDCl₃

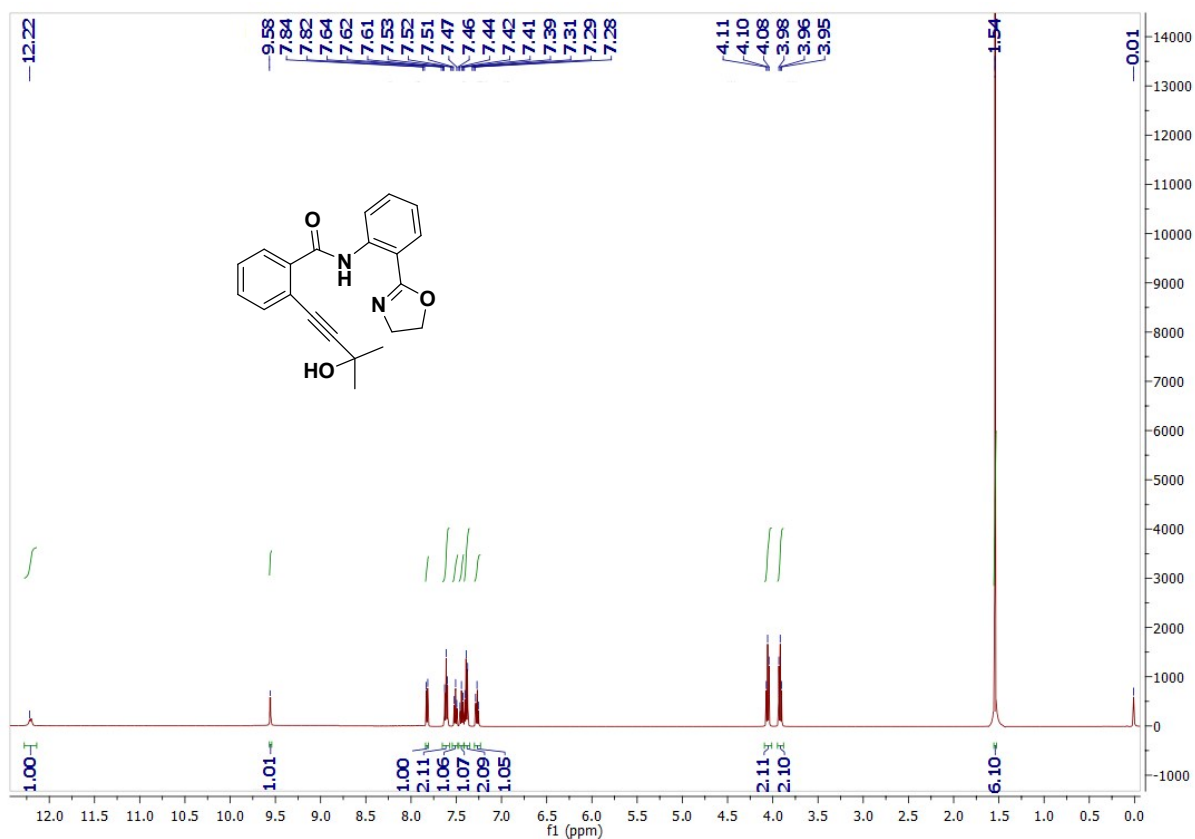


Fig. S43B ¹³C NMR spectrum of derivative **7m** in CDCl₃

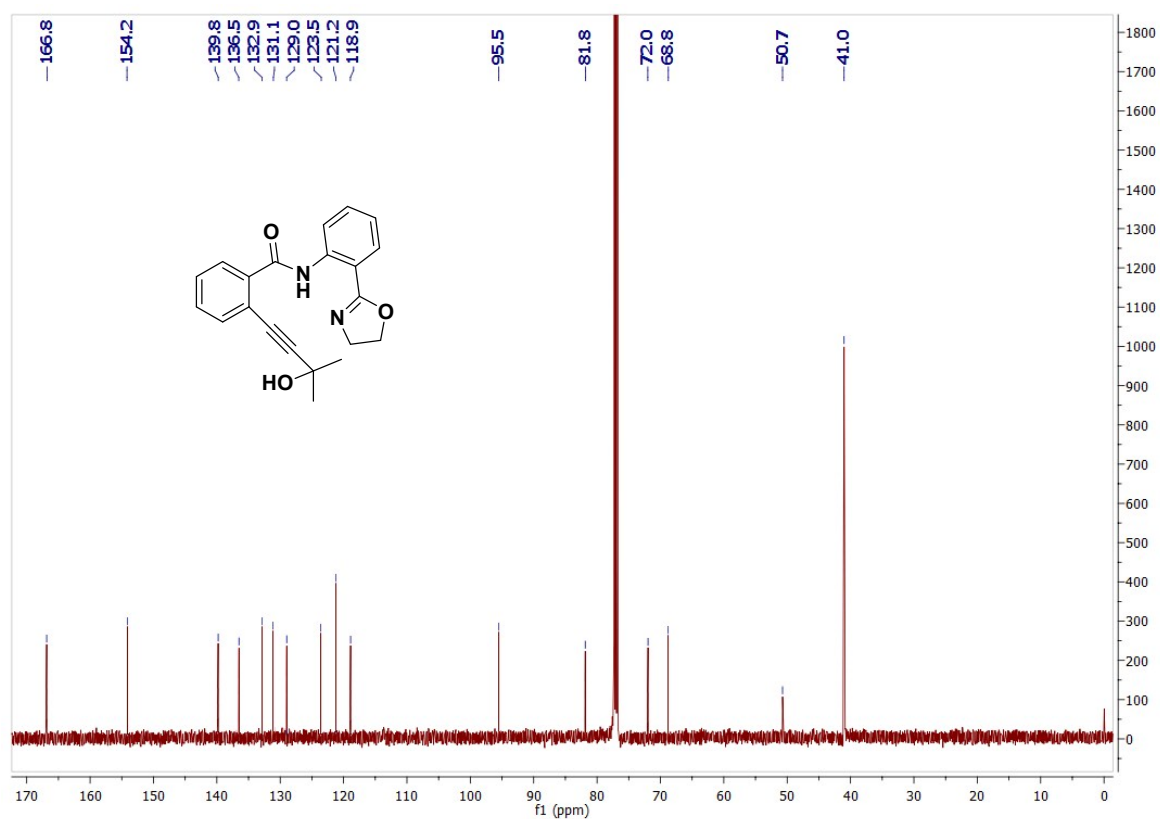


Fig. S43C ESI-MS spectrum of derivative 7m

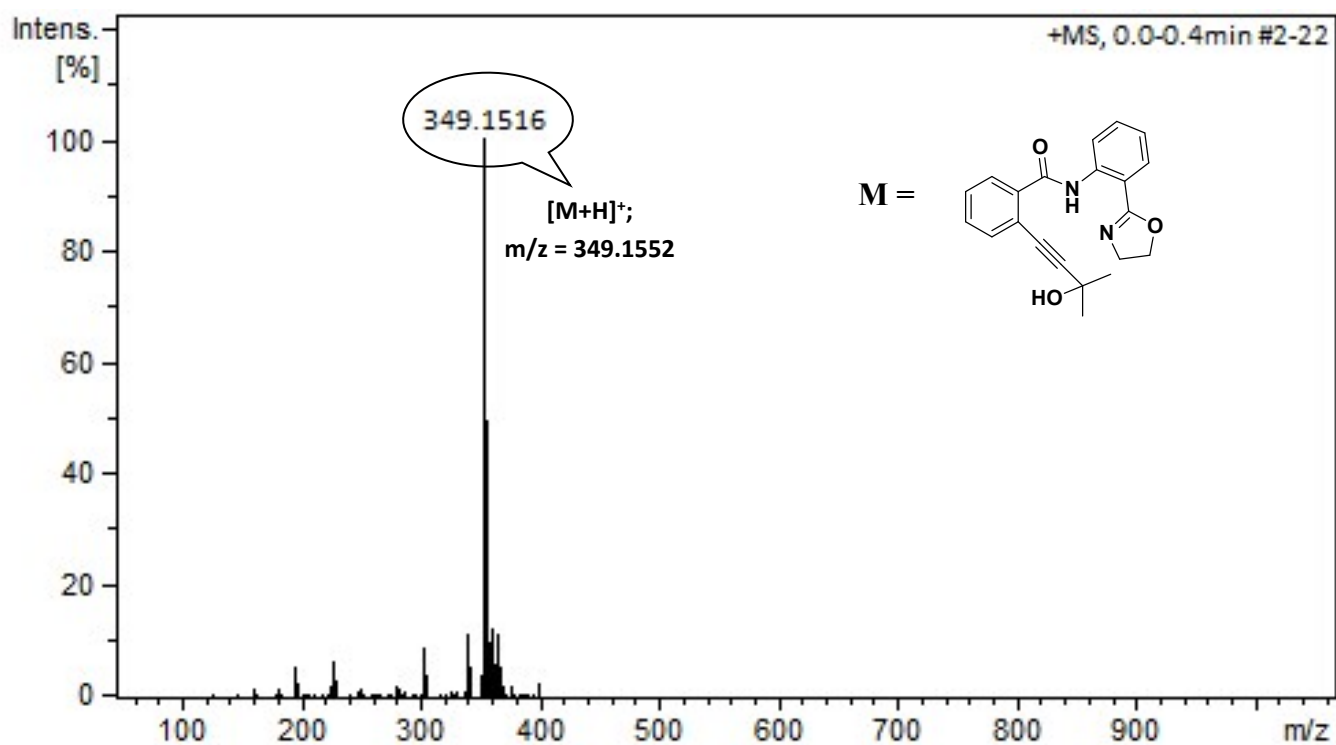


Fig. S44A ¹H NMR spectrum of derivative **6n** in CDCl₃

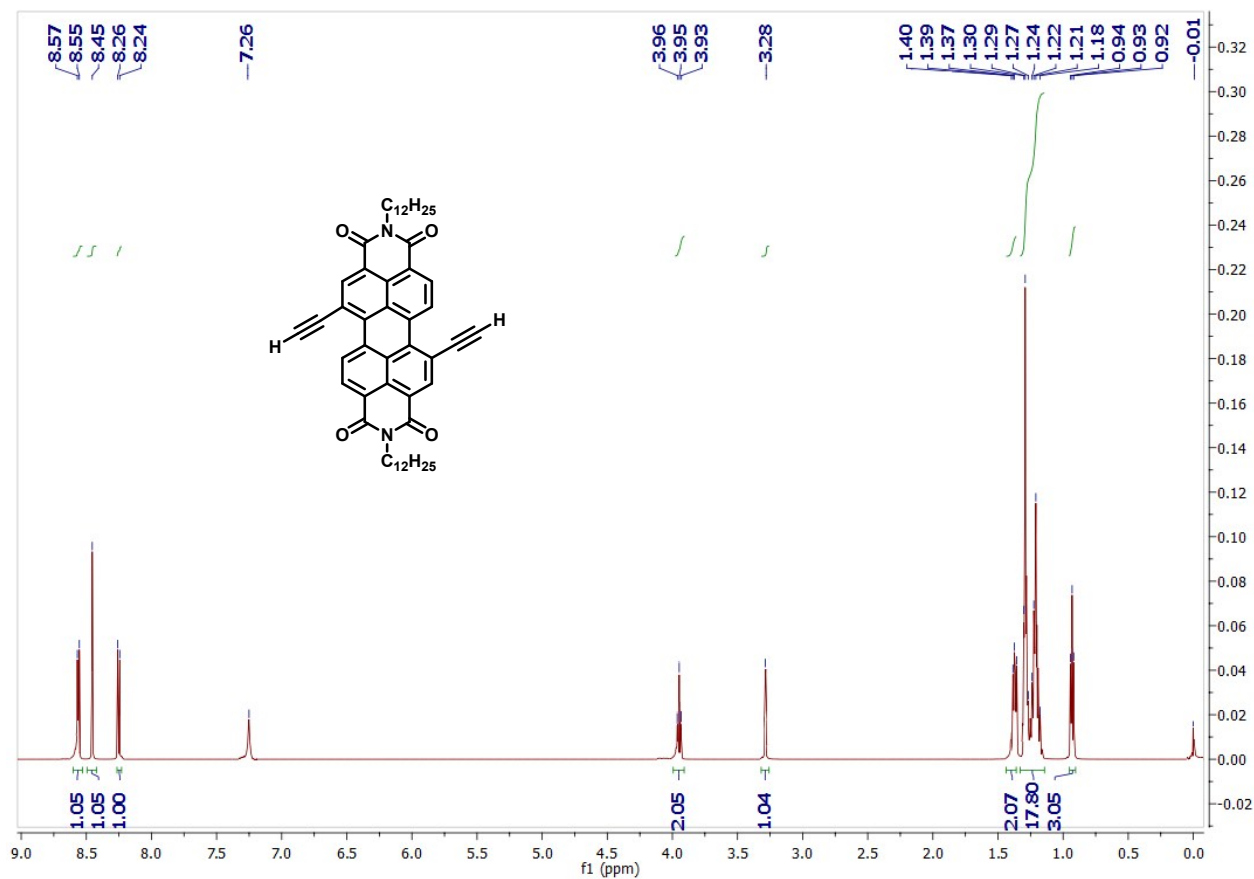


Fig. S44B ¹³C NMR spectrum of derivative **6n** in CDCl₃

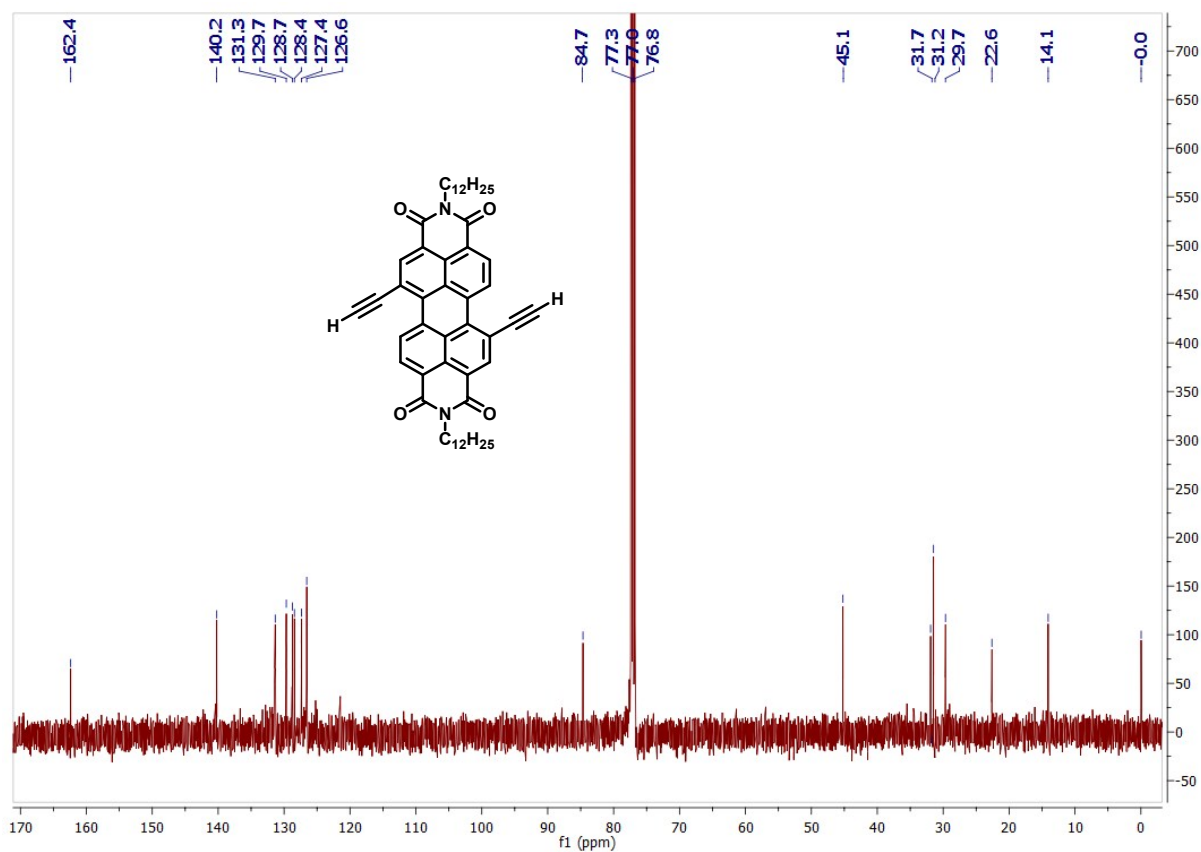


Fig. S44C ESI-MS spectrum of derivative 6n

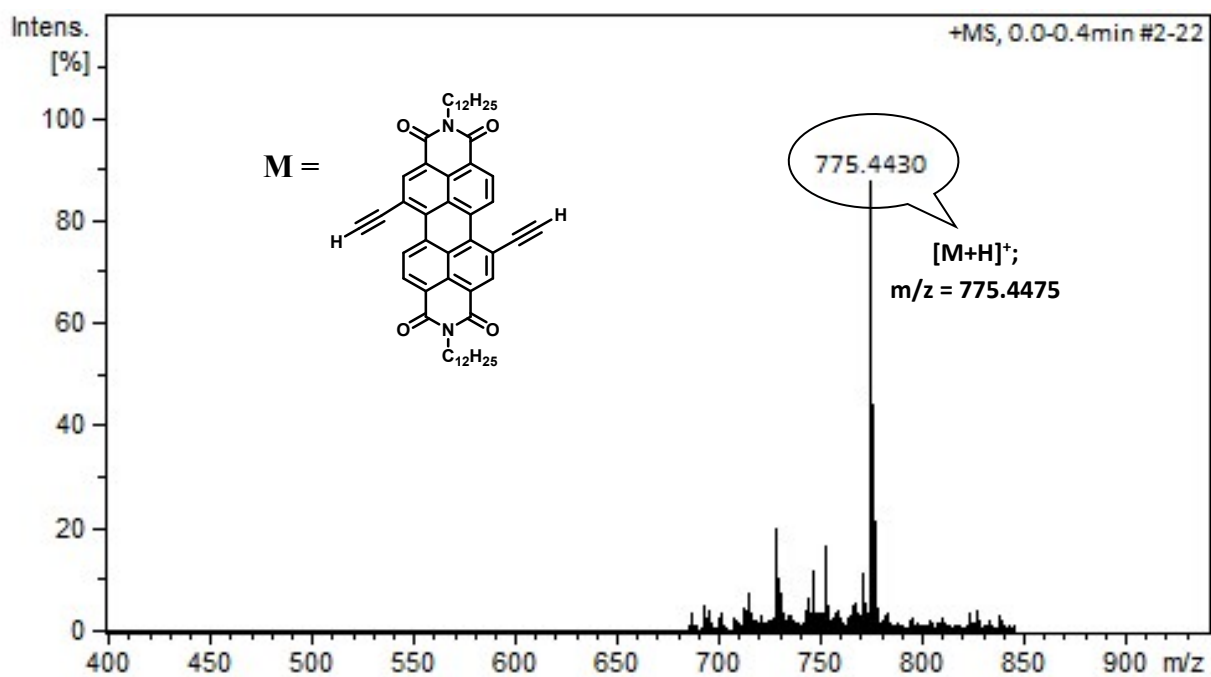


Fig. S45A ¹H NMR spectrum of derivative **7n** in CDCl₃

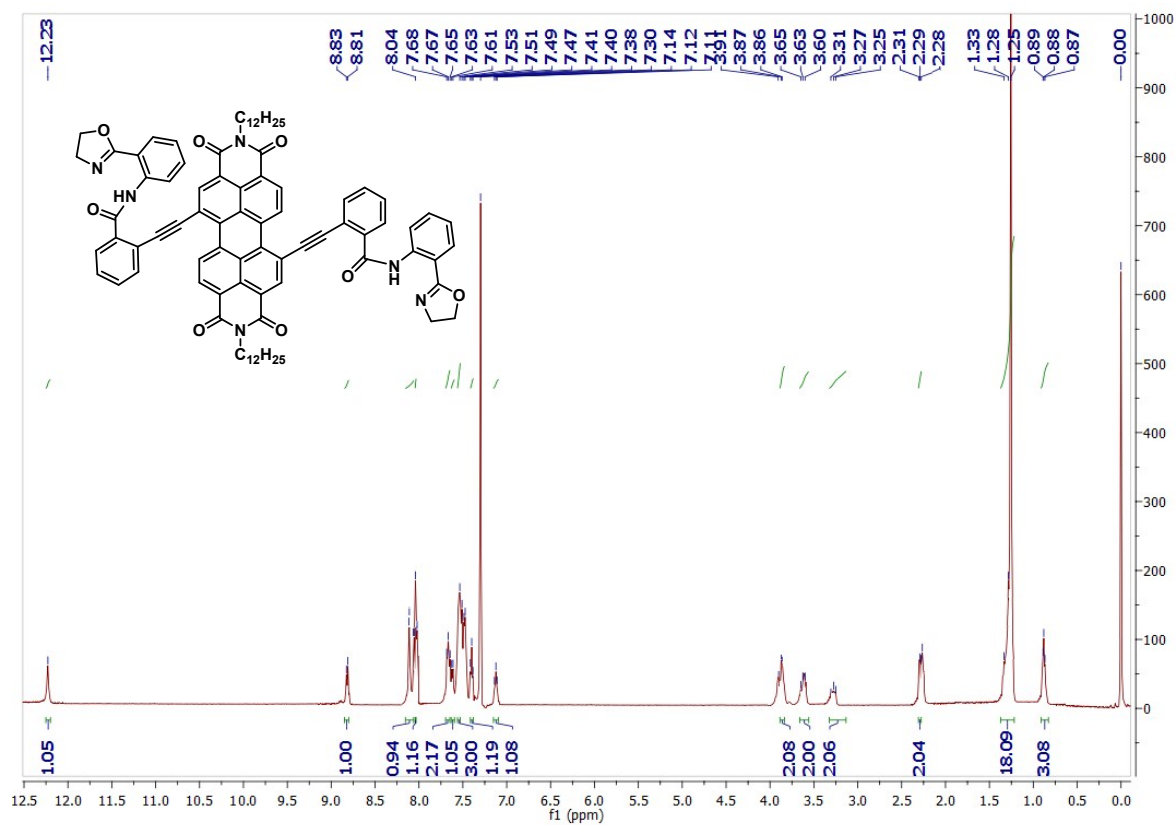


Fig. S45B ¹³C NMR spectrum of derivative **7n** in CDCl₃

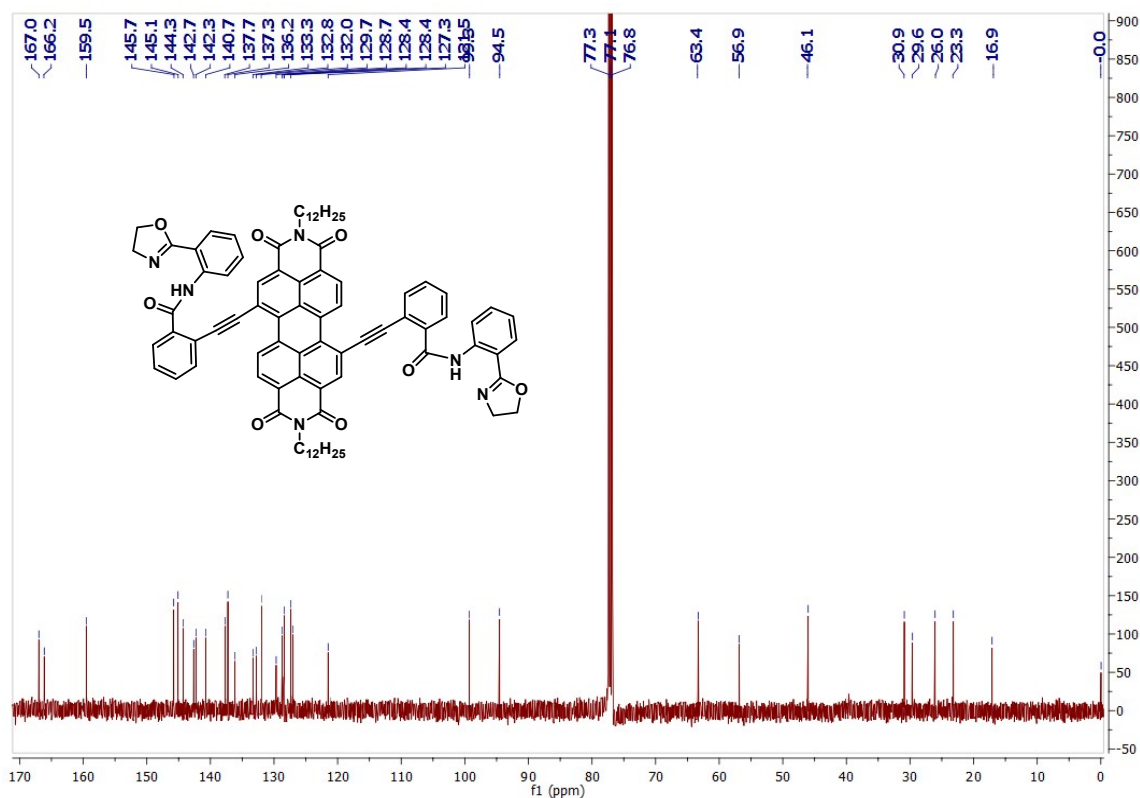


Fig. S45C ESI-MS spectrum of derivative 7n

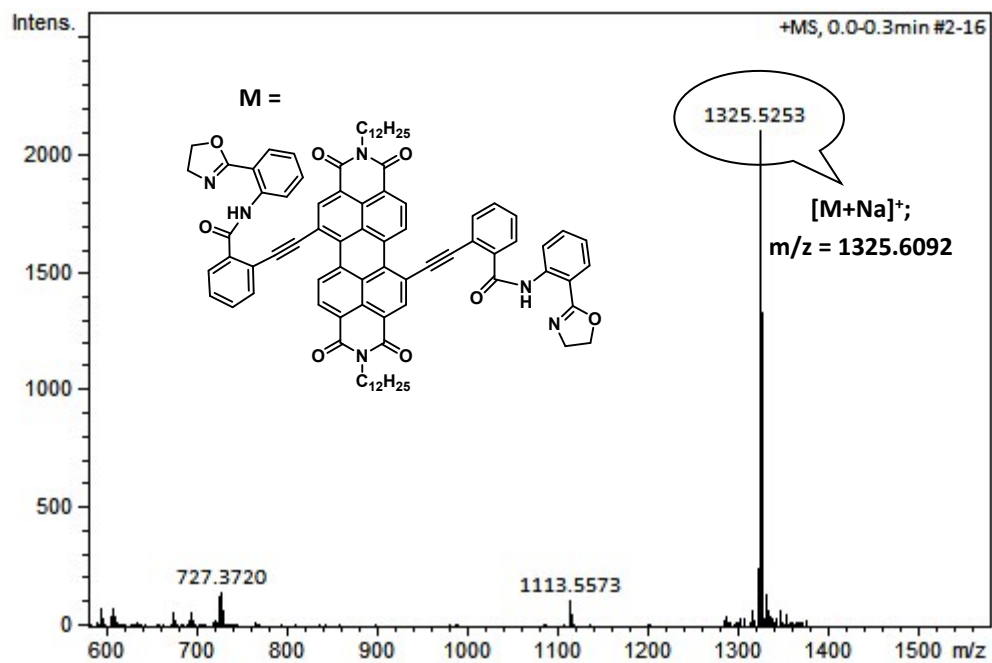


Fig. S46 ¹H NMR spectrum of derivative 10a in CDCl₃

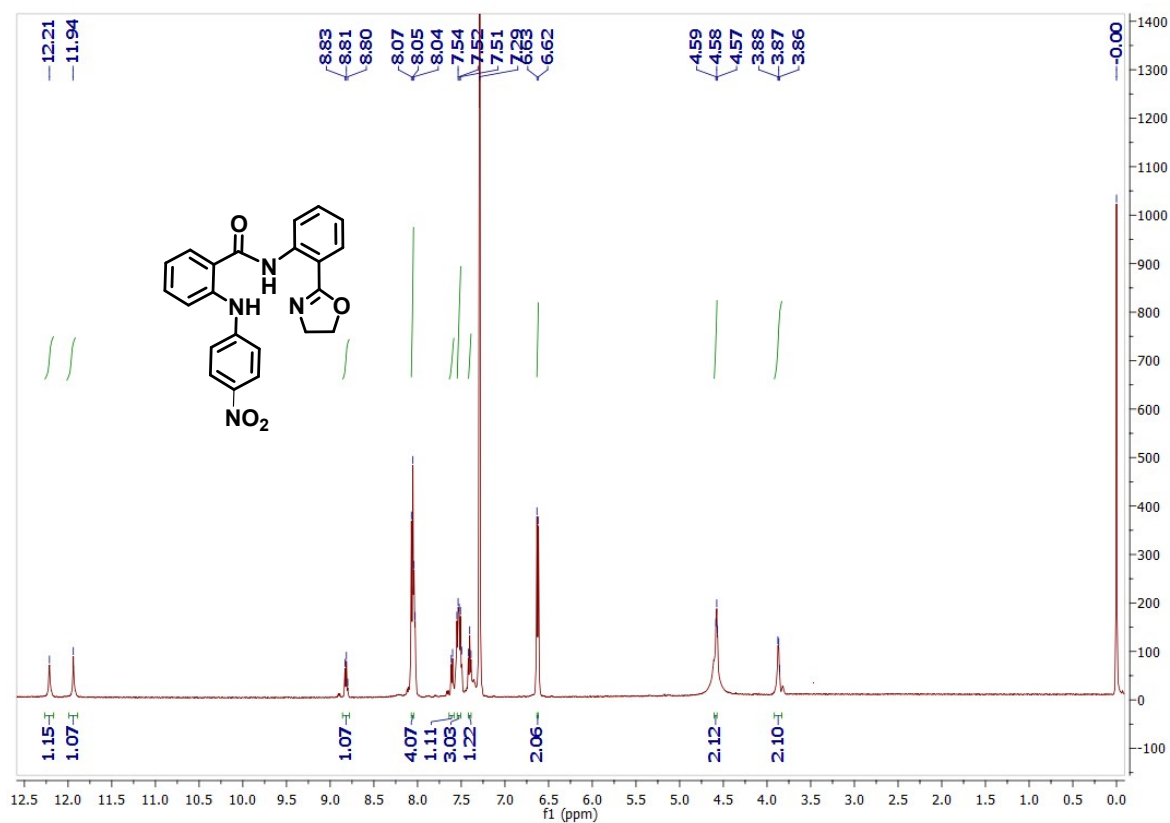


Fig. S47 ¹H NMR spectrum of derivative 10b in CDCl₃

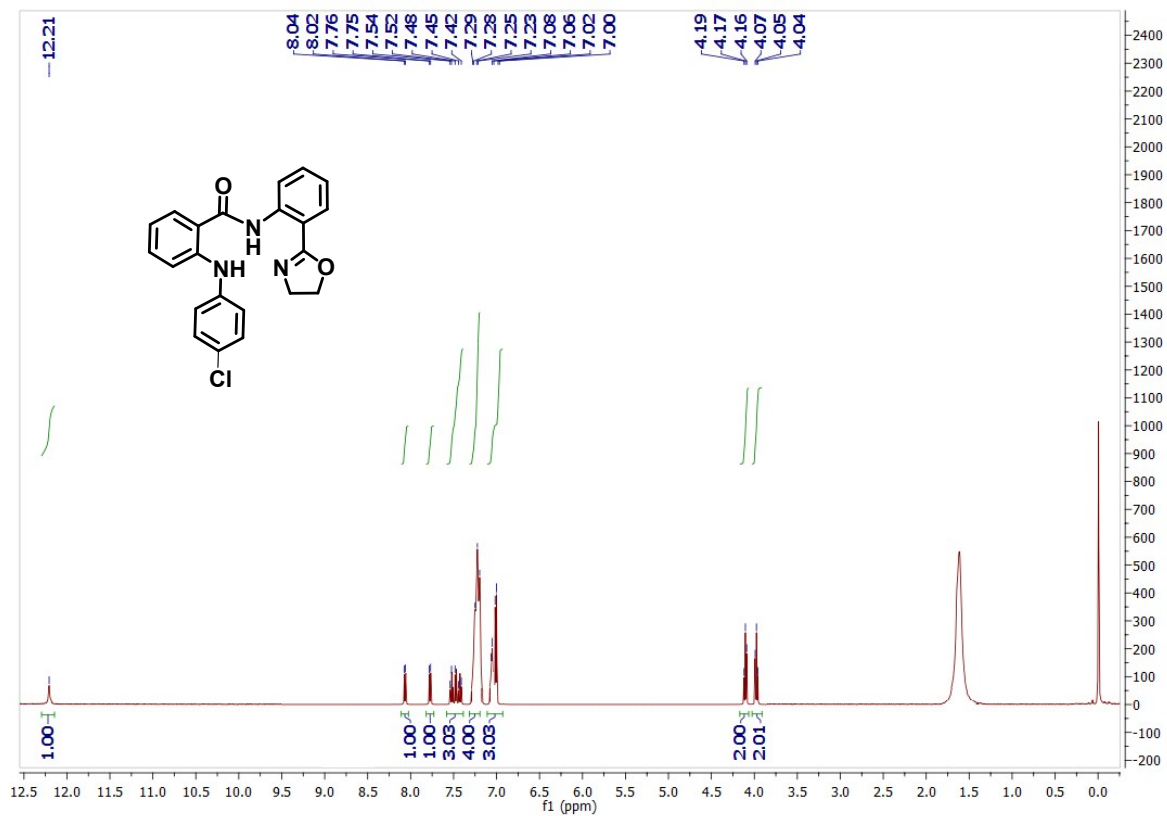


Fig. S48 ^1H NMR spectrum of derivative **10c** in CDCl_3

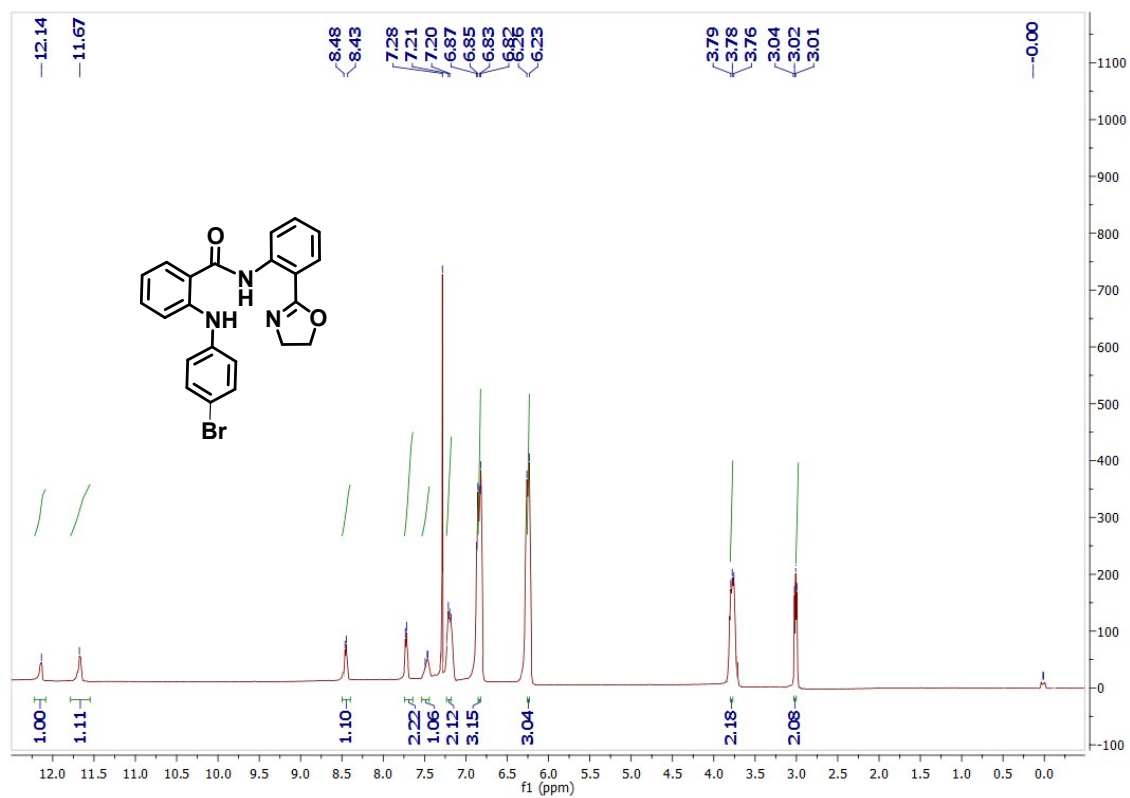


Fig. S49 ^1H NMR spectrum of derivative **10d** in CDCl_3

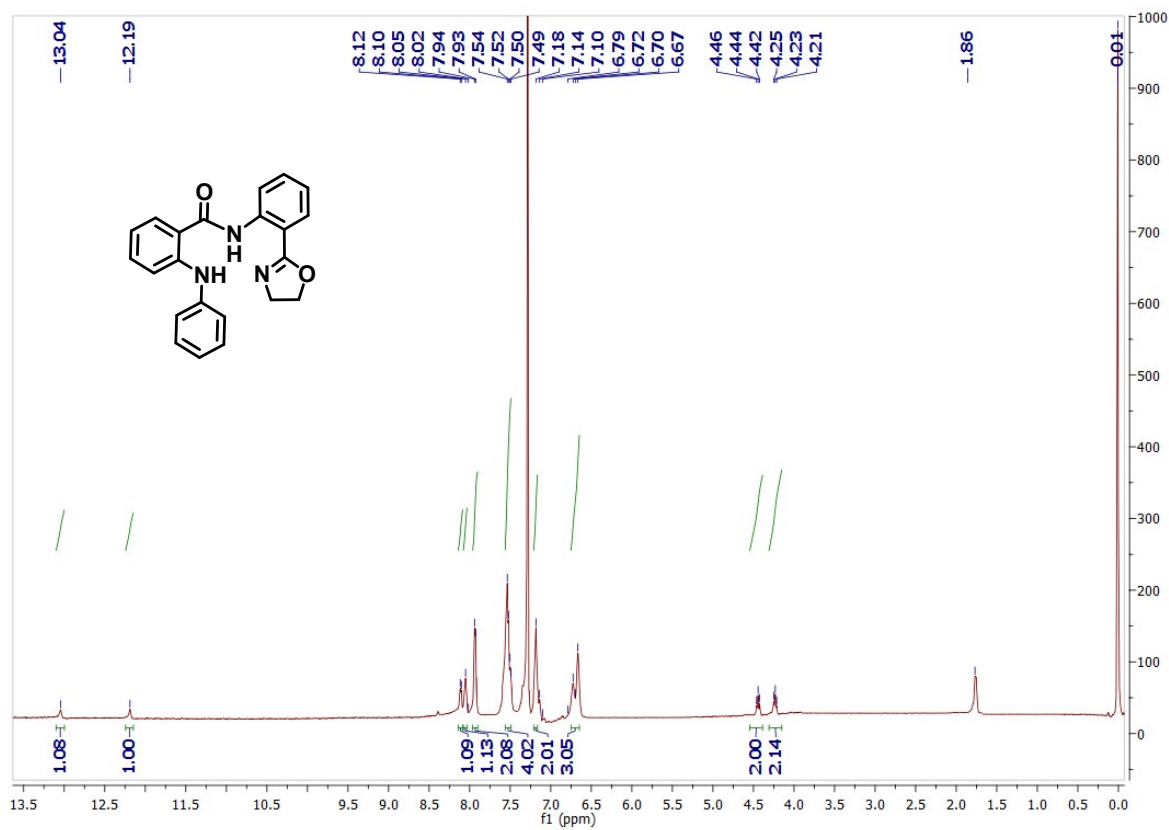


Fig. S50A ^1H NMR spectrum of derivative **10e** in CDCl_3

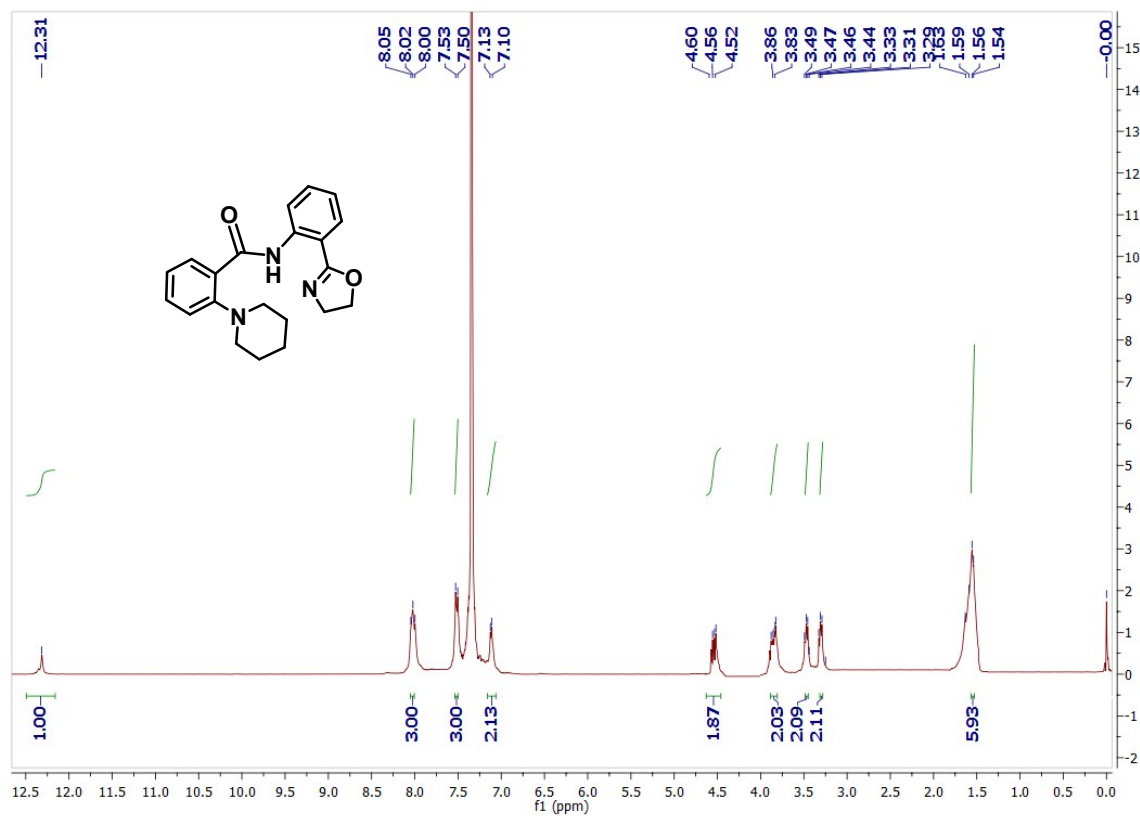


Fig. S50B ^{13}C NMR spectrum of derivative **10e** in CDCl_3

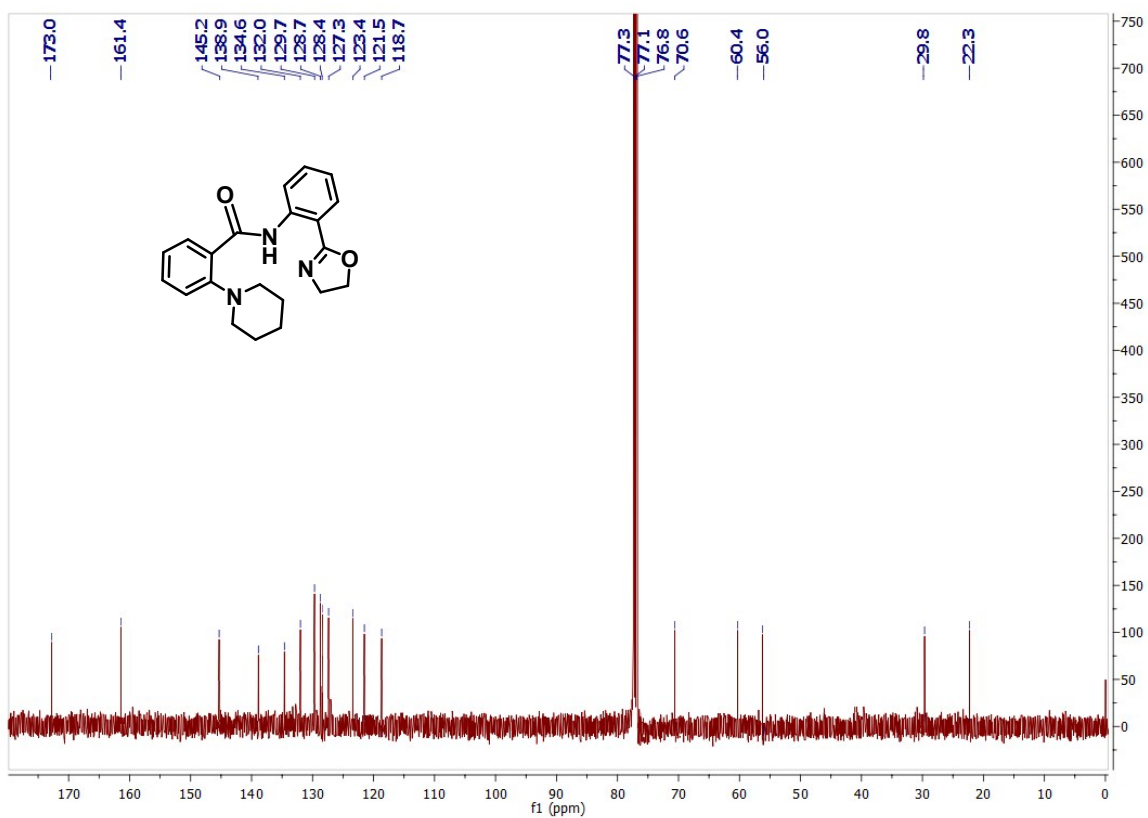


Fig. S50C ESI-MS spectrum of derivative 10e

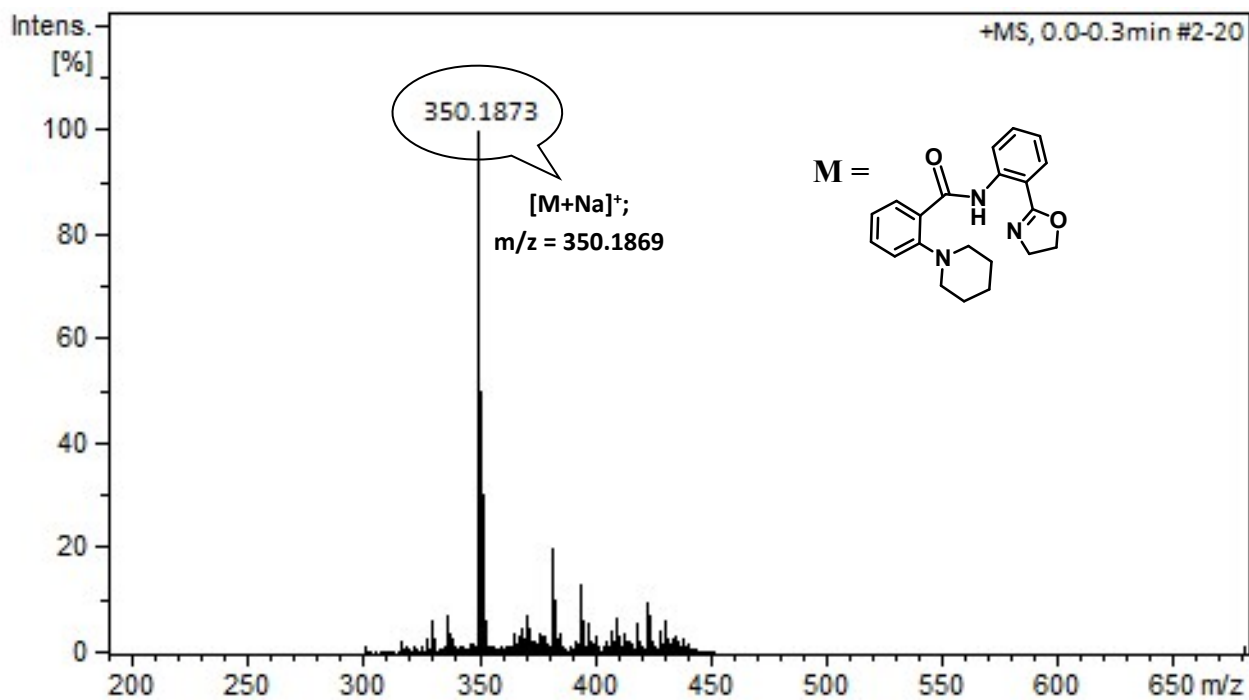


Fig. S51A ¹H NMR spectrum of derivative **10f** in CDCl₃

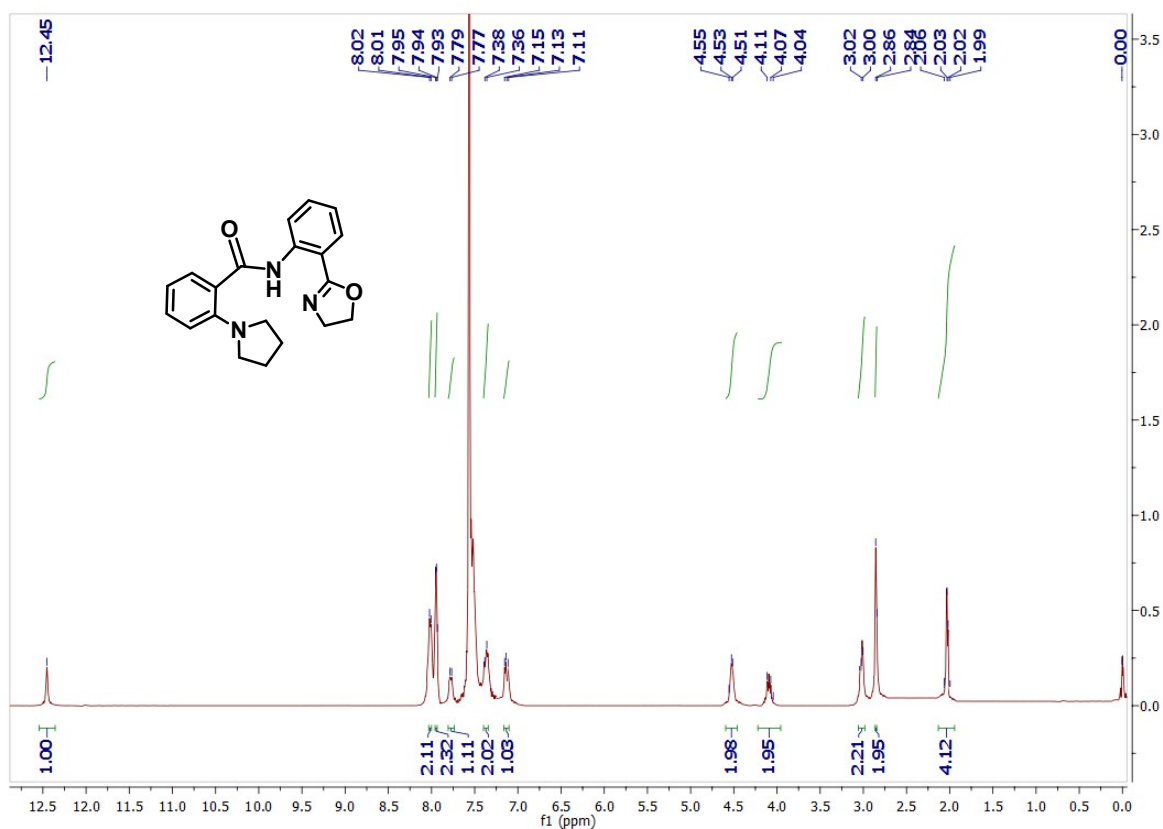


Fig. S51B ¹³C NMR spectrum of derivative **10f** in CDCl₃

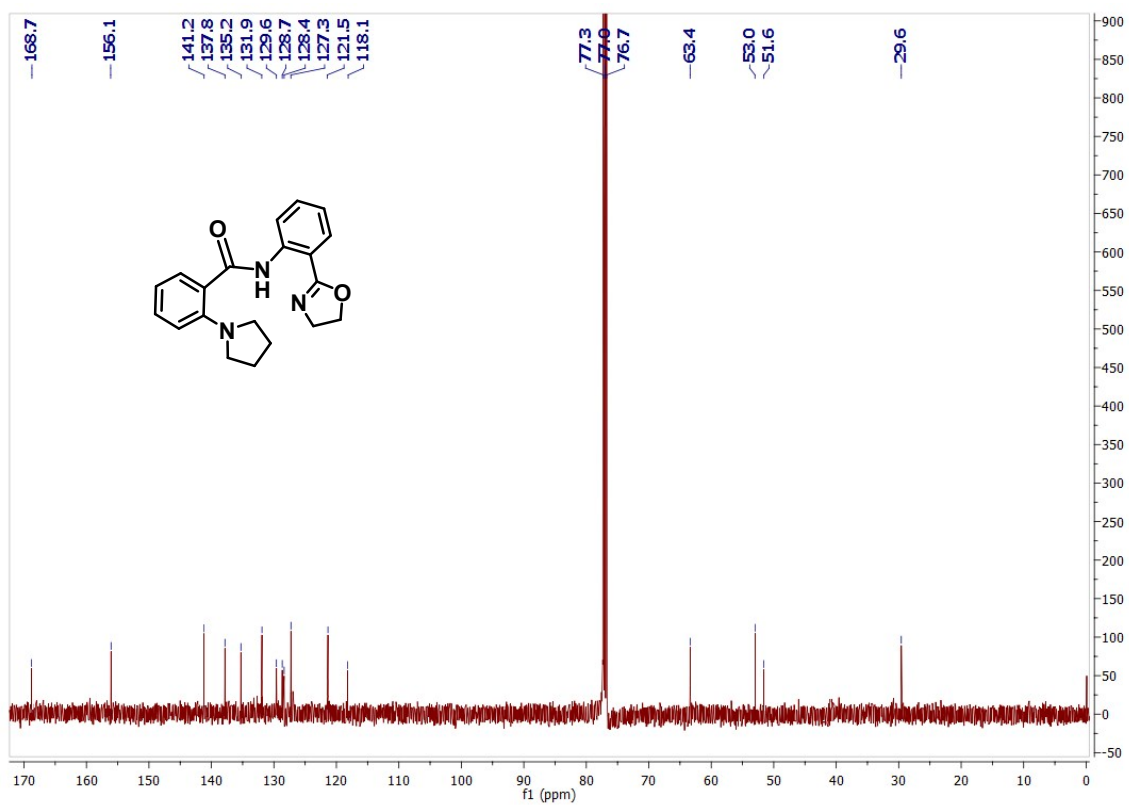


Fig. S51C ESI-MS spectrum of derivative 10f

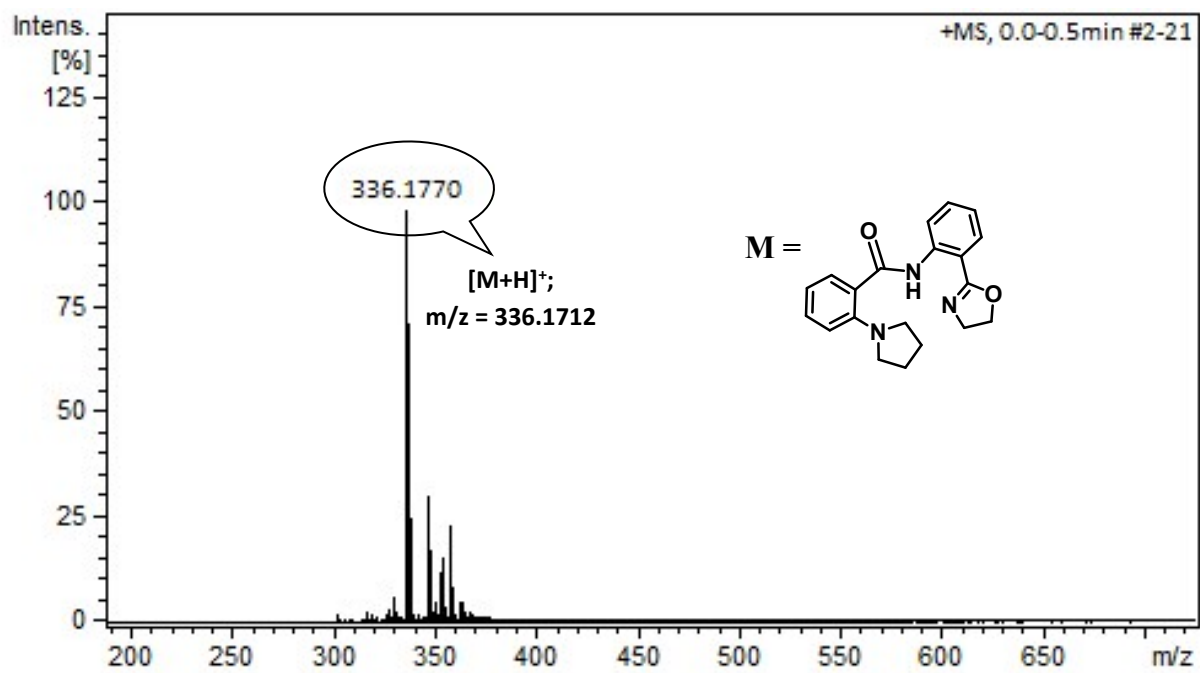


Fig. S52A ¹H NMR spectrum of derivative **10g** in CDCl₃

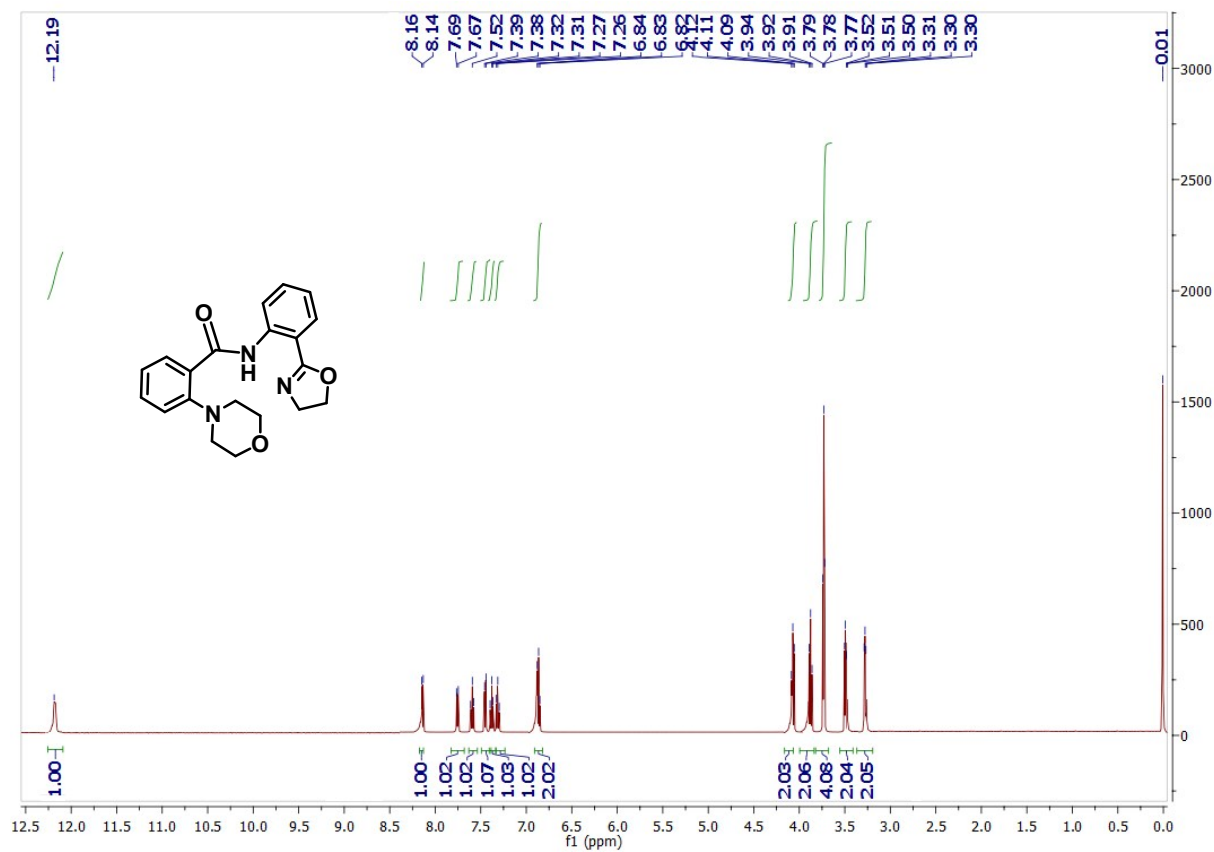


Fig. S52B ¹³C NMR spectrum of derivative **10g** in CDCl₃

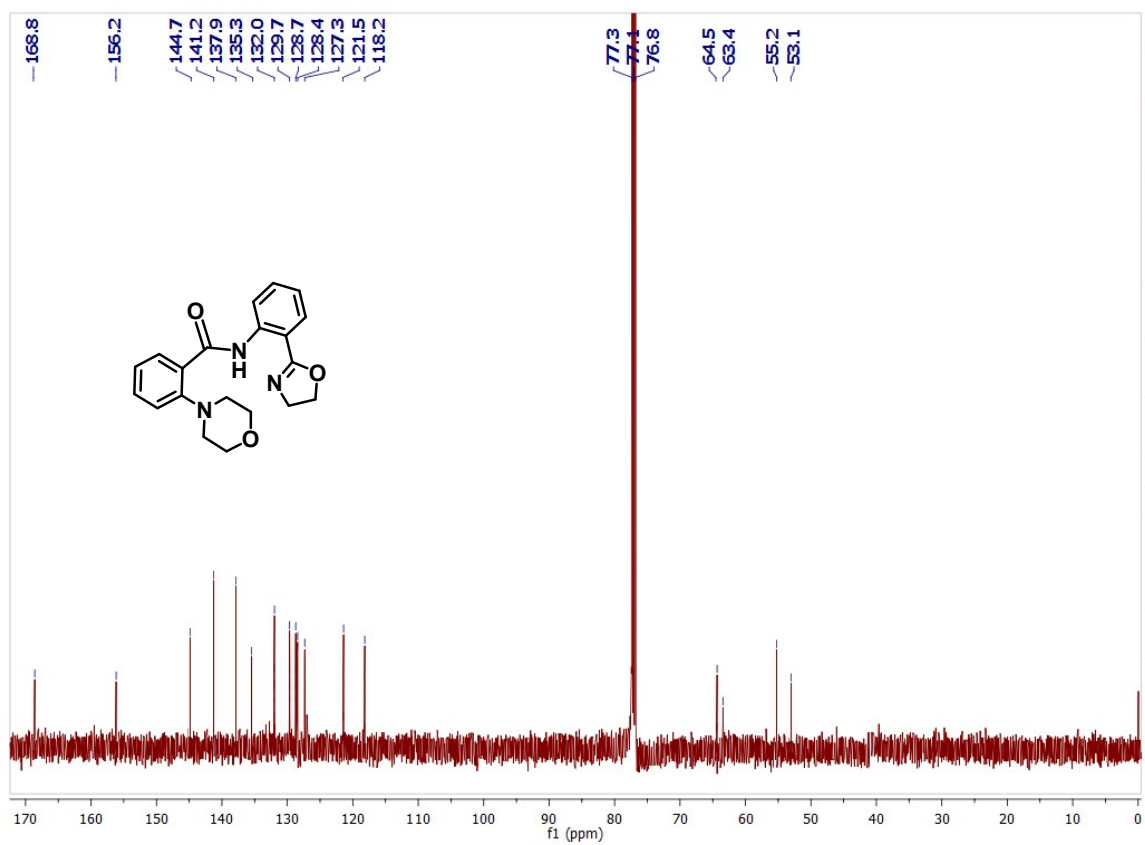


Fig. S52C ESI-MS spectrum of derivative 10g

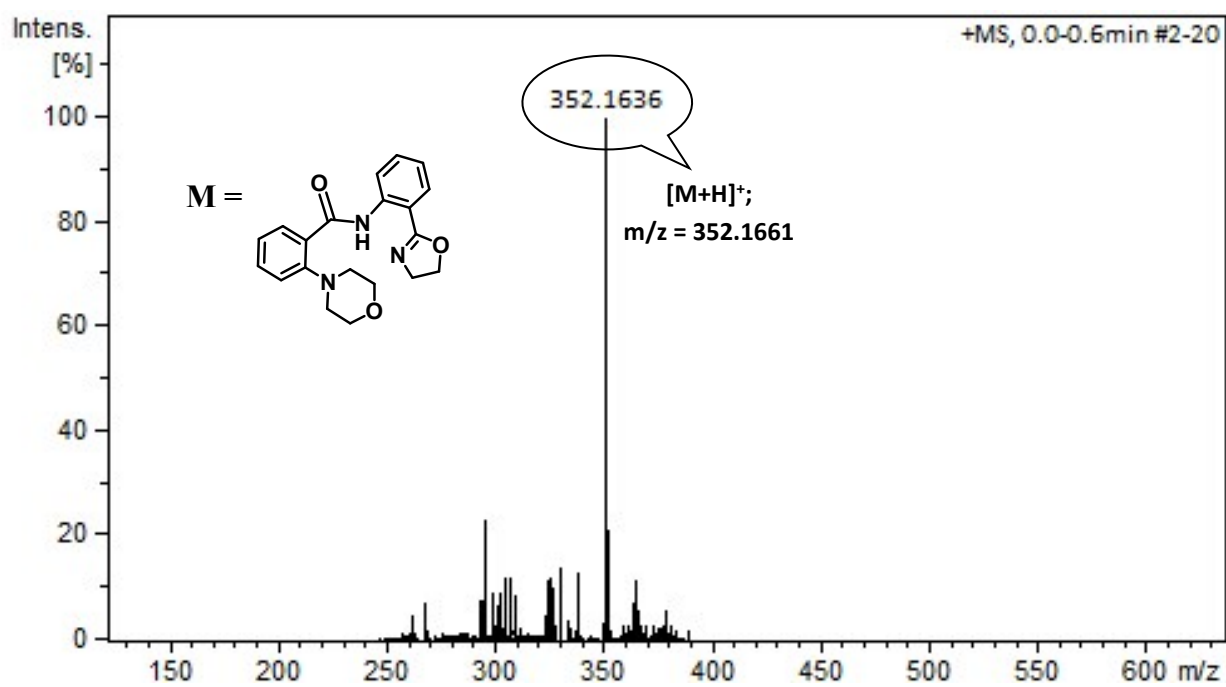


Fig. S53A ^1H NMR spectrum of derivative **10h** in CDCl_3

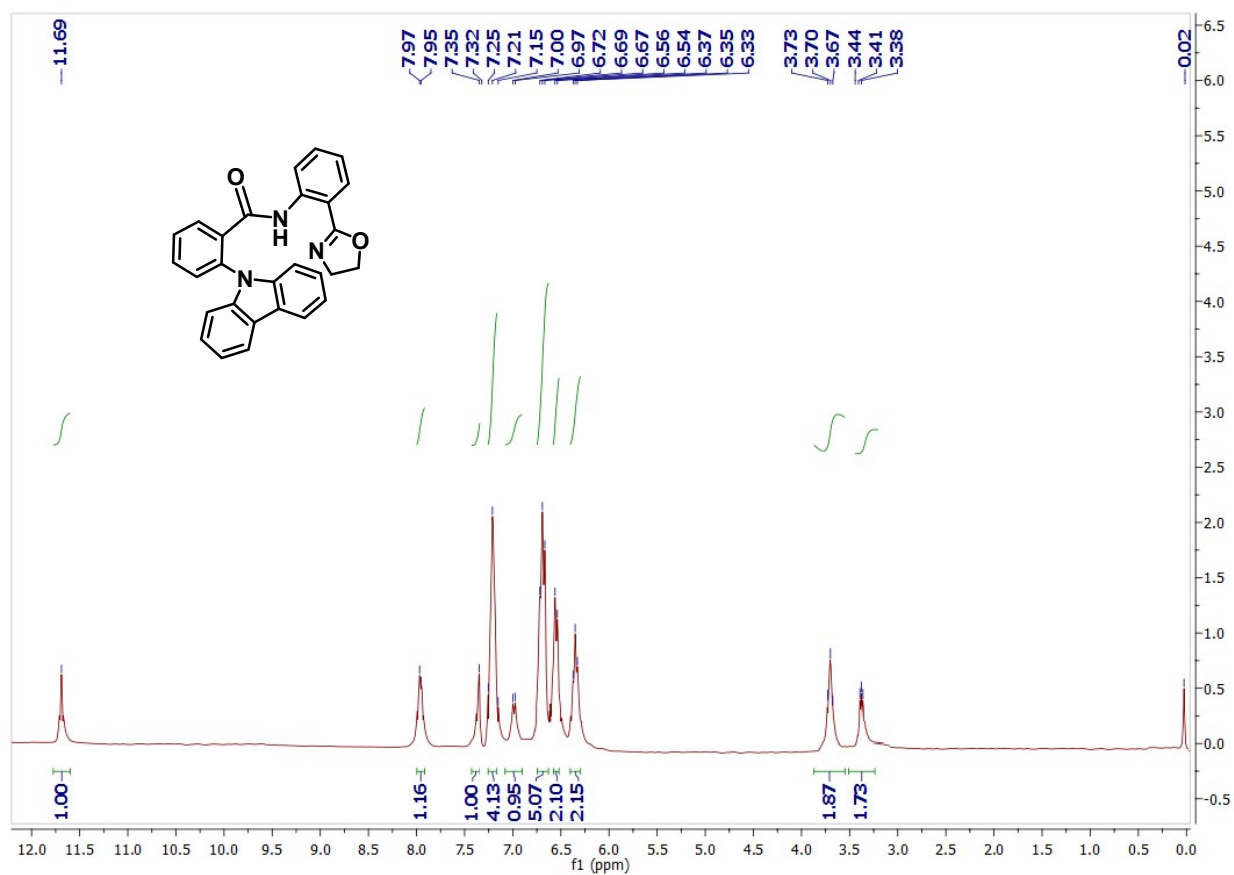


Fig. S53B ^{13}C NMR spectrum of derivative **10h** in CDCl_3

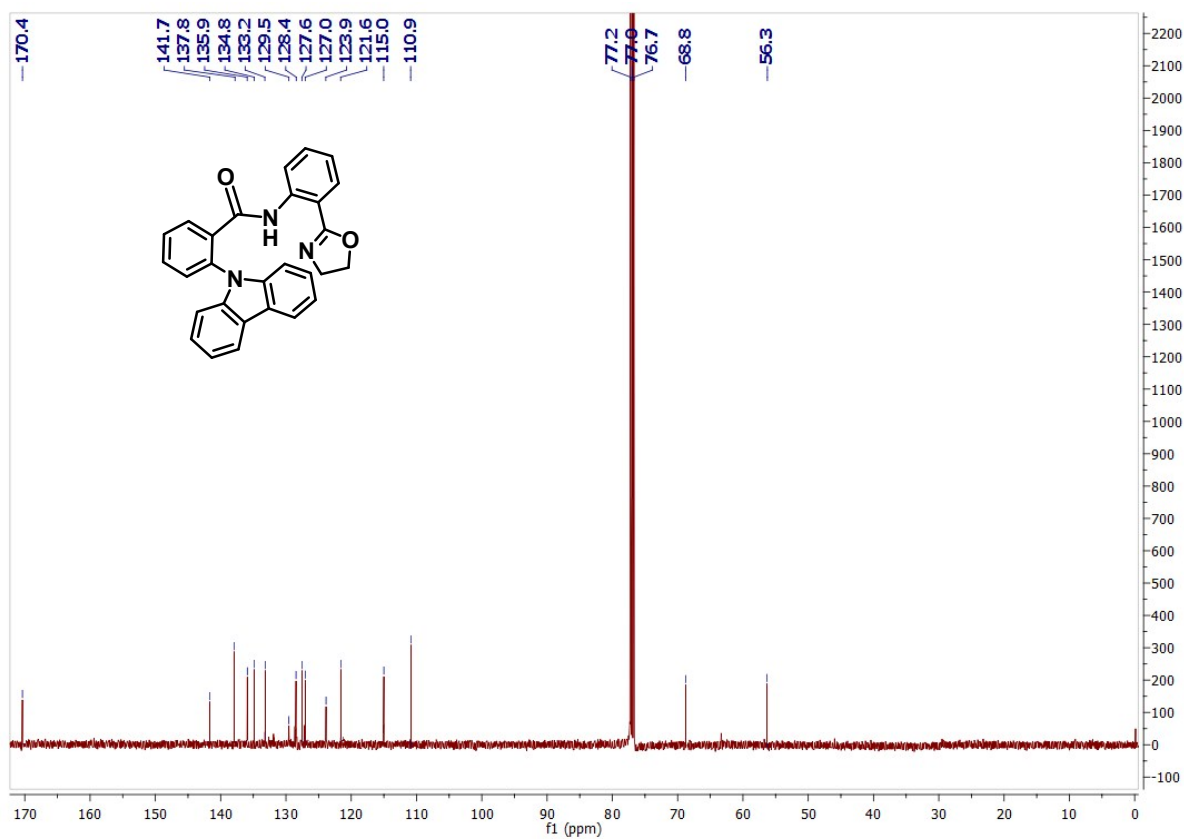


Fig. S53C ESI-MS spectrum of derivative 10h

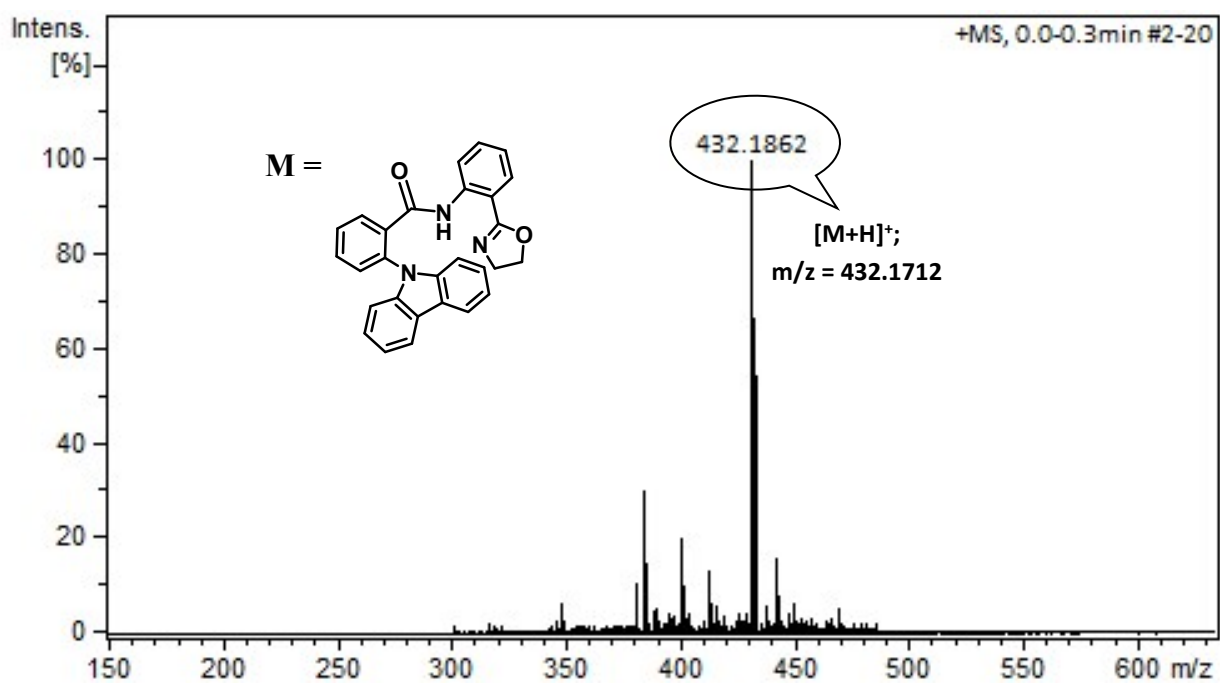


Fig. S54A ¹H NMR spectrum of derivative **10i** in CDCl₃

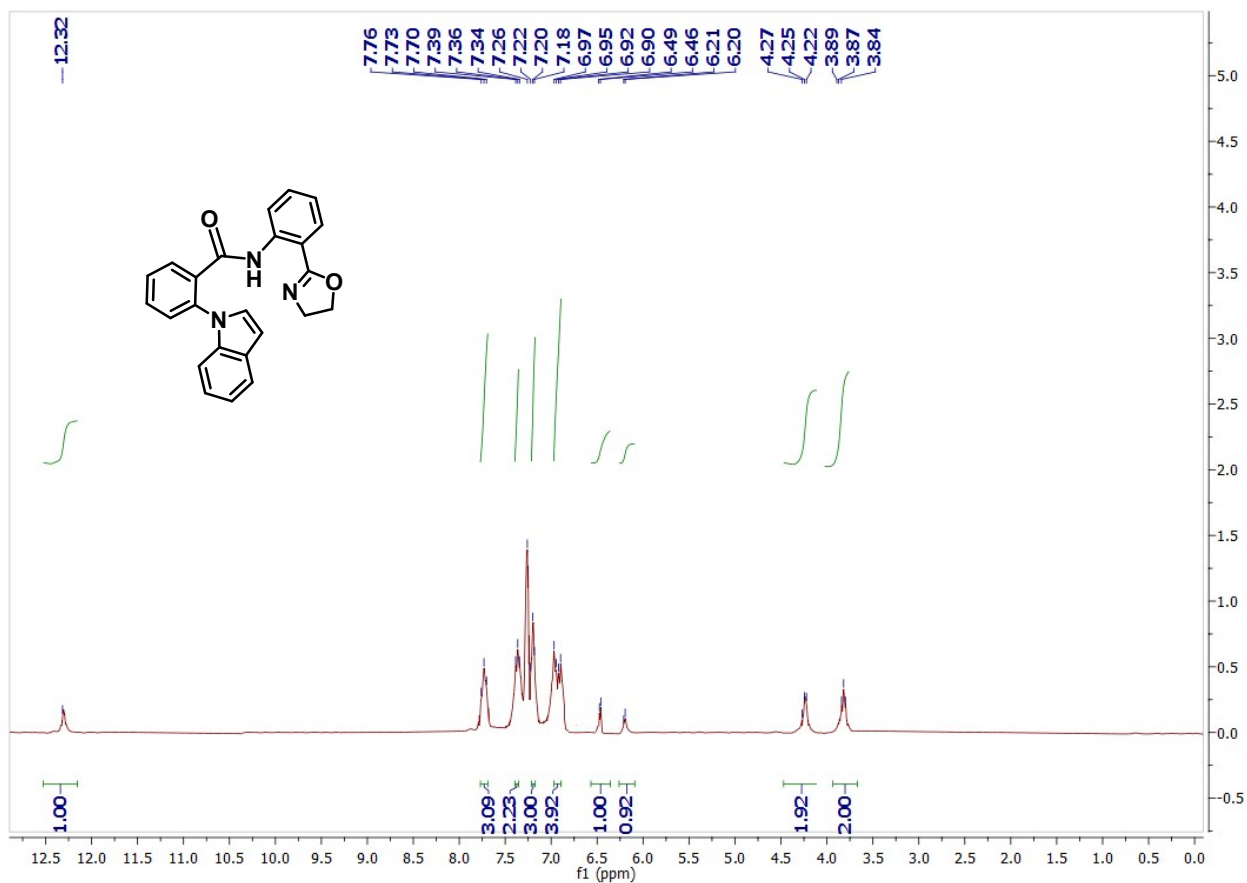


Fig. S54B ¹³C NMR spectrum of derivative **10i** in CDCl₃

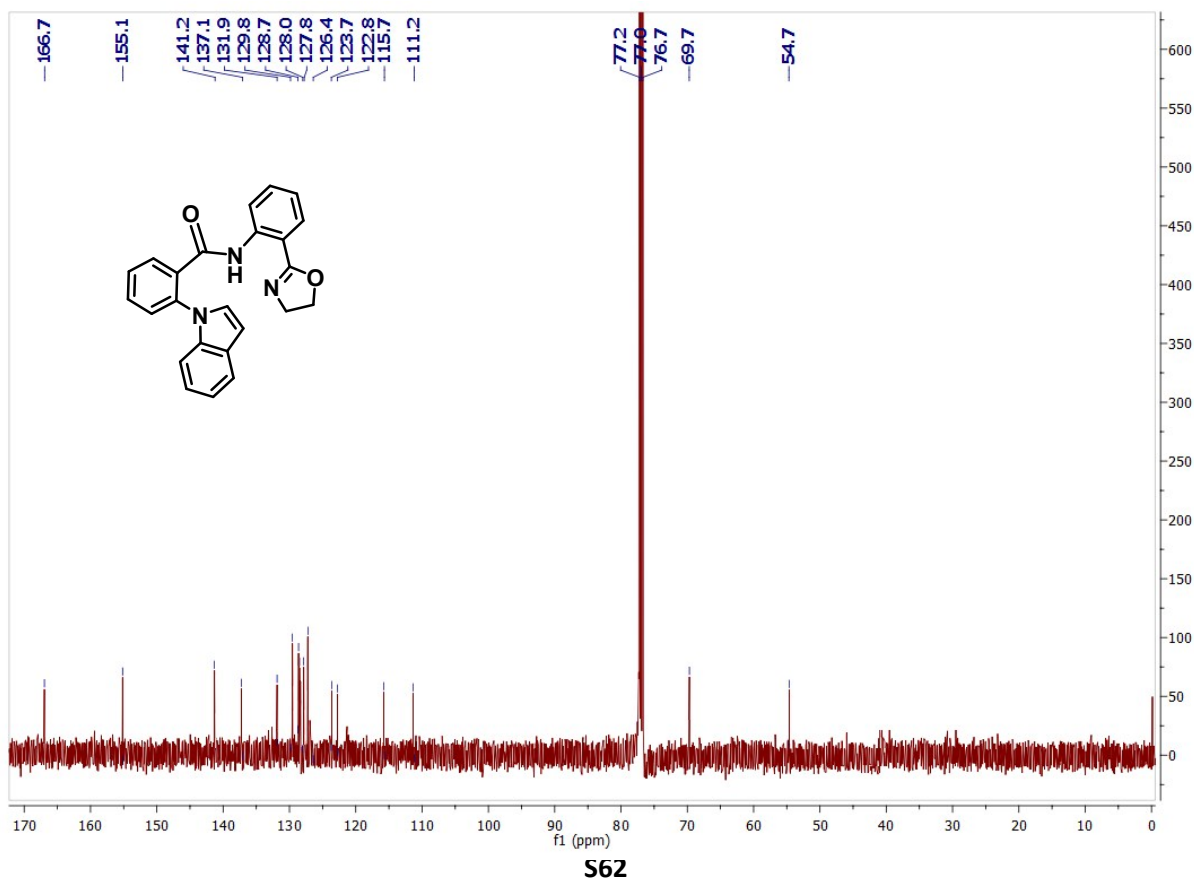


Fig. S54C ESI-MS spectrum of derivative 10i

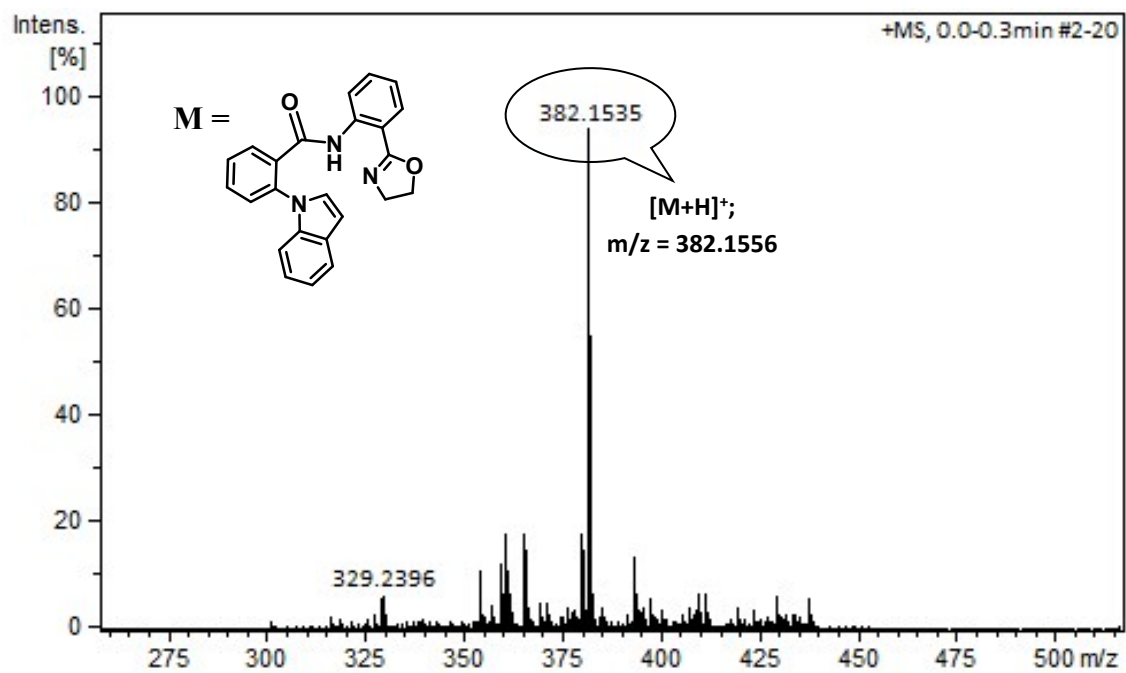


Fig. S55A ^1H NMR spectrum of derivative **10j** in CDCl_3

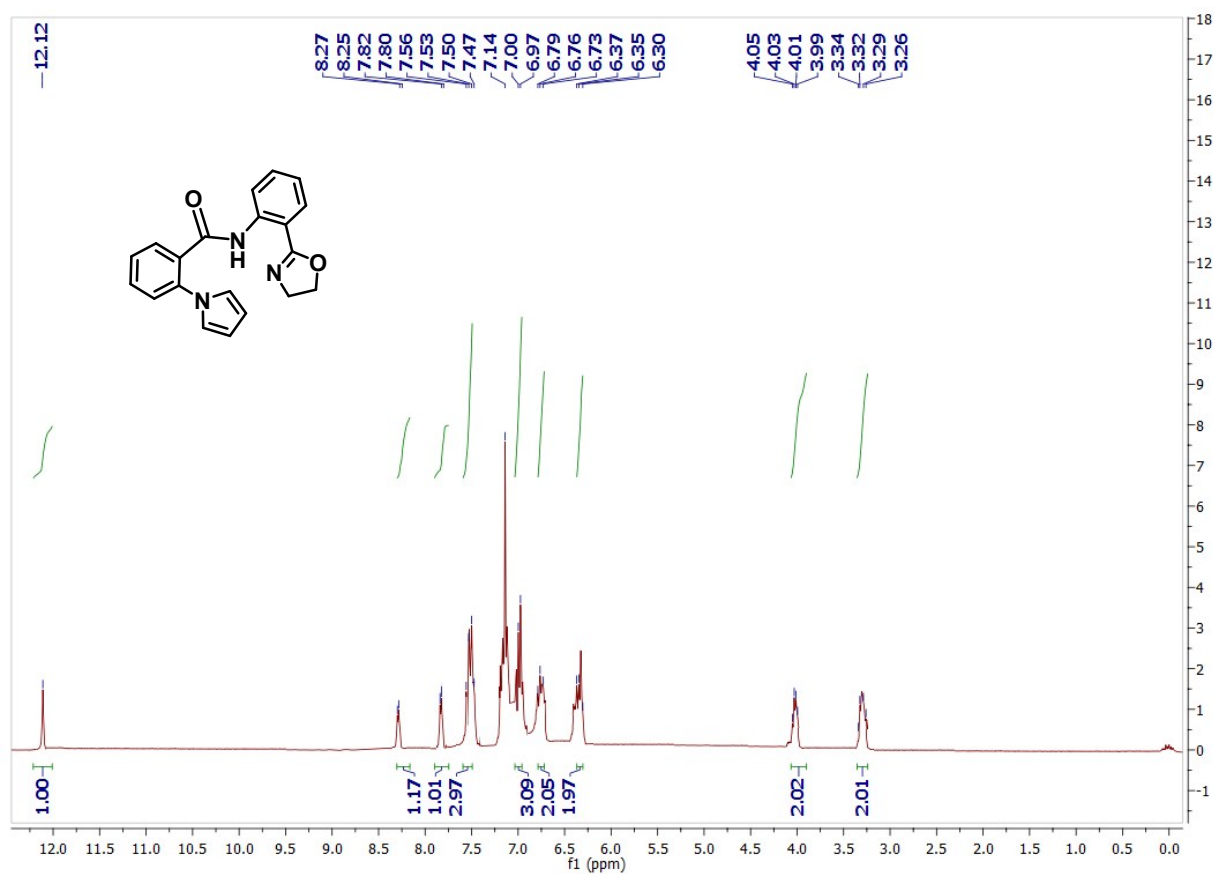


Fig. S55B ^{13}C NMR spectrum of derivative **10j** in CDCl_3

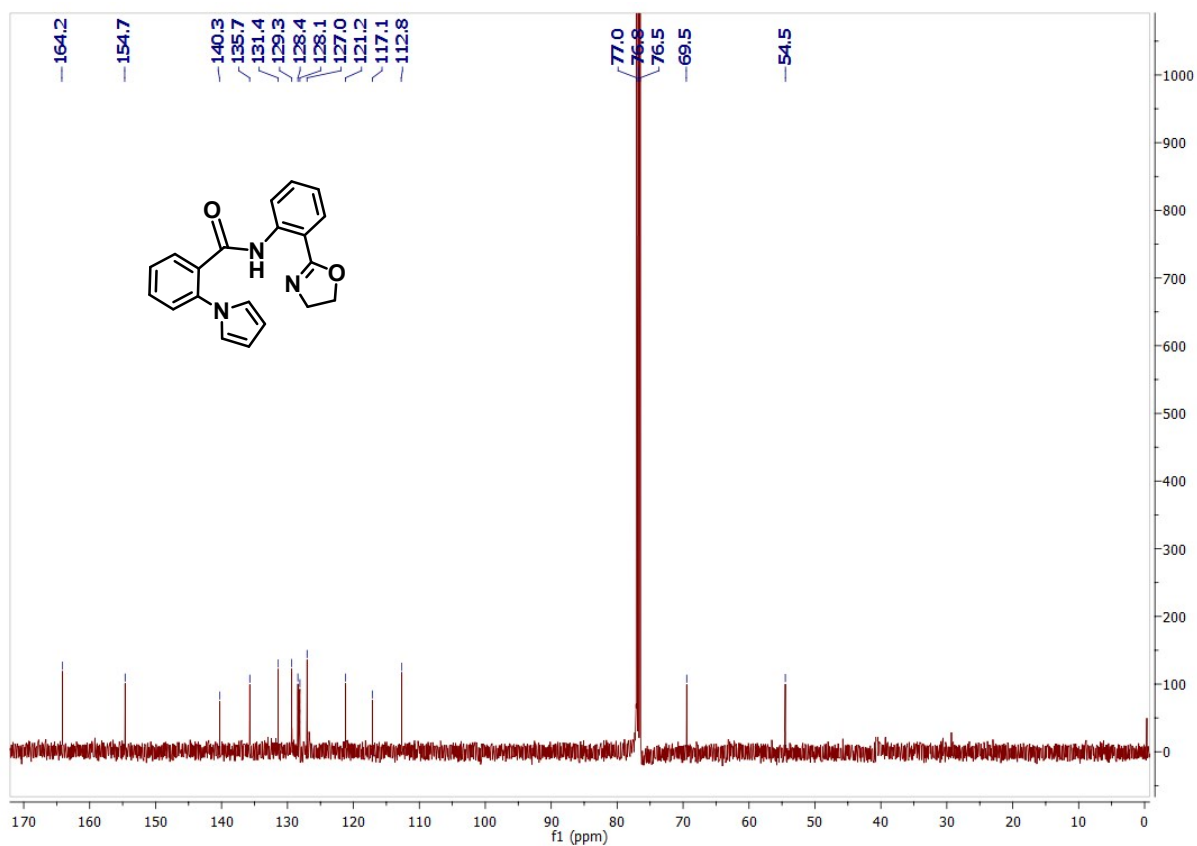


Fig. S55C ESI-MS spectrum of derivative **10j**

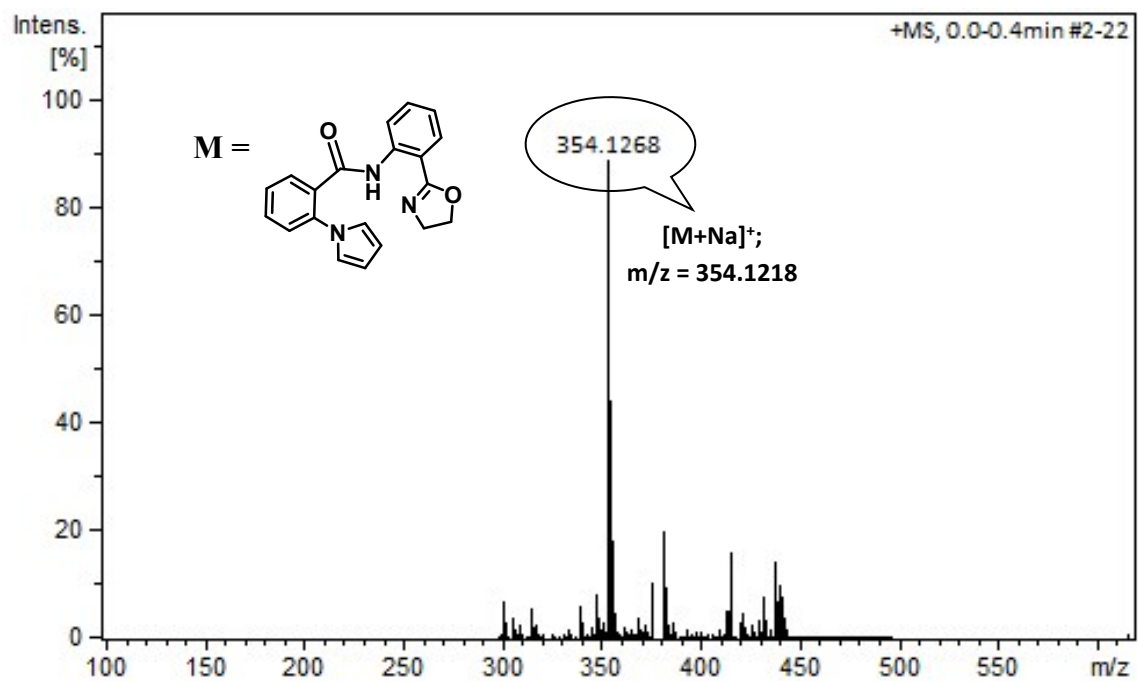


Fig. S56A ^1H NMR spectrum of derivative **10k** in CDCl_3

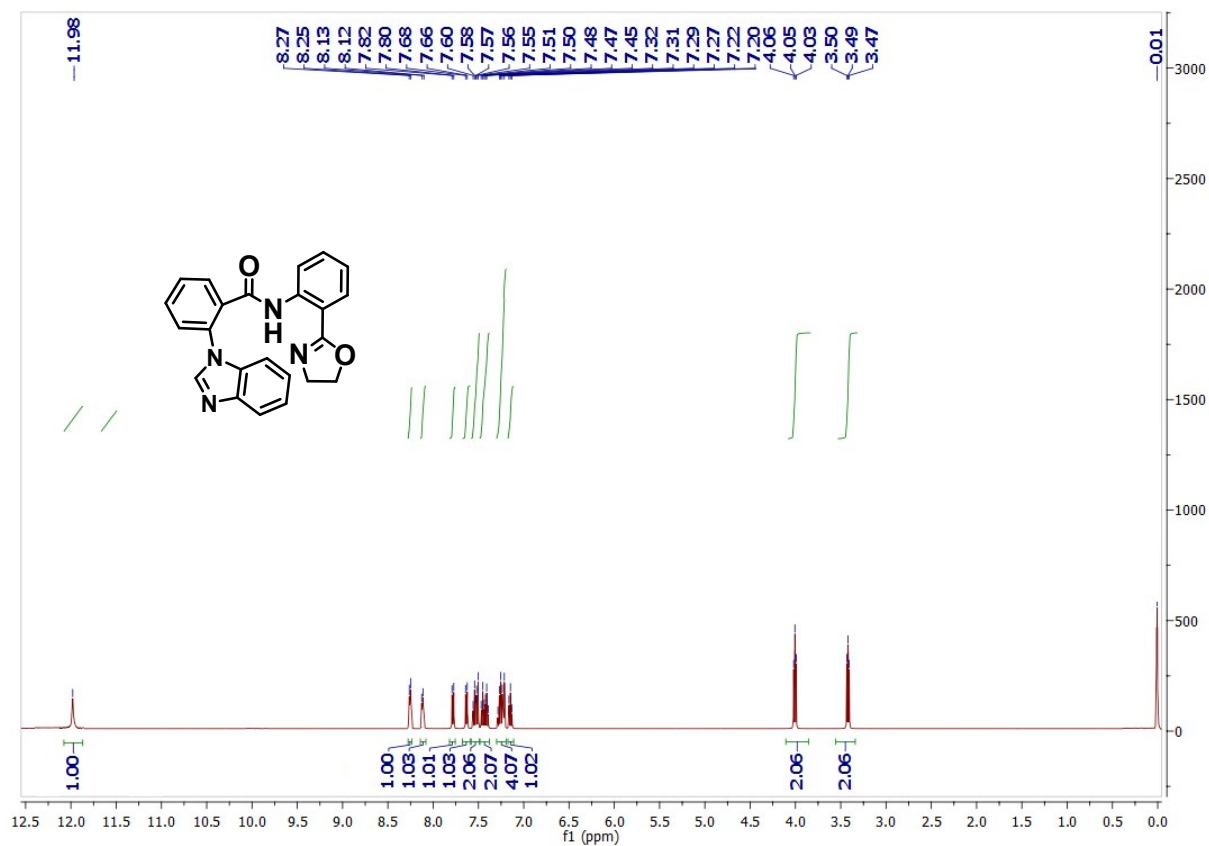


Fig. S56B ^{13}C NMR spectrum of derivative **10k** in CDCl_3

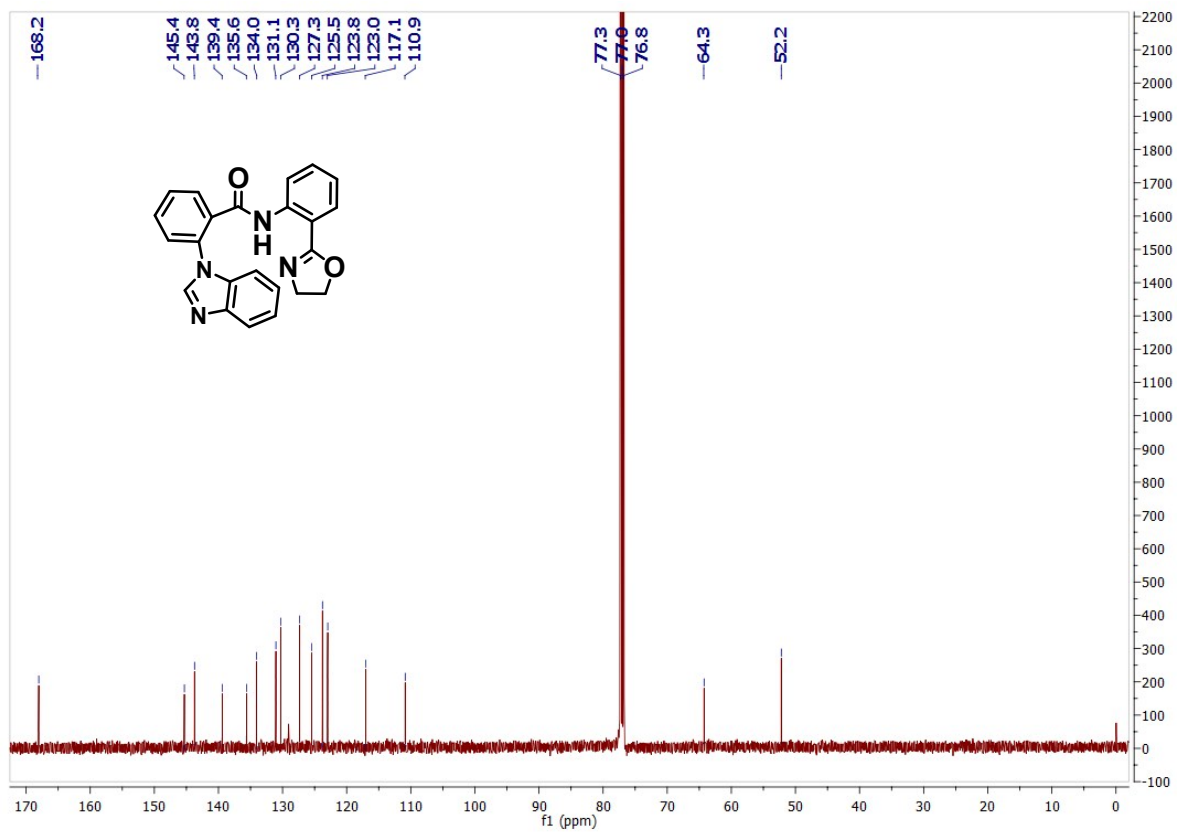


Fig. S56C ESI-MS spectrum of derivative 10k

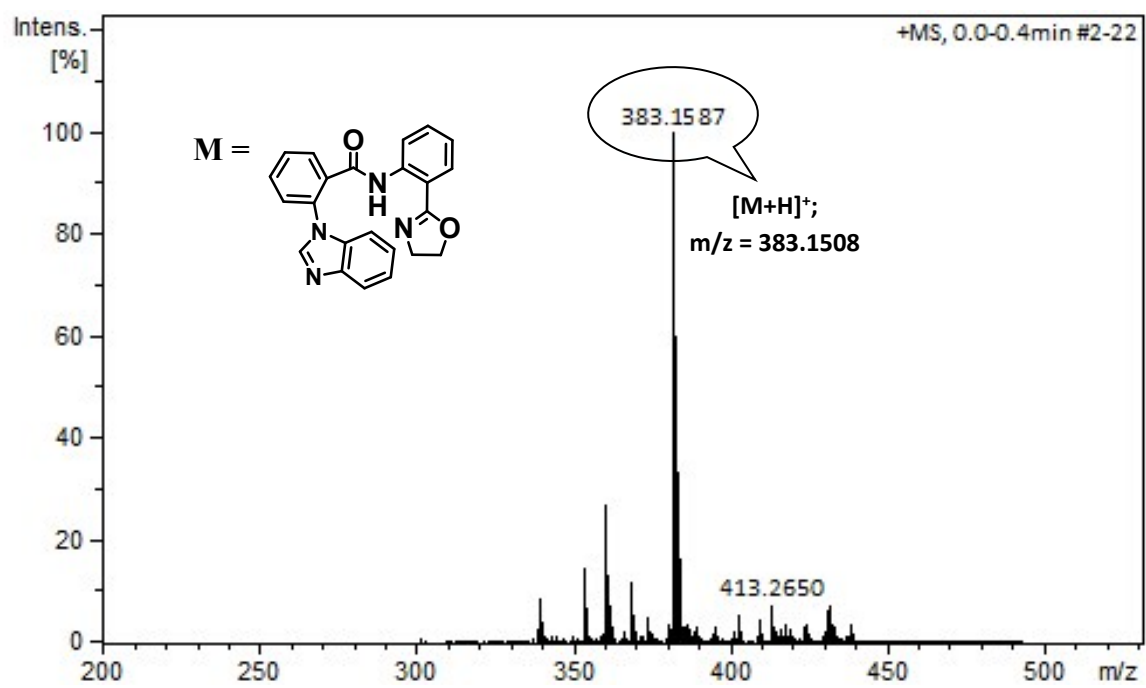


Fig. S57A ¹H NMR spectrum of derivative **101** in CDCl₃

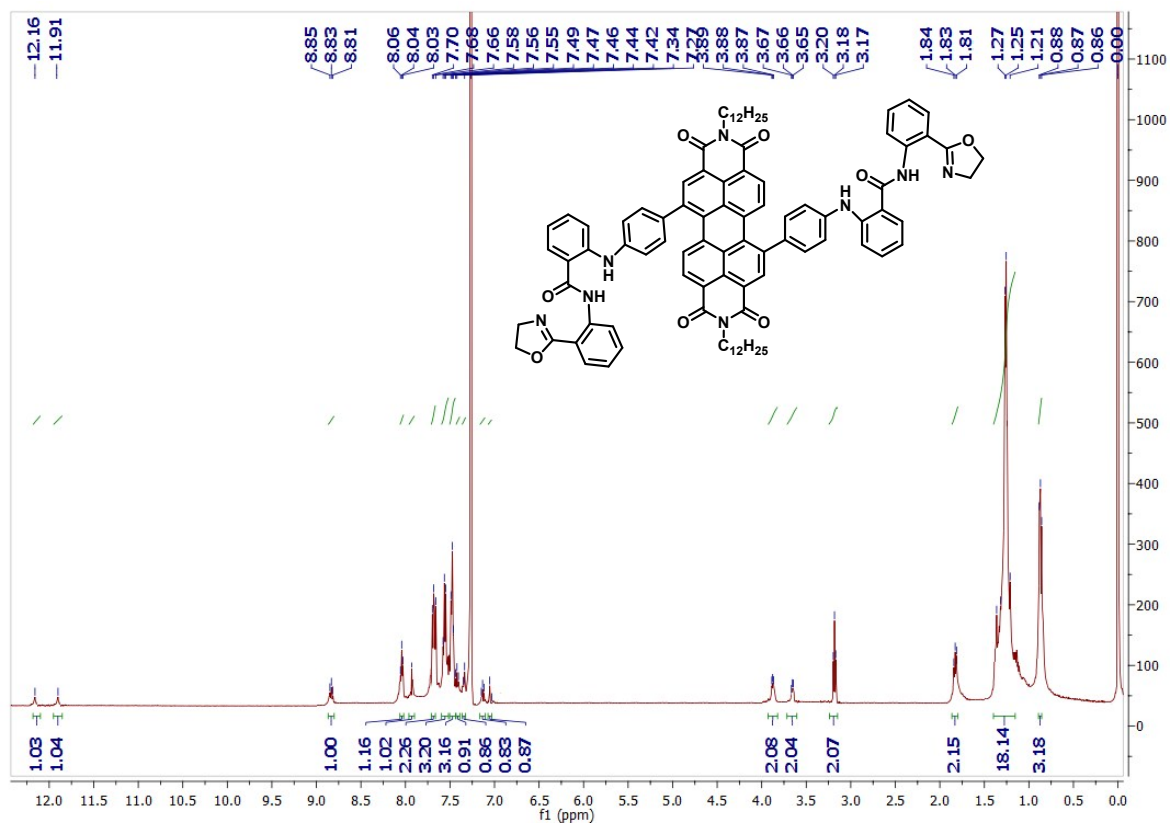


Fig. S57B ¹³C NMR spectrum of derivative **101** in CDCl₃

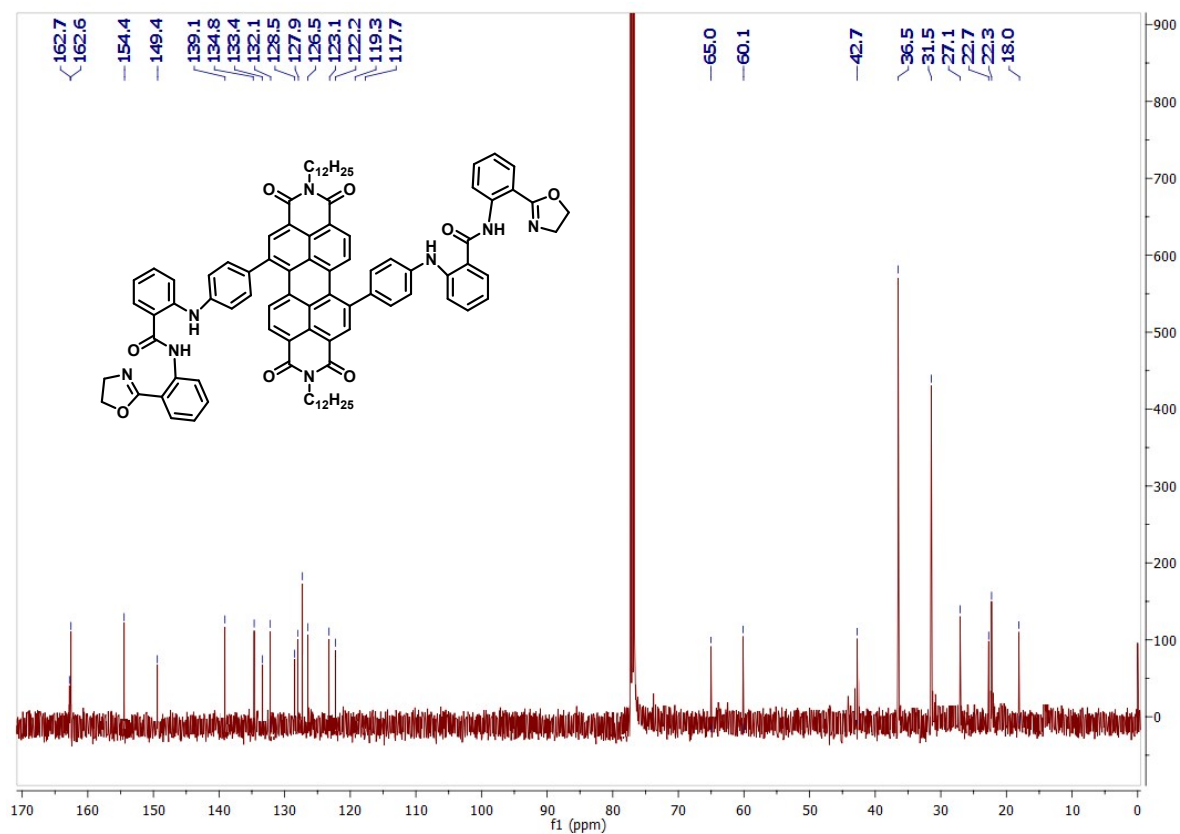


Fig. S57C Mass spectrum (ESI-MS) of derivative 10l:

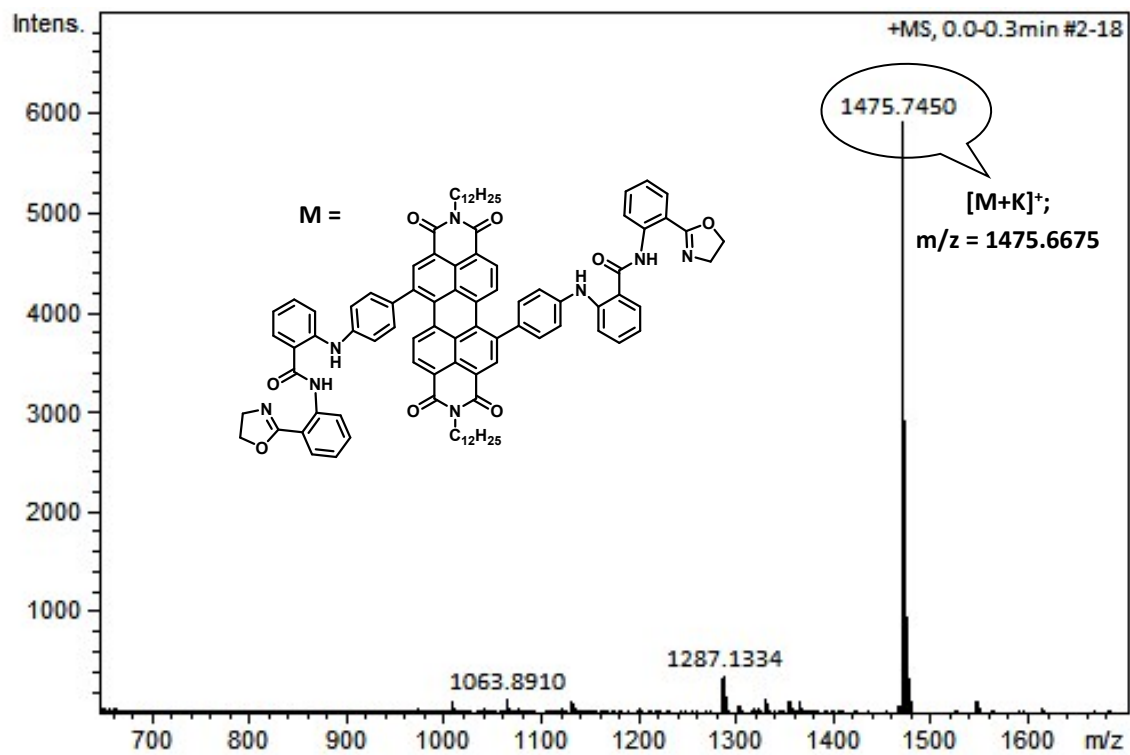


Fig. S58A ^1H NMR spectrum of derivative **11** in CDCl_3

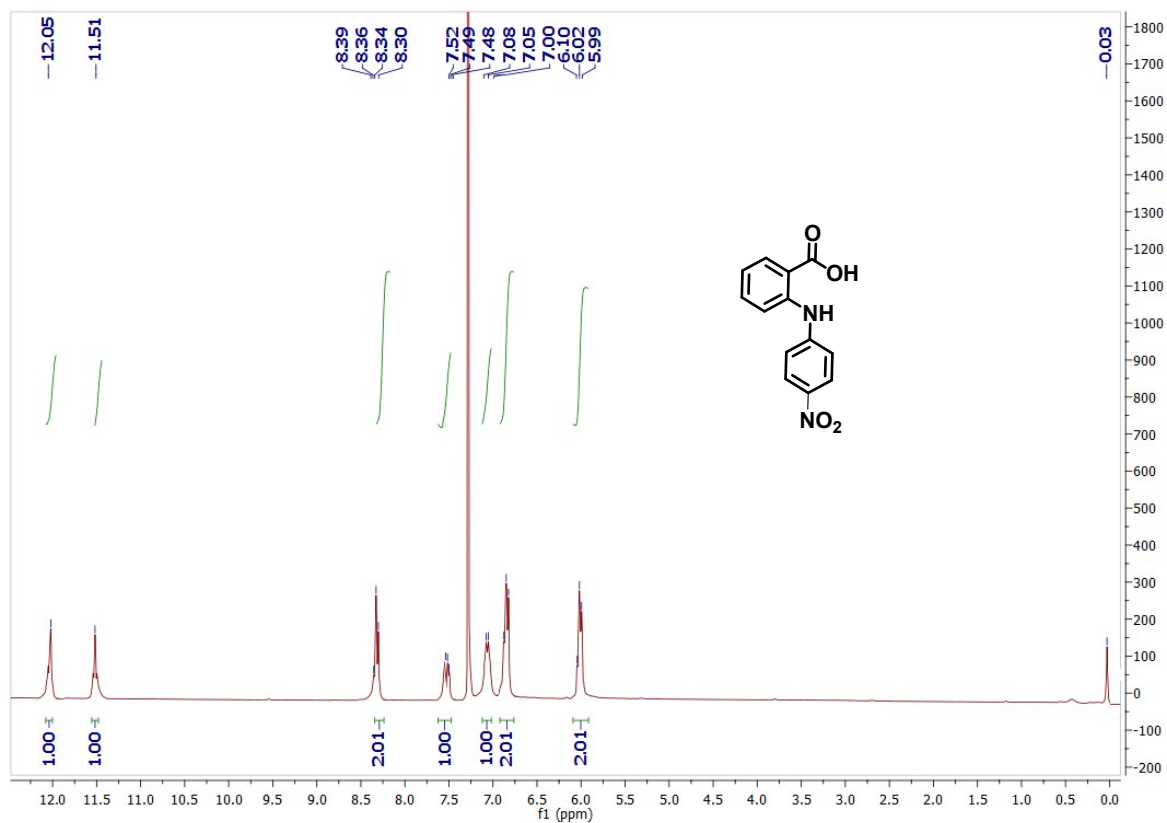


Fig. S58B ^{13}C NMR spectrum of derivative **11** in CDCl_3

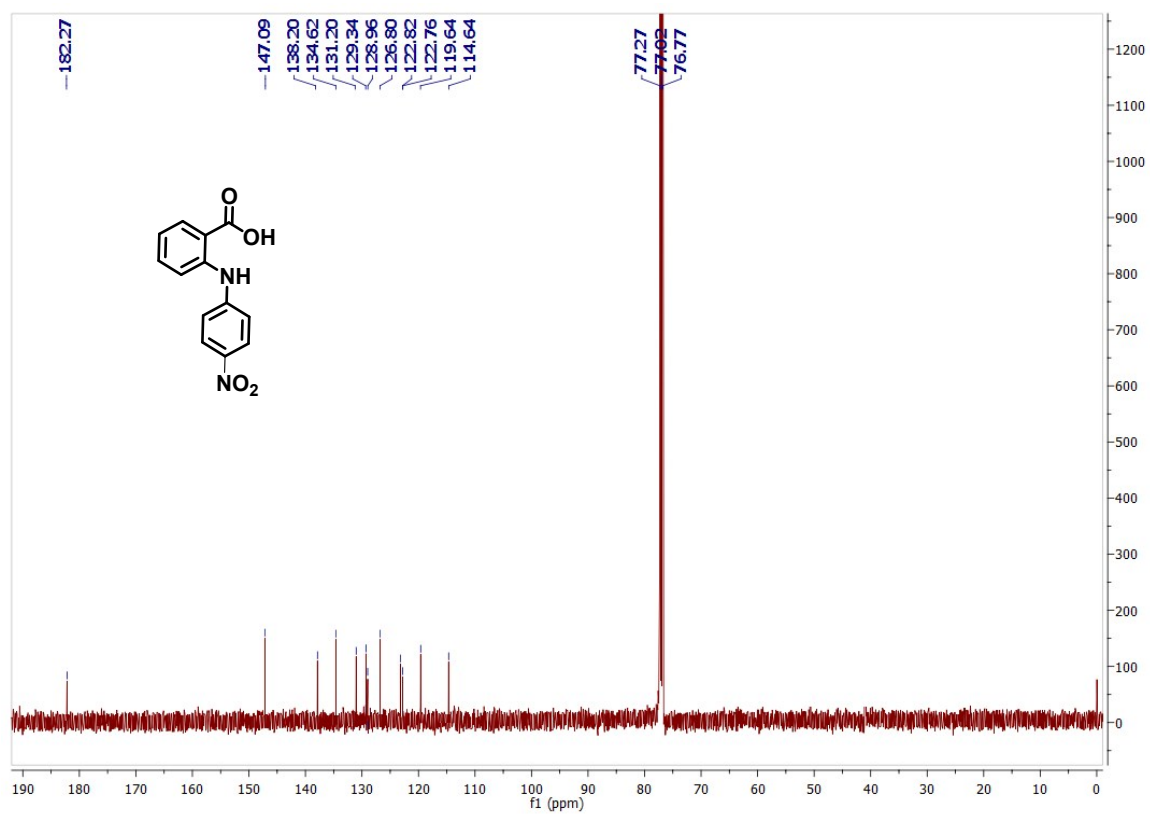


Fig. S59A ^1H NMR spectrum of derivative **12** in CDCl_3

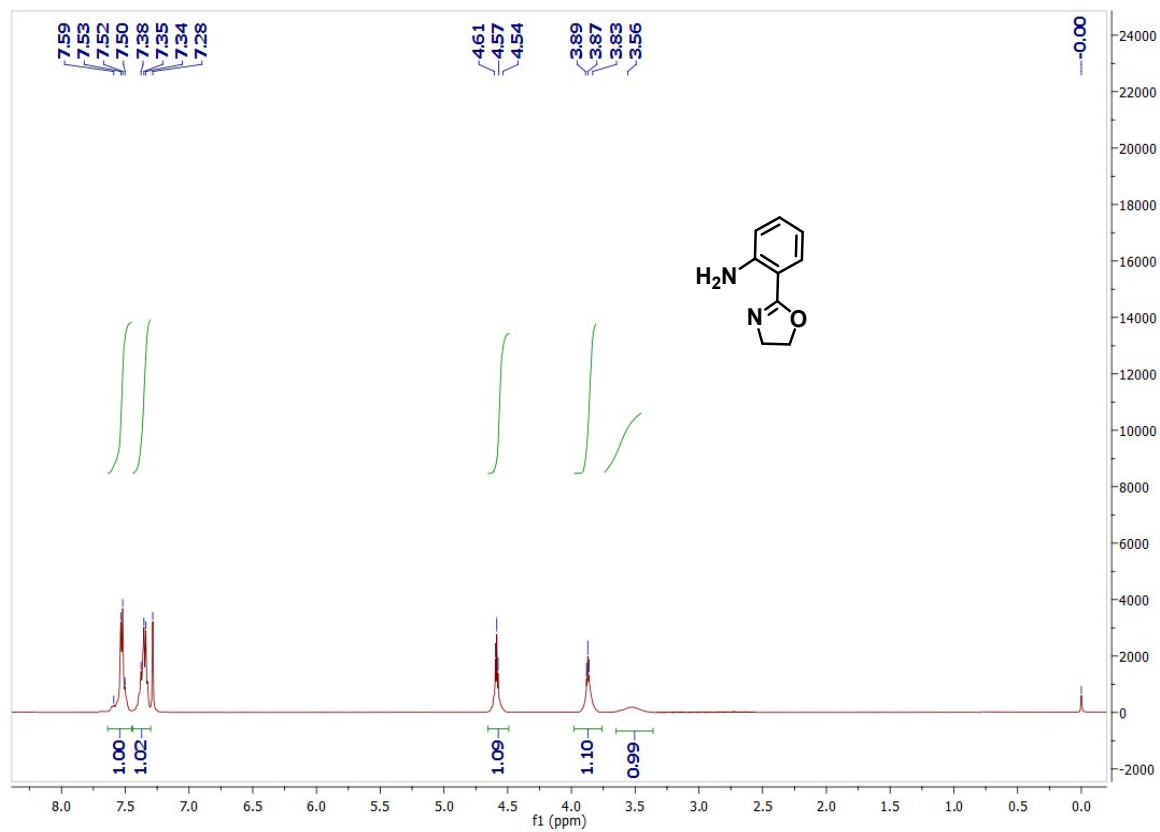


Fig. S59B ^{13}C NMR spectrum of derivative **12** in CDCl_3

